

Development of a Force-Feedback Laparoscopic Surgery Simulator

by

Ela Ben-Ur

B.S. Mechanical Engineering
Massachusetts Institute of Technology, 1997

Submitted to the Department of Mechanical Engineering
in partial fulfillment of the requirements for the degree of

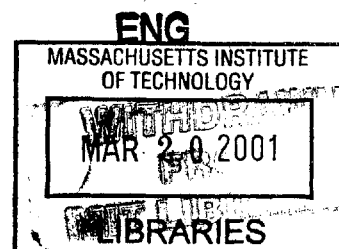
Master of Science in Mechanical Engineering

at the

MASSACHUSETTS INSTITUTE OF TECHNOLOGY

September 1999

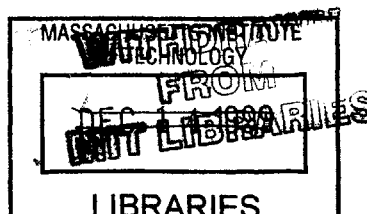
© 1999 Massachusetts Institute of Technology
All rights reserved



Signature of Author.....
Department of Mechanical Engineering,
July 28, 1999

Certified by.....
Dr. Kenneth Salisbury, Jr.
Principal Research Scientist
Thesis Supervisor

Accepted by.....
Professor Ain A. Sonin
Chairman, Committee on Graduate Students



Development of a Force-Feedback Laparoscopic Surgery Simulator

by

Ela Ben-Ur

Submitted to the Department of Mechanical Engineering
on August 6, 1999 in partial fulfillment of the
requirements for the degree of Master of Science in
Mechanical Engineering

Abstract

The work presented here addressed the development of an electro-mechanical force-feedback device to provide more realistic and complete sensations to a laparoscopic surgery simulator than currently available. A survey of the issues surrounding haptic (touch) displays and training for laparoscopic or "keyhole" procedures was performed. A number of primary and secondary sources including surgeon consultation, operating room observations, and task analyses were used to accumulate a list of needs. Subsequent requirements analysis translated these into a set of specifications for the kinematics, dynamics and actuators, and configuration of the device. These suggested a design with five actuated axes (pitch and yaw about the entrance to the abdomen, insertion, rotation about the tool axis, and gripper feedback) amenable to a configuration including two actuated tools in a lifelike torso.

These specifications were the basis for the generation and selection of design concepts. The PHANTOM haptic interface from Sensable Devices was chosen from among a number of existing devices and original designs to actuate the pitch, yaw, and insertion degrees of freedom. A separate end effector actuator was specified to supply feedback to the handle rotation and gripper. Mechanisms were proposed for each of these axes; a linear cable capstan was selected for the gripper and a cable capstan/drum for the rotation. The kinematics, bearings, transmissions, and user interface for both axes were designed in detail, and first- and second-generation prototypes were built. The finished devices were integrated with the PHANTOM hardware, electronics, and software. Performance and design evaluations were performed, and plans for future device improvements and user studies were outlined.

Thesis supervisor: J. Kenneth Salisbury
Title: Principal Research Scientist

Acknowledgements

I extend my sincere gratitude to Ken Salisbury for granting me the opportunity to sprinkle my engineering design pursuits with creative and humanistic moments through the wonderful field of haptics, and for going with me when they came along.

To Steve Dawson at Massachusetts General Hospital and Homer Pien at Draper Laboratory for bringing me on board this phenomenal project and helping to make everything happen, to David Rattner for his counsel and welcoming me to his operating room, and to the Center for Minimally Invasive Therapies and the National Science Foundation for their financial support.

To the extraordinary group that is “jks folks”, whose limitless support enabled me to grow as a designer and as a person. Mark, for your mentorship and patience, Brian for your energy and confidence, Don for your unique perspectives, Andrew for being sensible, Jessie for being whimsical, and Arrin for being honest and just being there (in our office).

To professors Woodie Flowers, David Wallace, Warren Seering, Ernesto Blanco, and Anna Thornton at MIT and Tony Field, my studio head while at IDEO Product Development, for helping me find a love and sensitivity for design, filling my toolbox, and instilling the importance of finding the right problem and doing things the right way.

To my lifelong friend, Jennifer Klein, for always helping me keep perspective and identity, and for continuing to support my creative side while becoming the artist and person I admire most.

To my sister Nurit who is so much a part of who I am, and what I aspire to be.

And to my parents, Joseph and Tamar Ben-Ur, for their unconditional love, for everything they have given and given up, and for always trying to make the world a place where I could follow my dreams.

This material is based upon work supported under a National Science Foundation Graduate Fellowship. Any opinions, findings, conclusions or recommendations expressed in this publication are those of the author and do not necessarily reflect the views of the National Science Foundation.

Table of Contents

CHAPTER 1 PROBLEM IDENTIFICATION & BACKGROUND	8
1.1 THE PROBLEM	8
1.2 BACKGROUND AND MOTIVATION.....	8
1.3 LAPAROSCOPY AND HAPTICS	10
1.4 COMPONENTS OF A SIMULATOR	12
1.5 PREVIOUS WORK	12
1.6 HISTORY OF THIS EFFORT.....	14
CHAPTER 2 PROBLEM DEFINITION AND REQUIREMENTS ANALYSIS	15
2.1 REQUIREMENTS DATA ACQUISITION.....	15
2.1.1 <i>Surgeon Input</i>	16
2.1.2 <i>Operating Room Observations</i>	17
2.1.3 <i>Documented Task Analyses</i>	17
2.2 REQUIREMENTS ANALYSIS.....	18
2.2.1 <i>Workspace and Kinematic Requirements</i>	19
2.2.2 <i>Transmission and Performance Requirements</i>	22
2.2.3 <i>Features and Configuration Requirements</i>	26
2.3 BENCHMARKING.....	29
CHAPTER 3 CONCEPT IDEATION AND SELECTION.....	31
3.1 PITCH, YAW AND INSERTION.....	32
3.1.1 <i>Existing Devices and New Concept Generation</i>	32
3.1.2 <i>Concept Comparison and Selection</i>	37
3.2 END EFFECTOR DEVICE.....	38
3.2.1 <i>Refocused Specifications</i>	39
3.2.2 <i>Device Configuration</i>	39
3.2.3 <i>Actuation Concept Generation and Early Refinement</i>	41
3.2.4 <i>Early Analysis and Concept Selection</i>	42
3.3 DESIGN SPLIT: 1 AND 2 DOF DEVICES	48
CHAPTER 4 DETAILED DESIGN AND FABRICATION.....	49
4.1 GRIPPER AXIS DESIGN.....	50
4.1.1 <i>Motion Constraints and Bearings</i>	50

4.1.2	<i>Shaft Constraint and User Interface</i>	54
4.1.3	<i>Cable Management</i>	57
4.1.4	<i>Actuation and Position Measurement</i>	58
4.2	ROTATION AXIS	59
4.2.1	<i>Configuration and Bearings</i>	59
4.2.2	<i>Shaft Constraint and User Interface</i>	60
4.2.3	<i>Cable Management</i>	62
4.2.4	<i>Actuation and Position Measurement</i>	62
4.3	PHANTOM AND SIMULATION CONFIGURATION.....	63
4.4	CONTROLS AND ELECTRONICS	67
4.5	SOFTWARE	68
CHAPTER 5 EVALUATION AND RECOMMENDATIONS.....		71
5.1	PERFORMANCE EVALUATION	71
5.2	DESIGN EVALUATION.....	73
CHAPTER 6 CONCLUSIONS AND EXTENSIONS.....		75
BIBLIOGRAPHY		77
APPENDICES.....		79
APPENDIX A. REQUIREMENTS ANALYSIS DATA COLLECTION FORMS		79
A1.	<i>Surgeon questionnaire</i>	80
A2.	OPERATING ROOM OBSERVATION FORM.....	81
APPENDIX B. DESIGN SPREADSHEETS		82
B1.	<i>Needs to Metrics</i>	83
B2.	<i>Specification Definition</i>	84
B3.	<i>Benchmarking and Platform Concept Selection</i>	85
B4.	<i>Gripper Subsystem Concept Selection</i>	86
APPENDIX C. CAD DRAWINGS		87
C1.	<i>1DOF Device</i>	87
C2.	<i>2DOF Device</i>	93
APPENDIX D. DEVICE MANUAL.....		99
APPENDIX E. PROGRAM CODE.....		101

Table of Figures

FIGURE 1-1. LAPAROSCOPY BEING PERFORMED, AND VIEW THROUGH THE LAPAROSCOPE IN HERNIA REPAIR.	10
FIGURE 2-1. AXES OF MOTION IN LAPAROSCOPIC SURGERY	20
FIGURE 2-2. LAPAROSCOPIC SCISSORS CONSTRUCTION..	21
FIGURE 2-3. EMPIRICAL TEST PERFORMED TO EXAMINE FORCE ON GRIPPER-ACTUATOR SHAFT.	23
FIGURE 2-4. TEST PERFORMED TO RATE FRICTION EXPERIENCED AT THE HANDLE IN TOOLS BEARING VARIOUS END EFFECTORS.	25
FIGURE 2-5. THE USE OF GRIPPERS TO SPREAD AND TEAR TISSUE IN CHOLECYSTECTOMY.	27
FIGURE 3-1. EXISTING SETUPS FOR ACTUATING THE PITCH/YAW AND IN SOME CASES INSERTION AXES.	33
FIGURE 3-2. COMBINED BEARING TO SUPPORT LINEAR AND ROTATIONAL MOTION OF THE TOOL SHAFT DEVELOPED BY THE BLEULER LAB.	35
FIGURE 3-3. CONCEPTS GENERATED IN BRAINSTORMING.	36
FIGURE 3-4. TOOL SIMULATION OPTIONS AND TRADEOFFS.	39
FIGURE 3-5. INITIAL BRAINSTORMING SKETCHES FOR THE END EFFECTOR DEVICE.	41
FIGURE 3-6. REFINED CONCEPTS. FROM LEFT TO RIGHT, LINEAR CAPSTAN, ARC-SECTION CABLE DRIVE, AND BALLSCREW.	42
FIGURE 3-7. ARC SECTION CABLE DRIVE SCHEMATIC.	44
FIGURE 3-8. HORIZONTAL EXCURSION CONSTRAINT FOR ARC SECTION CABLE DRIVE CONCEPT.	45
FIGURE 3-9. UPDATED CROSS-SECTION CONCEPT SKETCH OF THE SELECTED CAPSTAN-BASED DESIGN.	47
FIGURE 4-1. MOMENTS AND CONSTRAINTS ON THE GRIPPER CARTRIDGE.	50
FIGURE 4-2. TWO BRAINSTORMING IDEAS FOR THE GRIPPER MOTION CONSTRAINT.	51
FIGURE 4-3. FIRST EMBODIMENT OF GRIPPER MOTION GUIDE.	52
FIGURE 4-4. FINAL LINEAR GUIDE DESIGN FOR THE GRIPPER CARTRIDGE.	53
FIGURE 4-5. GRIPPER CAPSTAN DRIVE AXIS DETAILS.	54
FIGURE 4-6. OUTER SHAFT CLAMPING CONCEPT DEVELOPMENT.	55
FIGURE 4-7. INNER SHAFT CLAMP CONCEPTS.	56
FIGURE 4-8. CABLE FIXTURES FOR THE GRIPPER AXIS.	57
FIGURE 4-9. FINAL GRIPPER AXIS PROTOTYPE.	59
FIGURE 4-10. ROTATION AXIS DETAIL, AND AXIS SCHEMATIC.	60
FIGURE 4-11. PROGRESSION OF ROTARY CLAMP DESIGN.	61
FIGURE 4-12. ROTATION AXIS CABLE MANAGEMENT CONFIGURATION.	62
FIGURE 4-13. FINAL ROTARY AXIS PROTOTYPE.	63

FIGURE 4-14. THE FINAL EMBODIMENTS OF THE 1DOF (LEFT) AND 2DOF (RIGHT) DEVICES, INTEGRATED INTO THE PHANTOM GIMBAL.....	64
FIGURE 4-15. COMPLETE 5DOF HAPTIC DEVICE.	65
FIGURE 4-16. BOX SIMULATOR CONFIGURATION.....	66
FIGURE 4-17. SIMULAB TORSO (LEFT) AND LIMBS AND THINGS TORSO (RIGHT).....	67
FIGURE 4-18. COMPLETE SIMULATION SETUP.....	68
FIGURE 5-1. CONCEPT FOR INCREASED DEVICE ACCESSIBILITY.....	73
FIGURE 5-2. ORIGINAL AND REDESIGNED CABLE MANAGEMENT FOR THE ROTARY DRUM.....	74
FIGURE 6-1. SUGGESTED UTILITY TEST FOR SEVERAL TASKS.....	76

Chapter 1

Problem Identification & Background

1.1 The Problem

The motivation of this thesis was to develop an electro-mechanical force-feedback device to provide more realistic and complete sensations to a laparoscopic surgery simulator than currently available. This product development process presented two predominant challenges; the first was to understand relevant information about laparoscopic surgery and surgery simulation, and more specifically the critical requirements for this simulator. The second was to correctly interpret this information in the design and construction of a device to successfully fill this niche.

1.2 Background and Motivation

There are as many motivations for surgery simulation as there are academic and industrial efforts to develop dedicated machines for individual procedures of all kinds. These benefits extend to patients and apprentice surgeons alike, and as such providers of medical insurance stand to gain as well.

Most readily apparent is the interest in improving surgeon education. One advantage of surgical simulators is that they can be made available at any time to make frequent, self-paced practice possible for learning surgeons as well as experienced surgeons who may wish to practice a new surgery several times before performing it on a patient. This serves as a favorable contrast to the current “see one, do one, teach one” method which is restricted by the availability of operations which may be used as teaching cases, and which places a great deal of pressure on a new surgeon. Furthermore, simulators provide an opportunity for standardized, objective, and quantitative evaluation and feedback based on positions and forces which characterize the surgeons’ motions. Such information, including time on task, accuracy, peak force applied, tissue damage, and position error (Rosen et al, 1999), may be potentially used not only to give feedback to the learning surgeons about their performance and progress, but for testing, licensing, and re-validating surgeons. Simulators are also capable of presenting the trainee with multiple surgery scenarios, conditions, and pathologies that might be found in a real operating room (OR) with a real patient, but which are difficult to recreate with a cadaver, such as the onset of internal bleeding. Furthermore, they provide the opportunity to approach the same procedure multiple times in order to explore various surgical options. At the same time, simulation can decrease the time and cost associated with training for medical procedures, a matter of great importance to teaching hospitals in which resources must be distributed between patient care and education obligations (Caroll, 1994).

The real indicator, however, is the benefit to patients, and insurance providers are quick to help define these advantages. It is clear that better prepared surgeons can make a critical difference to the success of an operation, particularly in complicated procedures. Furthermore, the current practice of teaching through “on-the-job training ” (Rattner interview, 1999) can put patients at greater risk and result in unnecessary trauma to both trainee and patient. The use of simulator training prior to OR training may reduce the number of surgeries performed as “training cases” and allow students to initiate work on live patients when their skills are more developed.

1.3 Laparoscopy and Haptics

Laparoscopic surgery, considered here, amplifies some of these motivations since it is a particularly difficult procedure for the surgeon but provides many benefits to the patient. Laparoscopy is one of several types of minimally invasive surgery (MIS), which seek to minimize the size of incisions and exposure to infection by inserting tools into the body through either natural orifices (endoscopy) or tiny incisions with sealed ports (laparoscopy). One of these tools is generally a suitable camera (endoscope or laparoscope), and the surgeon performs the operation while watching this interior view on a monitor. In laparoscopic surgery, shown in Figure 1-1, one or more small incisions are made in the abdomen and a trocar, or plastic port, is inserted in each. Through the first, the laparoscope is passed to provide an image of the inside of the body on a monitor. Additional trocars are placed, and tools among a family of 33 cm long, 5-10mm diameter surgical instruments, are inserted as needed to perform the operation. In the course of the operation, the surgeon is frequently working with two toolhandles while looking away from the patient at a monitor.

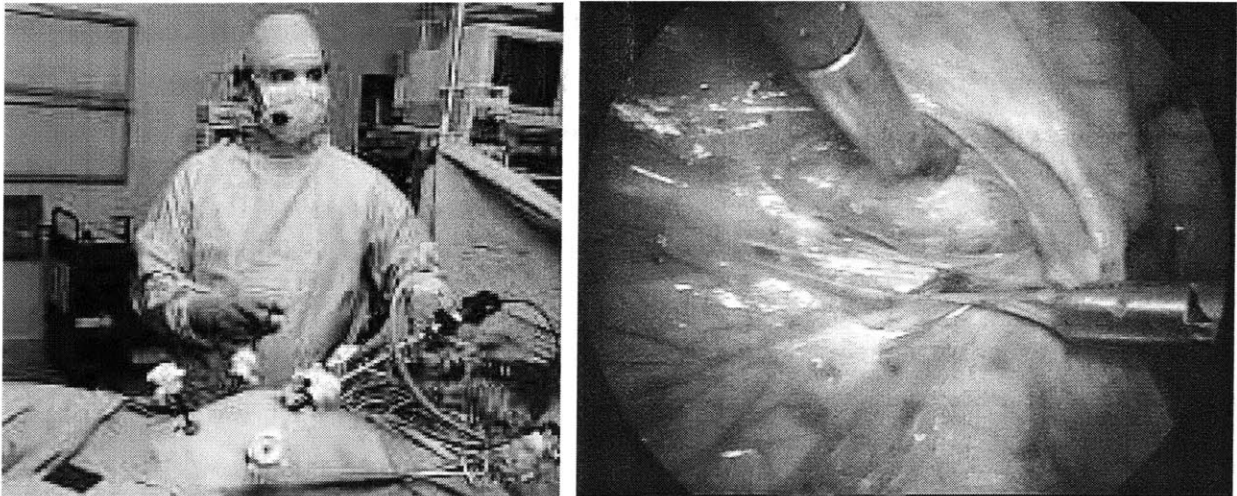


Figure 1-1. Laparoscopy being performed, and view through the laparoscope in hernia repair (Laparoscopy.com, 1999).

This configuration introduces several complications which require extraordinary hand-eye coordination. First, the surgeon is required to work in 3D while receiving only limited 2D

visual feedback on the monitor. Second, the surgeons work with long tools, for which the entry point into the body becomes a pivot. Consequently, motion of the surgeon's hands is reflected inside the body: when the hands move left, the tool moves right, and vice versa. Finally, maneuverability and access inside the body is significantly limited relative to surgery using traditional tools (Burdea, 1996), (Caroll, 1994).

However, the gain in terms of increased patient comfort and reduced risk, recovery time (patients often leave the same day), and scarring make laparoscopic procedures more than worthwhile. Increasing pressures to reduce hospital stays and related health care costs have promoted increasing use of minimally invasive procedures including laparoscopy. Under such motivation, engineering efforts have continued to produce new tools and procedures to further reduce patient trauma and risk. However, the added complexity and new procedures have stood as a barrier to the dissemination and acceptance of new technology in the medical community; a method of continuing education, which can be greatly facilitated through simulation, is pivotal to facilitating continued progress in medical care standards (Edmond et al, 1997).

As mentioned above, these new minimally invasive techniques place additional demands on surgeons' already impressive hand-eye coordination skills. Such skills are most rapidly acquired and internalized through hands-on "going through the motions", that is, practice makes perfect. As discussed earlier, simulators make it possible to practice more different procedures more frequently. However, an issue which was not certain, but very relevant to the current research, was the importance of haptic, or touch, information both in learning and performing laparoscopic tasks. The work of doctors at Penn State University College of Medicine revealed that haptic "learning" does occur as surgeons learn their trade. Experienced surgeons were much better at identifying shape and consistency of concealed objects using laparoscopic tools than medical students, and in some cases could identify grades of sandpaper as well as with an ungloved hand. (Gorman et al, 1999)

Given that haptic information is significant in surgery, it follows that providing accurate haptic sensations to surgeons as they practice is essential. There is potential for simulators to provide more accurate experiences to novices than currently available pre-OR training methods. Existing methods include the use of commercially available synthetic torso and organ models

intended for laparoscopic training, as well as cadaver or animal dissection. Synthetic and nonliving tissue can have dramatically different mechanical characteristics than live tissue, and live animal dissections are being phased out for ethical reasons. Finally, displaying tissue property data taken from live human tissue through a simulator can offer more realistic reaction forces to the student than working with these materials.

1.4 Components of a Simulator

The task of simulating both the visual and haptic sensations of surgery dictates a basic set of elements for any simulation system. Generally speaking, these components involve input/display devices and a computer which controls the simulation. Graphics display is provided by a computer monitor, and haptic display through an electro-mechanical force-feedback device, usually specialized for the type of surgery being simulated. The user interacts with the simulation through the haptic device, which measures the instrument position in the simulated workspace. The computer runs real-time software which uses this position (and its derivatives) as the input to tissue models based on simple mass-spring-damper relations, Finite Element methods, or other techniques to determine the geometric and dynamic behavior of the simulated tissue. These reactions are fed to software loops which continuously update the commands to both the graphical and haptic display devices.

1.5 Previous work

Extensive effort has gone into the development of each of the basic simulator system elements described above. As the present research was focused on the haptic display device, it is helpful to discuss significant work in this field.

Force-feedback devices as a field grew out of efforts initiated in the 1950's and 1960's to develop "master" manipulators for telerobotic applications. In these systems, a human interacts with the master device in order to control a second "slave" which performs a task. Telerobotics are generally implemented in environments unfavorable for human manipulation due to harmful

environmental factors or motion constraints, or for tasks that a robot can be specialized to perform. These input devices took on various forms: devices morphologically similar to the slave, joysticks, exoskeletons which encased the hand or more of the body, and more generalized kinematic configurations. (Madhani, 1998), (Burdea, 1996). The observation that human performance could be significantly improved by providing force feedback to the system user could be directly mapped into later efforts to develop masters to interact not with a distant real environment but with simulated or “virtual”. This led to the introduction of generalized force-feedback manipulators for virtual reality such as the PHANTOM haptic interface which would be the basis for a number of the systems described here (Massie, 1993).

The same trend can be seen for the field of medical robotics in particular. Force feedback telemanipulator systems have been introduced to permit motion scaling and filtering for microsurgery and to relieve the kinematic constraints on the surgeon in laparoscopy. Examples include an ophthalmic telerobotic system developed by Ian Hunter at MIT and a laparoscopic system designed by Akhil Madhani in the MIT Haptics Lab (Madhani, 1998). In such systems, forces reflected to the user can actually be amplified to effectively give the surgeon a “super-human” sense of touch and better control when working with delicate tissues. Some efforts to bring force-feedback into the surgery simulation arena have produced a variety of dedicated haptic devices while others, focusing on achieving sophisticated modeling and graphics, have taken the step of integrating one of these devices into their simulations. These configurations are predominantly 3-actuated-degree-of-freedom (pitch, yaw and insertion) devices which either actuate around the pivot point or can apply forces to the tool tip. Examples of the former include the commercially available Immersion Impulse Engine and the Force Feedback Device developed by Hauptabteilung Ingenieurtechnik. Devices which apply forces to the tool tip include a recent patent by Immersion Corporation (#5,828,197) (Martin, 1996) and the PHANTOM Haptic Interface made by Sensable technologies (Massie, 1993). A 2 DOF pitch-yaw device was developed by the University of Hull, and 6 DOF device using three parallel linkages and no trocar was implemented by the University of Tsukuba (Asano, 1997). Finally, the laboratory under Professor Bleuler at the Ecole Polytechnique developed a 4 DOF (pitch, yaw, insertion, and roll) device in which the first three axes are actuated similarly to the Immersion Impulse Engine. The Impulse Engine and the PHANTOM are the two predominant

devices which have been implemented by developers of full software simulations in order to provide force feedback for their systems. Thus, most simulations have feedback to the pitch, yaw, and insertion axes of motion, while the rotation of the tool and the opening and closing of the handle are passive. The device from the Ecole Polytechnique uses a crossed-roller configuration to introduce actuated tool rotation in parallel with the actuation of the insertion axis. Andrew Mor at Carnegie Mellon University made an interesting extension for the purposes of an arthroscopy simulator by providing feedback to the x-y positioning of the port using a pantograph planar linkage, thus actively simulating the reactions of the abdominal wall. These devices will be examined in light of specific system requirements in Chapter 3.

1.6 History of this Effort

The current effort was initiated by radiologist Dr. Steven Dawson with the Center For Innovation in Minimally Invasive Therapies (CIMIT) with the goal of taking laparoscopic simulation to a new level of “reality”. A team led by Homer Pien at the Draper Laboratory was enlisted to tackle the formidable software challenges posed by developing the computer model for both the graphics and haptics simulations. The MIT Haptics Laboratory was presented with two tasks that would be no less exciting from an electro-mechanical design standpoint. The first involved the development of a new force-feedback device to make it possible to display complete and high-fidelity touch in such a simulation while disguised in a realistic setting including surgical toolhandles and a human torso model. The second was to design one or more instruments for measuring tissue mechanical properties that could potentially be inserted through a trocar port to gather data from a living human. In this thesis, the author undertook the creation of the first device as a complete product design process from front-end task analysis through design, realization, and evaluation. Chapter 2 of this document details the sources and analysis of information used in design decision-making. These design strategy considerations are described in Chapter 3, while more detailed mechanical design and electronics/software integration is discussed in Chapter 4. Evaluation of, and recommendations for, the device based on both technical specifications and user expectations are presented in Chapter 5, and this assessment is the basis for conclusions and extensions discussed in Chapters 6.

Chapter 2

Problem Definition and Requirements Analysis

The most important and success-determining step in the development of a new product is the careful definition of the need or problem that the product serves; subsequent development must keep this need and associated requirements in constant sight. While absolute realism might ostensibly be assumed as the goal for a simulator, it is useful to precisely recall the function of the device in question: an *educational* laparoscopic surgery simulator. Requirements analysis for this project focused on understanding not only the elements of laparoscopic surgery but which of these elements are important for *learning* this complicated art. It was in fact possible to find a single underlying design problem to which all future design decisions could be submitted. While it was clear that ultimate realism would be an exciting achievement, and that high-fidelity haptics could be pivotal in teaching the nuances of procedures and distinguishing between healthy and unhealthy tissue, the single most important element of the learning surgeon's education is the development of a "systematic approach to problem solving" (Rattner interview, 1999).

2.1 Requirements Data Acquisition

Information about the qualitative and quantitative design requirements for the simulator hardware was investigated through several major sources: interviews, OR observations and documented task analysis.

2.1.1 Surgeon Input

The first resource for requirements information was expert testimony. Interviews were conducted with David Rattner, a pioneering laparoscopic surgeon at the Massachusetts General Hospital, and Steven Dawson, an interventional radiologist, also at MGH, who was the drive behind the development of this simulator. The questionnaire used as the framework for these interviews can be found in Appendix A1. It was designed with a common customer interview rule of thumb in mind: people are much better at recognizing features they do not want than at visualizing their ideal product. In addition to background questions about current training methods and other simulators they may have used, the doctors were asked directed design-driven questions which were structured in three different ways. The first set were yes/no questions regarding the importance of a number of technical parameters (use issues, workspace, configuration, feedback modes, etc.) to the effectiveness of a laparoscopic trainer. The second presented pairs of options for simulator configuration and required the interviewee to indicate which would be preferable. The final set listed major areas of design latitude and gave them the opportunity to suggest a “wish list” for each.

While detailed comments and requests will be categorized in the following section, it is worthwhile to make several general observations. The first of these is that the “important or not” and “choose one” questions type generally elicited a confident, detailed, and articulate response, while the doctors found it more difficult to describe their “wish list” even given specific topics. Second, haptic sensations appear to be very difficult to describe in an abstract, removed sense and are closely coupled to the context in which they are experienced. For example, there were a number of questions related to workspace and forces that Dr. Rattner, despite his vast experience, was better able to answer in the operating room with the tools in hand than in the preceding office interview. Similarly, while Dr. Dawson had drawn the conclusion from testing non-surgical PHANTOM demonstrations that this device was inappropriate for use in surgical simulations, when presented the same device with a laparoscopic tool attached and a more organ-like demonstration he was better able to assess the PHANTOM’s potential as the fundamental actuator for a simulator.

2.1.2 Operating Room Observations

The second major activity in data collection was observation of Dr. Rattner performing laparoscopic hernia repair and gallbladder removal (laparoscopic cholecystectomy or “lap choly”) in the operating room. These observations were performed twice in the course of the project: first at the start of the work and again after the device concept had been chosen but before detailed design decisions had been made. Both visits provided the opportunity to observe “training cases” in which an apprentice surgeon was present. In these cases Dr. Rattner was particularly careful in his narration of the procedure, and the student would perform segments of the operation under his guidance. The first visit was an instrumental in gaining familiarity with laparoscopy and associated terminology, instruments, and procedures, as well as in assessing preliminary parameters such as workspace, frequency of tool and port changes, and so on. These insights were invaluable during the generation and selection of design concepts. As the issues to be addressed in detailed design became clearly defined, it was possible to develop a directed task analysis study to address specific questions about design parameters. The operation observation form created for this purpose can be found in Appendix A2. The first part of this form was dedicated to recording the time spent by the surgeon manipulating tissues in specific ways which would place requirements on the simulator: grasping, cutting, and twisting. The second part prompted for observations regarding tool insertion points, removals, proximity and ranges of motion. The final element of the observation was the recording of the proceedings of the operation, including tools used, tasks done, and any comments made, particularly to the student surgeon.

2.1.3 Documented Task Analyses

Verbal and pictorial description of laparoscopic procedures can be found in various surgery texts, and excellent photograph and video coverage of many procedures is available online at www.laparoscopy.com. Cao, et al. (1996) breaks the procedures of cholecystectomy, inguinal hernia repair, and fundoplication (placing wrap around esophagus) down into a hierarchical set of steps and tasks, and measures the time surgeons spend in each over the course of an operation. A study carried out by Rosen, et al (1999) also presented a timed state analysis of the procedures of cholecystectomy and fundoplication, and further instrumented a laparoscopic grasper with

strain gauges to record surgeons' force profiles during actual cholecystectomy and fundoplication. Finally, Gupta, et al (1997) recorded forces applied to the laparoscopic handle during manipulation of various inanimate objects.

2.2 Requirements Analysis

Not surprisingly, a large amount of relevant data was collected from these three sources. The integration, organization, interpretation, and quantification of this information, as well as its application in concept selection, were carried out in several design matrices which proved to be powerful tools for maintaining the focus and integrity of the design process. These matrices were based on those suggested by Ulrich and Eppinger in their book *Product Design and Development* (1995) which is widely used as a product development text and guideline. However, the spreadsheets used here were somewhat customized, reflecting only the front-end design stages relevant to the current project, and frequently combining the operations of several suggested matrices into one matrix. These spreadsheets have been compiled in Appendix B in order to provide a concise and coherent summary of the decision-making process which led to the final design.

The first of these, entitled Needs to Metrics and found in Appendix B1, served as a forum to translate comments and observations into metrics relevant to design. Each was stated as a concise need and placed listed by source in the rows. Design metrics were added in the columns as new ones were suggested by reading through the needs. Darkened cells represent each of these correlations. Where possible, a numerical value was introduced to quantify this relationship in the spreadsheet Specification Definition found in Appendix B2.

In order to meaningfully process this wealth of information, each metric was associated with one of three major kinds of design parameters that would be addressed. These were workspace and kinematics, performance and actuation, and features and configuration.

2.2.1 Workspace and Kinematic Requirements

The first set of design considerations addressed the demands of replicating the workspace and axes of motion present in laparoscopic surgery, and would significantly impact the kinematic structure and axes designs chosen for the device.

The permissible size “box” for the device was governed by the desire to maintain the visual integrity of the simulation environment as well as to keep the setup relatively portable. Preferably, one or two such devices would fit beneath a human torso model, or alternately one with drapes lying across a width similar to that of a hospital bed, 3 feet across. The maximum total footprint for this machinery was then 1.5’x2’. The working volume of a surgical procedure varies somewhat with the type of surgery being performed, as does the location of this volume within the abdomen. The volume associated with the hernia repair was roughly 6”x3”x2” near the abdominal wall, whereas that used in the cholecystectomy was smaller, roughly 4”x2”x2”, and deeper within. Each device was to be responsible for the workspace of only one of two tools generally held by the surgeon. If the device was to remain in one position, its workspace would be required to be large enough to reach the areas of all procedures to be simulated; if the device could be moved between simulations of different procedures, only the largest individual operation volume would need to be considered. Both doctors indicated that it would be appropriate for a given simulator setup to be dedicated to a set of procedures with similar workspace constraints; as such, the minimum working volume was taken to be 6”x6”x6”. A subsequent specification was that hardware could not extend above the simulated interaction point by more than about 2”. This figure was achieved by considering the length of trocar typically inside the abdomen, about 3”, and assuming that while some may be cut back in order to allow the interaction point to approach the end of the *simulated* trocar, around 1” should be left inside to secure the trocar.

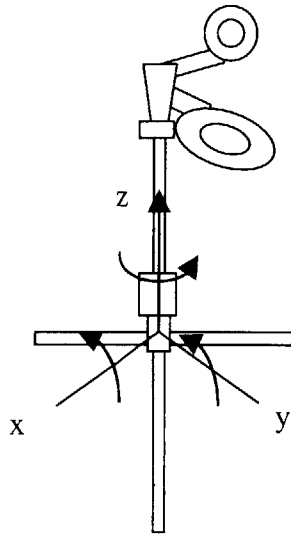


Figure 2-1. Axes of motion in laparoscopic surgery

The fact that the primary motions involved in minimally invasive surgery occur through a point constrained in the plane of the entrance to the body (a 2-dimensional constraint) reduces the degrees of freedom of the system to 4 from the 6 of an unconstrained spatial system. The remaining degrees of freedom for the laparoscopy tool as a whole include pitch and yaw rotations about the x and y axes, roll rotations about the z or toolshaft axis, and translation along the z axis, as defined in Figure 2-1.

In addition, many tools have an end effector which is controlled by a squeezing/opening motion of the tool handle. The details of a scissors tool are shown in Figure 2-2 below.

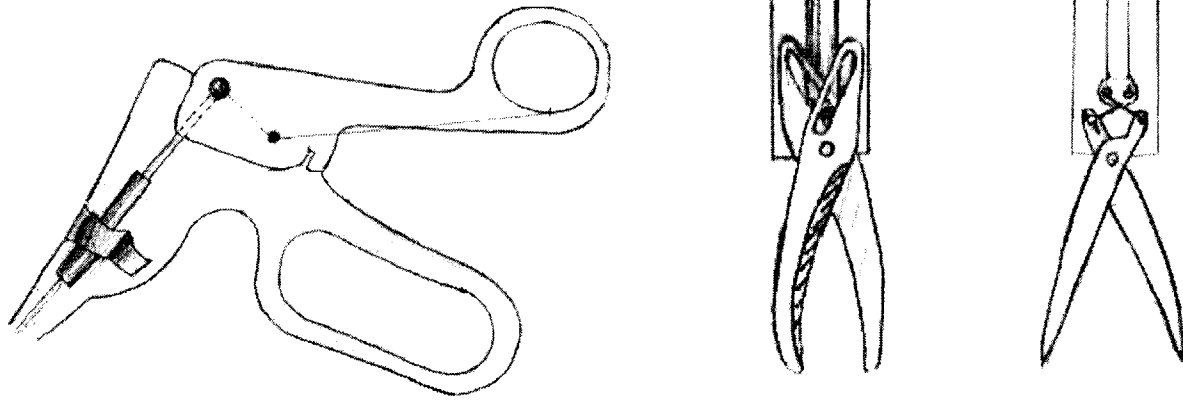


Figure 2-2. Laparoscopic scissors construction. The handle is at left, and end effector mechanisms from an AutoSuture tool and an Ethicon tool at right.

In general, the handle incorporates a lever which amplifies the force applied by the human hand by a factor of around 4 and transmits this force to an inner shaft which runs the length of the tool. The motion of this inner shaft relative to the outer shaft is used to actuate any one of a family of lever-based tools, but most frequently graspers and scissors. The travel of the inner shaft is dependent on the individual lever design for the brand of tool: for AutoSuture tools this was 6mm, whereas for Johnson & Johnson Ethicon tools it was only 2mm. The finger loops of the handle are actually decoupled from the twisting of the shaft, which can be controlled by placing the index finger on a wheel at the top of the shaft.

In total, there are five degrees of freedom to a laparoscopic tool. The comments from the doctors, as well as observations in the operating room, made it clear that the insertion force, pitch and yaw torques, and the gripper force are all significant in surgery and training. Active twisting along the tool axis was not apparent in the two procedures observed in the OR, but the doctors provided assurance that such torques are exerted in other procedures.

The next set of parameters to consider were the ranges of motion of each of the degrees of freedom, which can be deduced in part from the size and location of the work volume. Again, these varied with the procedure performed. Pitch and yaw motions reached a maximum of 60 degrees from vertical during cholecystectomy and as much as 80 or more degrees during the exploratory phases of the hernia repair. The tool insertion setpoint for a surgery varied between

near the surface (the tool frequently retracted into the trocar) for hernia repair to as deep as 6 inches during cholecystectomy; deviation from this point was around 3 inches in both cases. Finally, the maximum displacement for the roll axis, that is the extent to which the surgeon twisted the tool, was less than 90 degrees to either side of the rest position, or a total of 180 degrees of motion. It was verbally verified that there is rarely cause to rotate the tool more than this, and it is never rotated greater than 360 degrees.

The proximity with which two tools may approach, or appear to approach, one another placed much more stringent constraints on the volume of the device. Dr. Rattner emphasized to his pupil the need to use the tools “like chopsticks and spread” tissue during exploration in the hernia repair operation. In this process, the tools are crossed and come within 1-2 centimeters of one another. However, tool proximity was not as marked in the cholecystectomy.

2.2.2 Transmission and Performance Requirements

The second major set of considerations for which it was desired to gather information dealt with decisions that would have to be made regarding components (motors, encoders) and properties (backlash, backdriving force) of the servo loop.

2.2.2.1 Maximum Forces and Torques

The first of these were the maximum forces and torques applied to each axis of motion, and the duty cycle with which these were applied. As a first reference, the two aforementioned publications were consulted. Rosen, et al (1999) measured X-Y (plane perpendicular to the tool) forces and torques, Z (insertion) force, and the force along the inner gripper-actuated shaft during the grasping-pulling state of an actual laparoscopic procedure. Because this state placed significant demands only on the insertion and gripping axes, only those measurements were considered as envelope requirements. Gupta, et al (1997) made measurements of force applied to handle of the gripper during contact with materials such as cotton and PVC gel; although neither a specific lever ratio nor distance of the measurement from the fulcrum were given, this value could be compared to the inner shaft force by multiplying by a “worst case” ratio of 4:1. The two studies were fairly consistent, and suggested a maximum gripper shaft force of 17N (Rosen

et al, 1999), (Gupta et al, 1997). In order to achieve an idea of what this force would feel like to the surgeon, and as a rough check of these values, an empirical test was performed by suspending the corresponding mass from the inner gripper shaft while clamping the outer shaft to a table as shown in Figure 2-3.

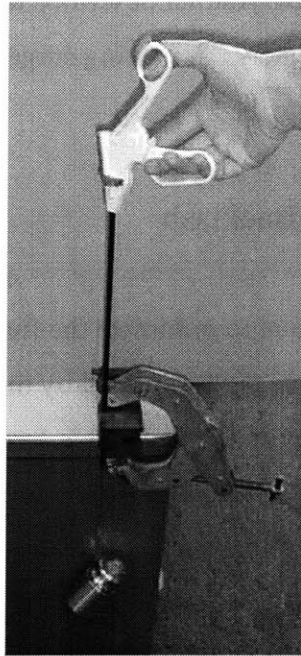


Figure 2-3. Empirical test performed to examine force on gripper-actuator shaft.

A significant amount of force was required to lift the weight by squeezing the handle; this appeared to be an appropriate upper bound (before safety factors) for a design force.

The insertion force documented by the University of Washington study was 17N. In order to verify this value as well as to better understand appropriate pitch/yaw torques, a PHANTOM was placed inside a box, and a laparoscopic tool inserted through a trocar in the lid and attached to the end of the PHANTOM gimbal. This setup was able to apply an effective insertion force and pitch-yaw torques to the tool handle. A simple demonstration simulation consisting of a large pink sphere of roughly “organic” stiffness (0.1 N/mm) was presented to Dr. Dawson. He was satisfied that the forces and torques which he experienced were as large or larger than those encountered during surgery. The PHANTOM can exert 8.5N in each translational direction, and the tool mechanical advantage in the pitch/yaw lever across the fulcrum reached a maximum of about 4:1.

Since the surgeon resists twist moments by placing a finger on the twist wheel, a maximum force of 6N was empirically chosen by the author, and would be applied at a radius of approximately 1.3cm, the radius of the wheel. Accordingly, a torque of 0.08 Nm was specified.

When questioned in the OR, Dr. Rattner described the forces in general as “very light” and could be seen working very delicately. A visiting surgeon from the Philippines confirmed this, saying that there is “no real resistance”.

2.2.2.2 Backdrive Friction and Backlash

For haptic devices in general, it is a goal to minimize the force required to backdrive the system resulting from friction and inertia in the device, scaled by the transmission ratio squared when reflected to the user, and in the transmission itself. This force will be felt in addition to the simulated forces displayed, and will be present when the user is moving in simulated “free space”. For generalized haptic devices like the PHANTOM, it is desired make backdrive friction as close to zero as possible for all axes. Because the present system was to work in conjunction with an actual, non-ideal, laparoscopy tool, this requirement was examined in more detail. In actual surgery, the trocar is able to pitch and yaw freely within the constraints of the abdominal wall. A fair amount of friction is associated with the insertion axis, however, due to the sliding of the tool shaft against the seal in the trocar. Since a realistic setup was required, it was assumed that this friction would be present as a consequence of using an actual trocar and tool, and that additional friction should be avoided. As regards the gripper axis, detectable friction is contributed by the linkage which drives the end effector in either grippers or scissors, and the sliding of the curved surgical scissors blades on one another made an additional significant contribution. These observations were quantified by clamping the stationary finger loop to a table and pulling on the mobile one with a spring scale with just enough force to keep the handle moving at a constant rate, as shown in Figure 2.4.

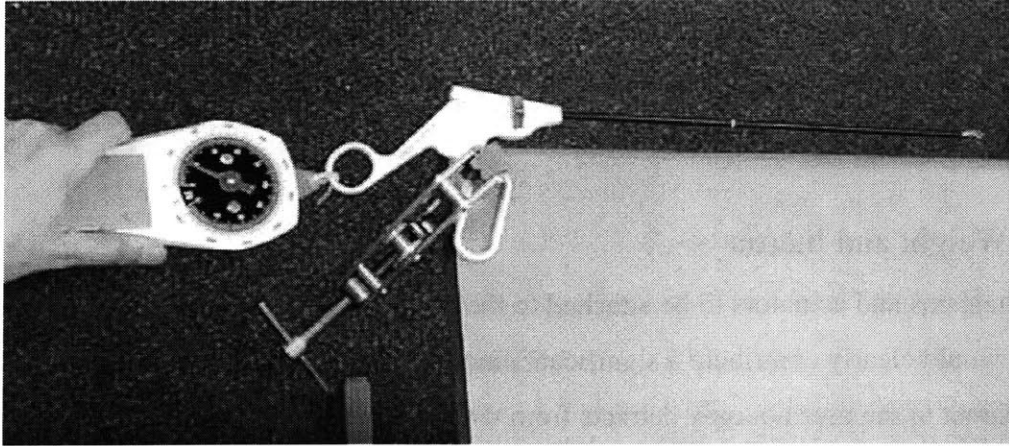


Figure 2-4. Test performed to rate friction experienced at the handle in tools bearing various end effectors.

It was found that scissors, which required 2.5 N, were characterized by dramatically greater friction than graspers which required 0.4 N, and that removing the end effector and linkage completely resulted in markedly lower friction than either tool, requiring less than 0.001N. As a result, it was concluded that an actuation scheme incorporating the tools as is should add no additional friction to this axis, but one which drove the inner shaft directly could have as much friction as the lowest-friction tool, graspers. The rotational axis of the tool carried an amount of friction as well, but this was part of the handle, which was assumed to be part of the final simulator. Consequently, friction in this axis was also to be minimized unless the handle would be altered by some method to compensate.

Similarly, in generalized haptic devices, it is desired for backlash in the system, as perceived by both the servo loop and by the user, to be zero. The latter constraint, that backlash between the position measured by the system sensors and the actuators be zero, was very much in effect for this project as well. Backlash at this point can cause instability in the servo loop because of the force nonlinearity caused by the delay in actuator engagement and because of the discrepancy between measured and actual position. The implications of this constraint were that backlash in the transmission between the motor and the measured position had to be minimal. However, a large amount of backlash is present in the lever and rotary dial mechanisms in the handle of the laparoscopic tools. There was 0.4 mm play in the gripper shaft travel, and 28

degrees of play was measured in the rotation dial. This backlash is apparent only to the user; it could and in fact should be left as is, since the surgeon's own internal "servo system" must be trained to compensate for this backlash .

2.2.2.3 Weight and Inertia

The mechanisms and actuators to be attached to the laparoscopic tool in order to provide force feedback would clearly contribute a significant amount of weight and inertia to the tool. Having these apparent to the user not only detracts from the realism of the simulation, but can contribute to muscle fatigue, particularly if the user must apply a constant force to support the weight of the device. If the simulator did add to the weight of the tool, then gravity compensation, or the application of a constant force equal to the additional weight in the vertical direction, could be implemented in software, or the weight could somehow be physically counterbalanced. Neither solution was ideal; gravity compensation requires constant effort from one or more actuators, and may require that this actuator be more powerful than otherwise necessary. Counterbalancing the weight contributes to the inertia of the system. Neither method is able to compensate for the apparent increase in inertia. Thus, it was a goal to minimize the weight of the device. This goal was generally consistent with a second requirement, that the inertia of the elements in each individual transmission be minimized in order to prevent excessive reflected inertia in any actuated axis.

2.2.3 Features and Configuration Requirements

The final set of requirements dealt with overall configuration options and alternatives for features and methods of use. As such, the source for this information was almost exclusively the opinions of the doctors.

The first group of these specifications pertained to the details of application of force-feedback in the simulator. Foremost was the question of how many of the 5 degrees of freedom in laparoscopy described earlier were to be actuated. The need for pitch/yaw and insertion feedback was immediately clear. As concerned the gripper axis, Dr. Dawson emphasized the need to be able to "feel increasing thickness", and it was observed in the OR that graspers were

used not only to squeeze but also to spread and separate tissue, referred to as blunt dissection, as demonstrated in the cholecystectomy pictured in Figure 2.5.

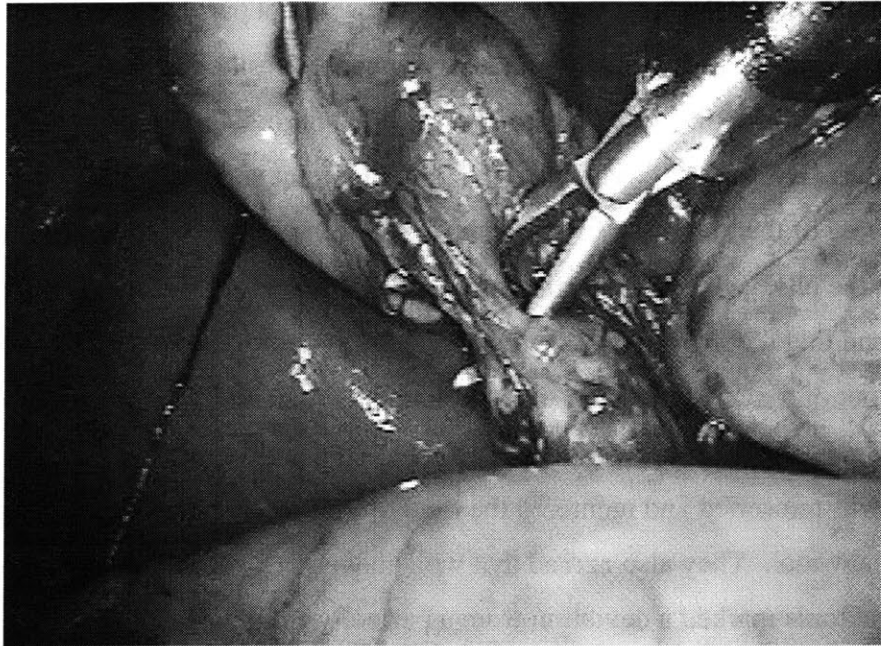


Figure 2-5. The use of grippers for blunt dissection in cholecystectomy (Laparoscopy.com).

Simulating such experiences clearly called for actively driven feedback to the gripper axis, since they could not be supplied by a mechanical spring or damper and these would in any case need to be coupled to a clutch of some sort to simulate empty space. Furthermore, both doctors stated that although less predominant, sensation from the rotation axis was nonetheless important in surgery and should be actively driven if the simulation was to be complete.

A subsequent issue was that of which laparoscopic tools were to be simulated. Dr. Dawson suggested three which would require gripper feedback, locking and non-locking graspers and scissors, as well as a scalpel. Furthermore, he specified that the difference in internal friction between the grasper tool and the scissors should be maintained. Another issue of concern regarded whether rigid objects, such as in the occurrence of the tools coming into contact with one another or with bone, would need to be simulated. Both doctors commented that these interactions do not occur in normal laparoscopy, but that it was for this very reason that they *should* be possible at least for pitch/yaw and insertion; the student surgeon should have immediate haptic feedback to indicate that such an error was made.

The next set of concerns regarded interface issues, and the paradigm for the use of the simulator. From the doctors and the surgery manuals it was understood that while port locations differ between different types of surgery, they are consistent within a particular procedure. Dr. Dawson specified that these locations should be changeable easily between simulations. With regard to the need to have the tool completely removable during simulated tool changes within a surgical procedure, Dr. Rattner commented that the important component that must be learned is the *re-registration* of the tool position after it has left the viewing area of the laparoscope. He confirmed that the physical act of inserting and removing the tool from the trocar was insignificant, and that requiring the student using the simulator to extract the tool to the edge of the trocar and out of the “field of view” before commanding a tool change would be appropriate. Both doctors agreed that a voice activated software tool change would be optimal at this point; when the tool was reinserted and reentered the field of view it would appear on the simulation display as the new tool. They also agreed that while having a single toolhandle instead of an array of surgical tools marked a deviation from a perfectly simulated OR, it would streamline the use of the simulator and reduce the number of components that might become broken or lost. Since the initial setup and possibly frequent movement of the tool between ports would likely be performed in a non-engineering setting, it was essential that this coupling be simple and robust and that it require at most one, preferably standard, tool. Additionally, the setup was to be as portable as possible.

A somewhat more subjective, but no less important, concern was the external appearance of the simulation. While Dr. Dawson envisioned a setup that could fit on one of an array of tabletops in a classroom as well as in a simulated OR setting, the station itself would be expected to maintain the visual integrity of the surgical environment. The exterior interface was to be a real laparoscopic tool handle emerging from a real trocar inserted in a lifelike human torso model, possibly including the drapes and covers used in the OR. Consequently, all hardware would have to reside beneath the torso model, and no visible instrumentation could be placed on the tool handle. The question was raised as to whether it would be appropriate to allow wires to emerge from the electrocautery port on the handle (to which in reality wires are attached during cautery); to this Dr. Rattner answered that the process of attaching and detaching the cautery wires, and learning to remember to do so, were essential, so this was not a possibility. Finally,

although Dr. Rattner commented that compliance of the abdominal wall, in which the trocar pivots, was not important, Dr. Dawson specified that if possible a model with a compliant torso be used to enhance the reality of the setup.

The final and very important insight that was achieved was to ascertain the overall development paradigm for the project. Dr. Dawson emphasized that while unprecedented realism and training potential were the goals set for the new simulator, wherever possible the most robust, simple, or inexpensive designs should be favored. To this end, he was not opposed to the possibility of using commercially available devices for one or more of the axes (for example using the Immersion Impulse Engine or the PHANTOM from Sensable Devices to provide pitch/yaw and insertion) if these devices satisfactorily met the aforementioned criteria.

2.3 Benchmarking

This defined understanding of the simulator requirements made it possible to conduct a more informative and objective comparison of both existing devices and new concepts in terms of their ability to meet each need. A full benchmarking comparison of several of the systems described in Chapter 1 was performed concurrently with concept selection for the first three axes (pitch, yaw, and insertion) and is presented in the following chapter. It was possible to obtain a small amount of feedback from doctors who had used simulators, but as mentioned earlier it could be difficult to elicit specific concerns. At the 1999 Medicine Meets Virtual Reality conference, many surgeons attending a human factors session voiced the concern that current “box trainers”, and particularly the Immersion device, were “too deep”; this referred to a deficiency in the insertion range of motion, and specifically to the constraint on how far the tool handle could be removed from the pivot. The other first-hand comments obtained were from Dr. Rattner, on his past experiences with simulators:

Q: Have you seen or used other simulators?

A: Yes-an Ethicon device, the “Preceptor”.

Q. Was it good or bad, and why?

A: It was lousy.

Q. Why?

A. Not realistic.

Q. Was it the haptics or the graphics?

A. Both -- the tactile feedback was terrible.

Q. Why?

A. The organs just didn't feel realistic, like real tissue.

Q. Why? Did they feel rubbery, or...?

A. Yes, rubbery, just different.

Again, a certain amount of interpretation and problem-isolation was in order. It is suspected that either part or all of Dr. Rattner's disappointment was the result of the software models used to calculate both the graphics and haptic reactions, and not necessarily in the mechanical attributes of the system hardware. Still, this gave an indication of the kind of feedback that could be gained through a direct interview but after the encounter with the device. Since more detailed comments could be expected in context, it would be useful to be present while the surgeons used other systems.

In addition, it was possible to speak with an engineer at Immersion Corp. regarding feedback received about the Impulse Engine. The unfilled needs he cited were feeling stiff objects such as bone or other tools, receiving feedback to the rotary and gripper axes, and getting two such tools close to one another.

Chapter 3

Concept Ideation and Selection

As mentioned earlier, the most practical design solution which met all design criteria was sought, and either developing a complete 5 DOF device from the ground up, or using one of the aforementioned devices (as available) as a platform were considered plausible options. As such, all possible configurations for the axes were considered and weighed by the merit of the design independently of whether they were represented by a previous device. Early in the brainstorming process it became apparent that certain axes tended to require design in parallel, while others stood alone with respect to design considerations. Pitch and yaw, and in some cases insertion, were generally coupled and considered together. These also largely governed the overall configuration of the device. The mechanisms for actuating the roll and gripper axes were for the most part each considered independently, but packaged together as the second major stage in the device.

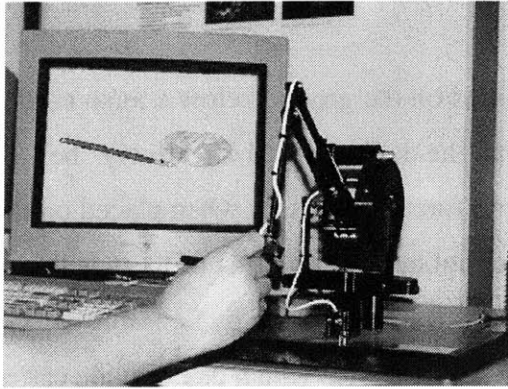
The characteristics of a concept generation, or “brainstorming” session which are most likely to lead to a successful product are to take an open-minded approach, considering any mechanisms at one’s disposal. It is best to defer judgement on these, and to allow one idea to grow into another. The brainstorming sessions which produced many designs, some of which are described here, followed such a course. Two stages of concept selection followed; in the first cut, obviously impractical solutions were dismissed without further analysis, which was reserved for differentiating between plausible designs in the second selection.

3.1 Pitch, Yaw and Insertion

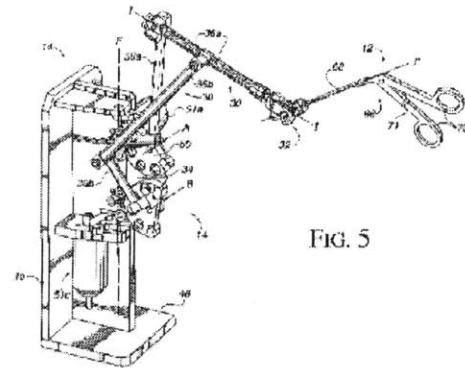
As discussed earlier, a fair number of devices exist which provide either the first two (pitch and yaw) or three (pitch, yaw, and insertion) actuated degrees of freedom. As such, many different designs had been pursued by earlier efforts. These designs as well as several original ones are presented and evaluated here.

3.1.1 Existing Devices and New Concept Generation

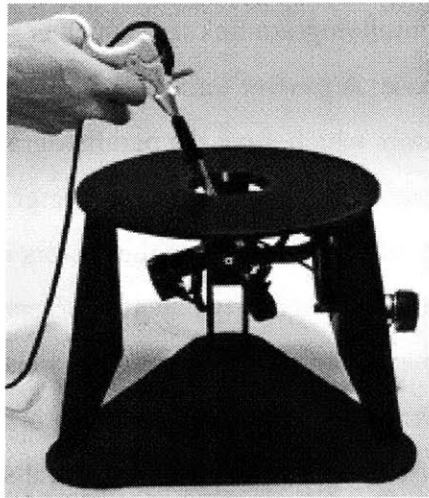
It is appropriate to first display the existing devices, since this background research was the inspiration for further brainstorming. These are displayed in Figure 3-1.



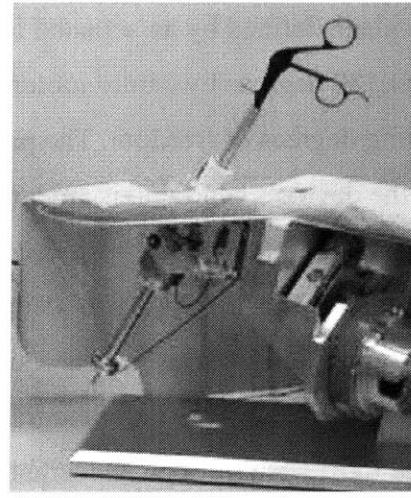
(1) (Krumm, 1999)



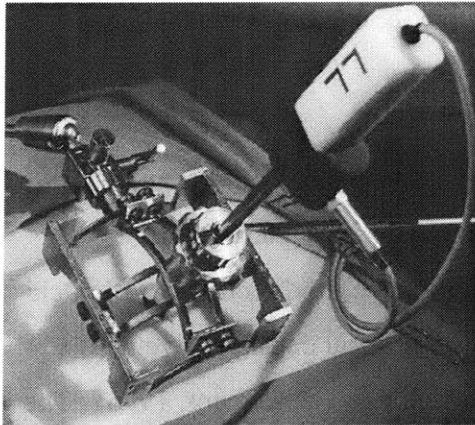
(2) (Martin, 1996)



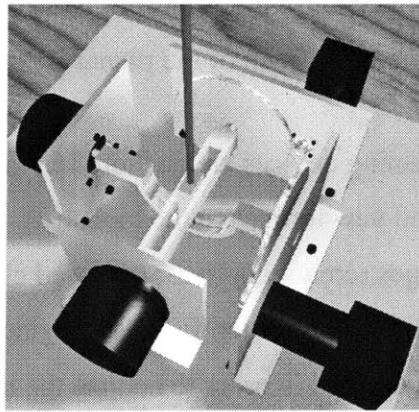
(3) (Immersion Corp., 1999)



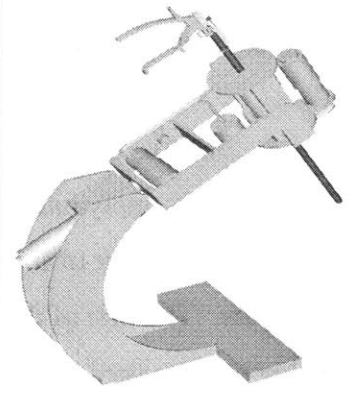
(4) (Vollenweider, 1999)



(5) (Krumm, 1999)



(6) (U. Hull, 1999)



(7) (Krumm, 1999)

Figure 3-1. Existing setups for actuating the pitch/yaw and in some cases insertion axes. (1) PHANTOM by Sensable Devices. (2) Newly patented device by Immersion Corp. (3) Immersion Impulse Engine (4) Bleuler Lab (Vollenweider) device. (5) Hauptabteilung Ingenieurtechnik (HIT) Force Feedback Device (6) Karlsruhe Input Device. (7) U. Hull VEGA Haptic Feedback Manipulator.

The first two devices shown could be stationed on the ground below a torso model and connected to the tip of a laparoscopic tool, such that the device would effectively “be” the tissue. Both would provide pitch, yaw, and insertion forces to the tool when placed on the opposite side of the abdominal pivot point from the tool handle. The first of these is the cable-driven PHANTOM designed by Thomas Massie at MIT and produced by Sensable Technologies. This is an “all-purpose” open-chain haptic device which can provide cartesian forces to simulate point contact with virtual objects. Its roughly hemispherical workspace consists of a plane defined by an actuated four-bar parallelogram linkage, which is rotated through about 180 degrees by a third motor on the base. A passive terminal gimbal provides the three remaining degrees of freedom. The pair of motors which drive the parallelogram linkage from across the device’s central axis are positioned such that they balance the weight of the linkage and gimbal at the starting position, allowing the “rest” forces on the motors to be zero near this position. (Massie, 1993) The second such device is a newly patented invention by Immersion Corporation. While bearing a similar kinematic configuration as the PHANTOM, the four-bar planar linkage is not a parallelogram. Furthermore, all of its driving motors are placed on the base of the device through an insight which uses idlers to establish a vertical section of cable between capstan and drum which is colinear with the central rotation axis of the device. (Martin et al, 1996) While this configuration is not balanced like the PHANTOM, it should dramatically decrease the inertia of each of the planar linkage axes.

All five of the remaining devices are anchored in the plane of the fulcrum from which they directly apply pitch and yaw torques to the tool shaft. The first two devices use a perpendicular pair of linkages (creating a five-bar closed chain linkage) to directly control pitch and yaw. The first of these, the Immersion Impulse Engine, uses a linear capstan drive with a cable running the length of the tool in order to actuate the insertion axis (Rosenberg, 1996). The Bleuler Lab at the Ecole Polytechnique developed a similar device, and have designed a crossed-roller bearing structure which supports both the linear and rotational of motion using pairs of opposing rollers angled at +/- 45 degrees from the tool shaft. This configuration is shown in Figure 3-2.

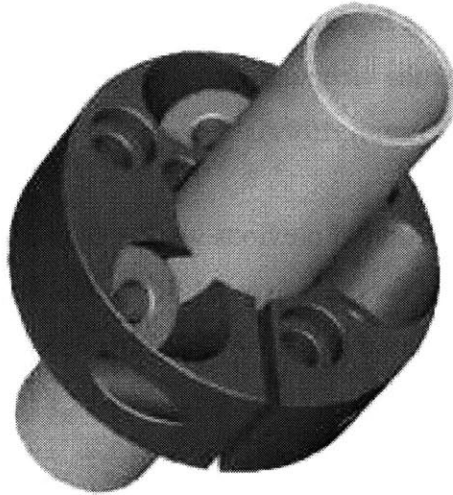


Figure 3-2. Combined bearing to support linear and rotational motion of the tool shaft developed by the Bleuler Lab (Vollenweider, 1999).

Limited information was available about this device, but it was understood that when the tool is moved in pure insertion the rollers turn in the same direction, and when the motion is pure rotation, the rollers turn opposite one another. These axes are apparently not actuated, but it is conceivable to design active degrees of freedom on this principle (Vollenweider, 1999).

The next pair of devices are again closed-chain linkages which make use of two slotted links to support the pitch and yaw axes. The first of these, developed by Forschungszentrum Karlsruhe (FZ Karlsruhe) is actually not a force-feedback device but rather a passive position input device bearing a kinematic configuration similar to that found in some joysticks; again, it is plausible to consider an actuated version of this device. In this design, the tool passes through the crossing point of the two curved, slotted links, thus dictating the position of the tool within a semispherical workspace around the pivot at the intersection of these axes (Krumm, 1999). The second device was made by the University of Hull VEGA group and uses a slightly different method: the center of curvature of one curved link is coincident with the center of a straight link to which the pivot of the tool is affixed. Here, sliding contact is made with only the curved link. This device does not include an insertion degree of freedom (University of Hull, 1999).

Finally, the Hauptabteilung Ingenieurtechnik (HIT) device (5) could be found only as a rendered model on the FZ Karlsruhe webpage, but from this rendition can be described as an open-chain serial manipulator (Krumm, 1999).

Taken together, this collection of previous work constituted a very comprehensive examination of the design options for these axes. Still, a couple of concepts were generated, including one inspired by the structure of the FZ Karlsruhe device and a differential-based device are shown in Figure 3-3.

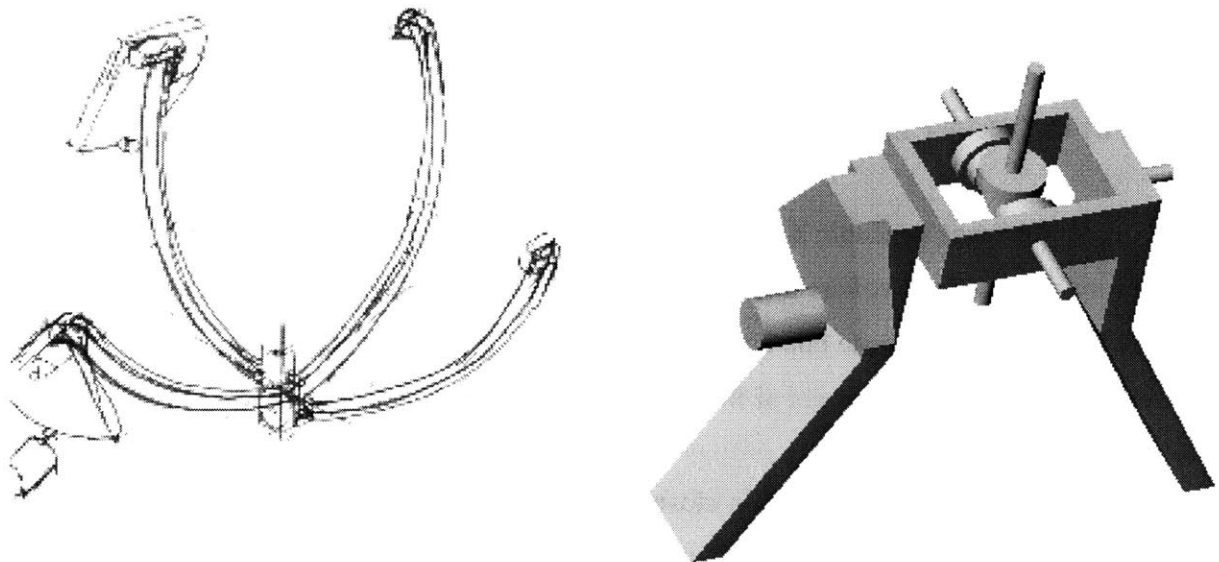


Figure 3-3. Concepts generated in brainstorming.

The first of these was essentially an inverted version of the FZ Karlsruhe input device in which the slotted links were replaced by rails on which rolling element bearings could be mounted. In the second design, a first motor would pitch a second stage which supported a cable differential capable of providing yaw and rotation feedback in parallel. Actuation for the linear insertion motion could be added to either of these using a linear capstan or crossed rollers.

3.1.2 Concept Comparison and Selection

The criteria discussed in Chapter 2 were now put to use in evaluating these possibilities. First, the design on which the U. Hull device was based, and the concept it inspired during brainstorming, were eliminated due to friction, manufacturing, and robustness concerns associated with the two curved, slotted links. The remaining concepts were compared in the Pugh-type spreadsheet Benchmarking and Platform Concept Selection, which can be found in Appendix B3. The PHANTOM was used as a baseline concept, to which the performance of all others in each requirement was compared. The most distinguishing of these comparisons will be discussed here. First, a tradeoff was offered between tip- and pivot-actuated devices on kinematic issues: tip-actuated devices kept all hardware well below the pivot point, making it possible to bring trocars closer together, offering better compatibility with torso models, and allowing a larger range of motion for the pitch/yaw and insertion axes. However, because the pivot-actuating devices kept the tool tip completely free of additional hardware, it would theoretically be possible for the tips of two instruments to interact much more closely, particularly for the very compact cable differential design, but also for designs such as the Immersion and Bleuler devices in which the bulk of the hardware lay to one side.

Furthermore, an effort was made in the design of several of these devices to ground as many motors as possible, since those which traveled with one or more axes contributed to the perceptible inertia of these axes. As a beneficial corollary, actuators fixed to ground could be chosen to be as powerful as needed, making higher maximum forces and torques possible. In this sense the design of the Immersion patent, with grounded pitch, yaw, and insertion actuators was most favorable; the Impulse Engine, Bleuler Lab and U. Hull devices grounded both pitch and yaw. The second distinction in dynamics considerations was in the somewhat increased stiffness that could be offered by the closed-chain devices (Impulse Engine, Hull, differential) over the open-chain ones (HIT, PHANoM, Immersion patent); it was expected, however, that this would be perceptible mainly in the representation of rigid objects far stiffer than human tissue. Since these objects, namely bone and other tools, were to be simulated predominantly as placeholders to indicate errors in the user's trajectory rather than for extended engagement and palpation, this was not necessarily a concern. In addition, it was predicted that the U. Hull concept, in which

one axis required the sliding motion of the tool within a slotted guide, would display significantly more friction than the other axis configurations considered here, all based on rolling-contact bearings. Finally, it was expected that the tip-actuating designs—the PHANTOM and the Immersion patent—would make the actuation paradigm somewhat cleaner and more elegant; the device would actually *become* the tissue, resisting with the same forces which the tissue models calculated. In the pivot-actuating models, the torque to be applied to the tool shaft would be not only a function of the interaction of the virtual tool tip and tissue, but also of the distance of the tool tip from the fulcrum.

The configuration issues largely reflected the tip-actuation versus pivot-actuation dilemma. The former offered the advantage of greater compatibility with a more realistic external environment and compliant body wall, and more flexibility in repositioning for different trocar ports. The latter provided the convenience of holding the receptacle for the tool near the trocar, making reinsertion of the tool more straightforward. However, these were unable to provide insertion force feedback without adding a cable along the length of the tool, which would compromise visual integrity, or using rollers, compromising bandwidth by the addition of friction and compliance.

The conclusion from the above considerations was that the device suggested by the Immersion patent would likely be the best choice for the first three actuated axes. The PHANTOM was the next choice, and was commercially available. Therefore, the PHANTOM was chosen, but the decision was made to build the additional degrees of freedom in such a way so as to make a later change in choice of platform possible.

3.2 End Effector Device

Thus began a new, refocused design effort to develop an actuation device for the rotary and gripper axes. This device was again subject to the established set of metrics; however, a more focused, specific set of requirements for this subsystem was first compiled which would map to the desired characteristics for the simulator as a whole.

3.2.1 Refocused Specifications

In order to be able to establish a set of design criteria which were truly useful for the new problem, a subset of specifications were listed which embodied the overall needs but were directly relevant to the end effector actuator. Issues including minimizing overall volume and weight while striving for simplicity and low part count, manufacturability and usability were in mind. At the axis level, friction, backlash, and inertia were to be minimized while maximizing stiffness. These considerations were first applied in the choice of an overall configuration for the device, then in selecting an actuation scheme for each axis.

3.2.2 Device Configuration

The three possible paradigms for tool setup were: (1) tools could be captured and remain at the same port and tool changes during a procedure would be accomplished in software, (2) tools could be removed between sessions to change ports and tool changes would be again in software, and (3) the structure of the individual end effectors of would be maintained, and tools could be removed and interchanged like real tools during the simulation. These options and tradeoffs are summarized in Figure 3-4.

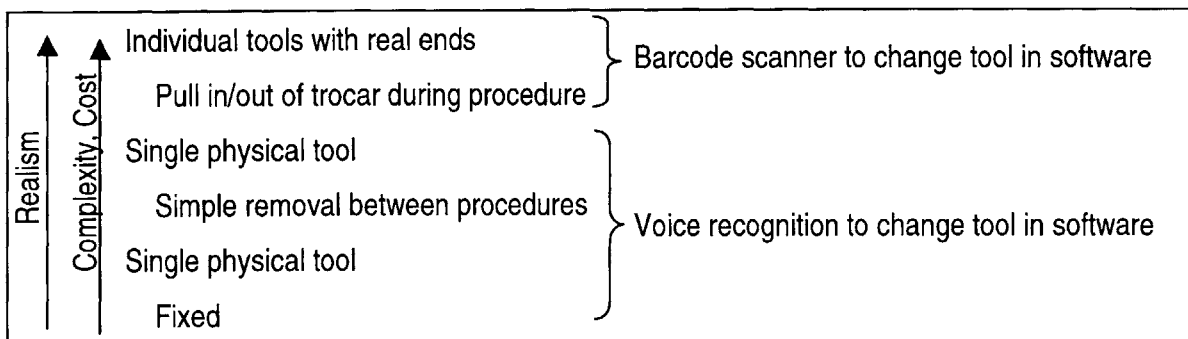


Figure 3-4. Tool simulation options and tradeoffs.

It was seen early on that while option 2 would be somewhat more challenging and complicated to design than 1, the third option would increase complexity many times over. In order to be able to insert and remove varying surgical tools into the same port to receive force feedback, an automatic latching mechanism would be required. Early brainstorming of possible embodiments suggested that it would be very difficult to accomplish this without introducing an additional

actuator, significant backlash, or loss of stiffness (from spring-loaded devices), such that visual realism could be gained only at the expense of haptic realism. Furthermore, this mechanism would be required to take many unknowns (gripper and rotational orientation) and still be able to precisely locate each axis and securely couple it to the haptic device. Ensuring robustness of this mechanism, both in terms of seamless use and functioning lifetime, would be nearly impossible.

Furthermore, the gripper could be driven by actuating at either the handle or at the tool tip. The latter could be accomplished by actuating the end effector as is, providing a force in parallel with any end effector forces by actuating the inside shaft, or by removing the tool end effector altogether and actuating the inside shaft alone. The option of actuating the handle was first eliminated, since it would be impossible to add an actuator and associated transmission, encoders, and wires without compromising the integrity of the tool. It was then observed that driving the motion of the inside shaft relative to the outside shaft would require a much less complicated coupling mechanism than attempting to actuate each individual tool end effector. Furthermore, this coupling mechanism would not need to be dedicated to a particular kind of tool, since both scissors and graspers bore the same internal shaft.

The final choice of whether or not to keep the individual tool end effectors intact required a closer look at the operating paradigm of the simulator. It was further observed that removing the tool end effector would be consistent with the operating paradigm described earlier, in which tool changes would be implemented in software. As anticipated during requirements analysis, this would allow the tool to remain engaged to the simulator for the duration of a simulation, and require the tool to be removed and replaced only to simulate a procedure which made use of different ports. This scenario relaxed the requirements on the changeover time. However, as mentioned earlier, while the tools bore an identical mechanical structure above the end effector, this final mechanism imparted its own characteristic friction (noticeably higher for scissors than for graspers) to the feel of the tool, and was in fact responsible for the majority of the friction in this axis. It was decided to remove the end effector and to restore the “force signature” of the individual tools by commanding a modeled damping (that is, proportional to speed) force to the actuator.

3.2.3 Actuation Concept Generation and Early Refinement

The challenge of actuating the two concentric shafts in relative linear and rotary motion was now examined. The assumption was made at the outset that a transmission of some type would be required for both axes, since otherwise very large actuators would be required to generate the torques specified. With this early assertion made, a first brainstorming session was used as a broad exploration of possible transmission schemes. This session produced the ideas sketched in Figure 3-5.

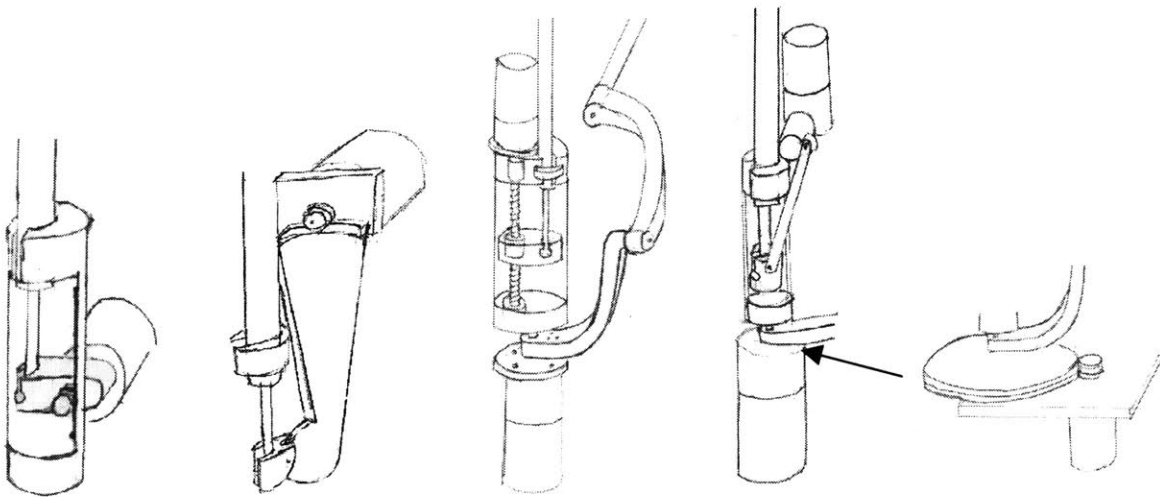


Figure 3-5. Initial brainstorming sketches for the end effector device. From left to right, the proposed designs were a leadscrew, slider-crank, arc section, or capstan.

The concepts for the rotary axis were fairly straightforward: either a simple gearbox transmission coupled directly to the axis, or a motor with or without a gearbox coupled to the transmission by a capstan and cable drive. Ideas for the linear transmission included a linear capstan, arc-section cable transmission, ballscrew, and slider-crank. In each case, a motor rigidly attached to an outside housing would be used to drive the motion of the inner shaft of the tool relative to the outer shaft via the transmission and a cartridge which clasped the tip of the inner shaft. At this stage the design of the housing and the mechanical couplings between the tool and the transmissions were not addressed.

Before further analysis was done, these concepts were refined somewhat. The slider crank was eliminated for the sake of stiffness and simplicity of both manufacturing and control,

as it would be characterized by a nonlinear output force. The linear capstan and ballscrew designs were each changed in order to make the output force of the rotary-to-linear transmission collinear with the axis of motion, thus eliminating extraneous moments and increasing the potential stiffness of the design. An analogous change was made to stiffen the arc section cable drive design, in which the tip of the inner shaft would be directly captured in the driving section. The possibility of using a right-angle transmission of some sort was proposed in order to bring the motor for the linear axis closer to the tool shaft to reduce rotational inertia. The resulting set of sketches is shown in Figure 3-6.

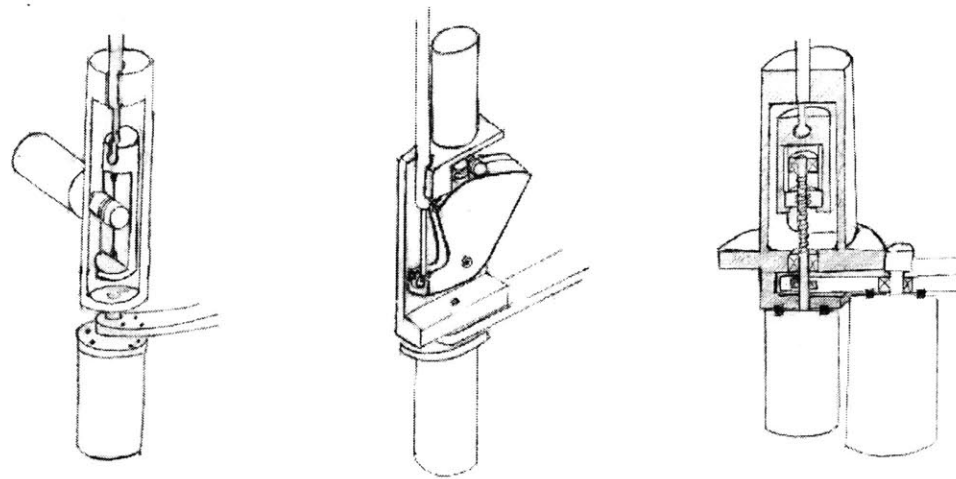


Figure 3-6. Refined concepts. From left to right, linear capstan, arc-section cable drive, and ballscrew.

3.2.4 Early Analysis and Concept Selection

In order to further differentiate between these possible designs, more detailed analysis of the actuation requirements for each of the proposed transmissions was required. These considerations are summarized in the table Gripper Subsystem Concept Selection found in Appendix B4. For reference, it is useful to recall the specifications asserted in Chapter 2. The rotary axis required a minimum travel of 180 degrees and a torque of 0.08Nm, and the linear axis required a travel of up to 6mm and a force of 17N. For design purposes it was assumed that the actuators and transmissions should provide at least twice the force or torque specified.

As a point of reference, it was useful to investigate the maximum continuous output torques of motors available. Maxon rare earth (RE) motors had long been favored in the Haptics Lab for their particularly high power output to motor weight ratio. It was noted that it would be preferable to use a motor no larger than the 16mm diameter, 4.5W, 5.44 mNm maximum continuous output motor weighing 40g, since the next larger motor, 25mm, was much more powerful and also much at 130g. Thus, a baseline for motor output was 5mNm, with a short term recurring overload capability of up to 25 mNm. These motors were available with planetary gearboxes with low backlash; single-stage gearboxes (4.4:1 or 5.4:1) were preferable for backdriveability, but the 19:1 gearbox was also a possibility.

The requirements for the pure rotation transmission for the tool twist axis were direct to calculate. The design torque could be produced using a transmission ratio of 15:1. This would be achievable using the 4.4:1 planetary gearbox and a 3.3:1 or greater cable transmission ratio, given by the ratio of the drum diameter to the capstan diameter.

Actuation options for the linear axis concepts were similarly determined. For the linear capstan, these calculations were straightforward. Glancing at a Sava steel cable selection chart suggested that to carry 17N, an 0.018" diameter 7x19 cable would be required and that a minimum capstan diameter of about 0.25" or around 6mm could be used, with a safety factor of 8.8. The required output torque would then be 108Nm, and would be possible with the 16mm motor and 19:1 gearbox.

A bit more geometry was required to evaluate the arc section cable drive possibility. The problem parameters were defined as shown in Figure 3-7.

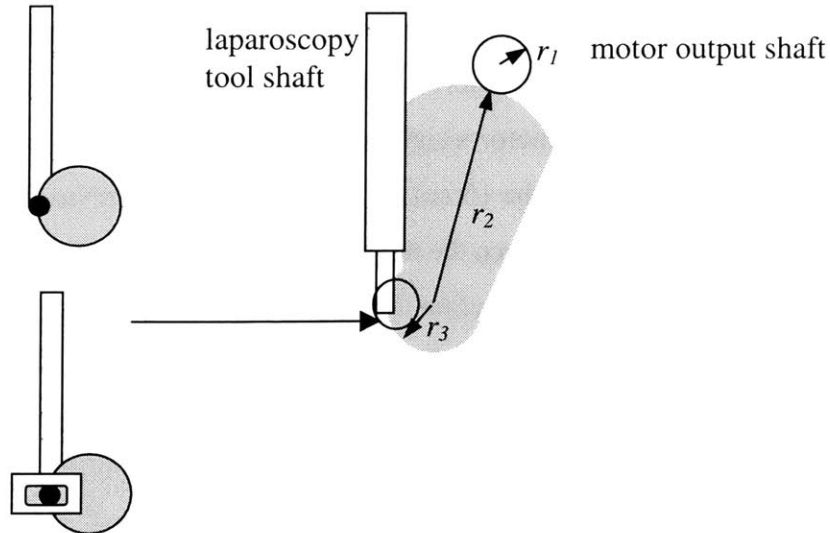


Figure 3-7. Arc section cable drive schematic. At left are two possible coupling configurations between the inner tool shaft and the arc section.

The transmission ratio for this cable drive is simply $\frac{T_2}{T_1} = \frac{r_2}{r_1}$. If the coupling between the output capstan and the tool tip were to be a “pin joint”, that is, allowing rotation only, a finite horizontal displacement would be imposed on the tool tip. If this coupling were to consist of a pin sliding in a horizontal slot coupled to the tool tip, this undesired motion could be eliminated; however, a moment would be induced when the drive pin was not directly under the shaft. Furthermore, in order to ensure that this sliding took place under a 17N load, a linear bearing would likely be needed. Given these considerations, it was decided instead to use the estimated maximum allowable deviation of the tool tip from pure vertical before friction would cause the inner shaft to stick inside the outer shaft in order to determine the minimum output radius, r_3 . The simple geometry of this problem is sketched in Figure 3-8.

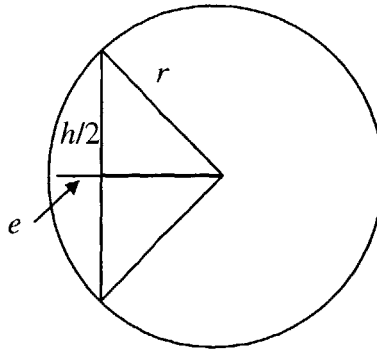


Figure 3-8. Horizontal excursion constraint for arc section cable drive concept.

The relation $e = r - \sqrt{r^2 - \left(\frac{h}{2}\right)^2}$ was used to estimate the minimum output radius r ,

where h , the total vertical travel, was assumed to be 6mm according to the device specifications, and e , the minimum excursion, was estimated as 0.5mm. The suggested output radius found by this method was 10mm, requiring a swing of +/- 37 degrees. This placed the required output torque at 340mNm. In this configuration it was preferable to use no more than the 4.4:1 gear reduction, since the significant friction contributed by higher ratios would again be amplified to the user by the cable transmission. This would require the cable transmission ratio to be 14.2:1, clearly involving an enormous mechanism. It was estimated that the largest feasible reduction would be about 8:1, which would require the major arc section radius r_2 to be 48mm long and require space for 29mm of horizontal travel.

Finally, the plausibility of the ballscrew mechanism was investigated using the power balance relation $T = \frac{F_v}{\omega} \cdot \frac{SF}{\eta} = Fl \cdot \frac{SF}{\eta}$, where T was the required motor output torque, F the force in the gripper shaft, l the lead of the ballscrew, SF a safety factor, and η the efficiency the ballscrew. A starting search was conducted to find a miniature ballscrew with the highest available lead-to-diameter ratio for maximum backdriveability. Schneeberger Linear Technology offered a 3mm ballscrew with the appropriate load bearing characteristics: a backlash-free (preloaded) nut, and a lead of up to 1mm. Using the 1mm lead ballscrew as a

guideline, an efficiency η of 0.75, and a safety factor of 2, the required motor output torque was determined to be 45 mNm. It was again desired to use the smallest reduction planetary gearbox with the motor, since the ballscrew would not only amplify the gearbox backdrive friction but would itself contribute significant friction, particularly with a preloaded nut. However, neither the 4.4:1 or 5.4:1 gearboxes would sufficiently amplify the motor torque, and a different motor/ballscrew combination would have to be found.

Several additional observations were made which contributed to the final decision. First, it was realized at this time that it was possible to decouple the twist and gripper axes of the tool.

This resulted from the fact that only the outer shaft was directly attached to the wheel on the handle. The inner shaft was supported by a rotating bearing in the handle, and forced to turn with the outside shaft only by the main linkage pin in the end-effector driving mechanism, which was mounted through the outer shaft. When the end effector was removed, the inner shaft and outer shaft were able to rotate independently; consequently, it was possible to keep the inside shaft stationary while the outside shaft was rotated. The significance of this observation was that it would be possible to actuate the gripper and twist axes in parallel, so that the motor and transmission driving the gripper axes would not also rotate when the user rotated the shaft of the tool. This quieted concerns about additional rotational inertia contributed by the gripper axis. As a result, there was little advantage in pursuing the ballscrew design, which aligned the gripper motor with the shaft axis but raised concerns about backdriveability, backlash, and the bending strength and stiffness of a small-diameter screw. Similarly, there was less incentive to try to implement a right-angle drive for the gripper axis, which would not be an easy task.

Of the two remaining cable designs, the arc section was less preferable although it provided additional reduction without gears and eliminated the need for linear bearings or sliding, it was again governed by a nonlinear force relationship and required significant additional space. The linear capstan was chosen as the most mechanically straightforward and compact solution, and it was assumed that a well-crafted sliding contact would bear less friction than that inherent in the grasper actuator mechanism described in Section 2.2.2.2.

A final concept sketch, shown in Figure 3-9 was made in order to update the linear capstan design such that the linear and rotary axes were decoupled.

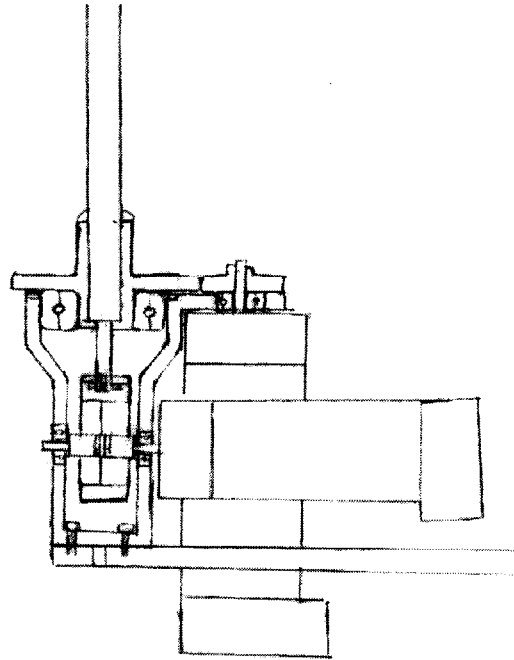


Figure 3-9. Updated cross-section concept sketch of the selected capstan-based design.

In this configuration, the outer shaft was no longer fixed in the main housing, but was coupled to a drum which rested in a bearing set in the top of the housing. Again, since only the outer shaft transmitted axial torque to the user, the main housing could now be fixed to the final link of the PHANTOM gimbal. The rotary drum and outer tool shaft were rotated separately by a motor mounted to the housing parallel to the shaft axis. The inner shaft of the tool was again coupled to a linear capstan, driven by a motor fixed to the same housing, and extending perpendicular to the tool shaft. While earlier it was of concern that this motor position increased the rotational inertia of the device about the tool shaft axis, this was no longer a factor since the motor and housing no longer rotated. The contribution to inertia in the pitch, yaw, and insertion axes would not be any significant function of the motor position.

3.3 Design Split: 1 and 2 DOF Devices

At this time it was decided to first build a device which actuated only the gripper axis, since the need for this feedback was more clearly defined. Furthermore, this provided the opportunity to debug one axis before adding the second, and produced two devices for the purposes of comparing efficacy in surgical training. It was determined, however, that the designs would be identical an extent as possible for mechanical consistency and so that the components for the two gripper axes would be interchangeable.

Chapter 4

Detailed Design and Fabrication

Many further issues needed to be addressed in order to fully specify and fabricate the device, as well as to make it “come to life”. The preceding design process was repeated in miniature in defining the details of each axis as well as the structures which formed user interface components. The rapid 3D sketching capabilities of SolidWorks were used for a great deal of the concept development, and dimensioned drawings were created as each part became satisfactorily defined. The process of fabrication of a first-generation prototype of the 1 DOF design provided a fair amount of additional insight, which was reflected in the final generation designs and prototypes for both the 1- and 2-DOF devices. These devices were then integrated into the PHANTOM hardware and electronics, and software developed was to drive graphics and haptics for all five axes. While some details are given here for the purpose of discussion, dimensioned SolidWorks models can be found in Appendix C, and all other required specifications in Appendix D, Device Manual. All components were designed in English units for ease of manufacture in the United States.

There were several themes which ran through the design efforts, and which were clearly visible in the final design. These reflected the device specifications from the previous chapter, and included a conscious effort to save space wherever possible.

4.1 Gripper Axis Design

In order to fully specify a working axis, it was first necessary to consider how the axis would be constrained and supported in order to yield the desired motion. Couplings between the laparoscopic tool and the required axis components were designed, and the details of the cabling layout were finalized. Finally, the requirements of actuating and controlling the axis were addressed. This was done first for the gripper axis, since it was the foundation for both devices and was to be built as the first prototype.

4.1.1 Motion Constraints and Bearings

Among the first considerations was how to constrain each moving part to only the desired motion, taking into account forces and moments to which it would be subjected. The first of these was the motion of the gripper cartridge within the housing. An analysis of the existing constraints and applied forces may be found in Figure 4-1.

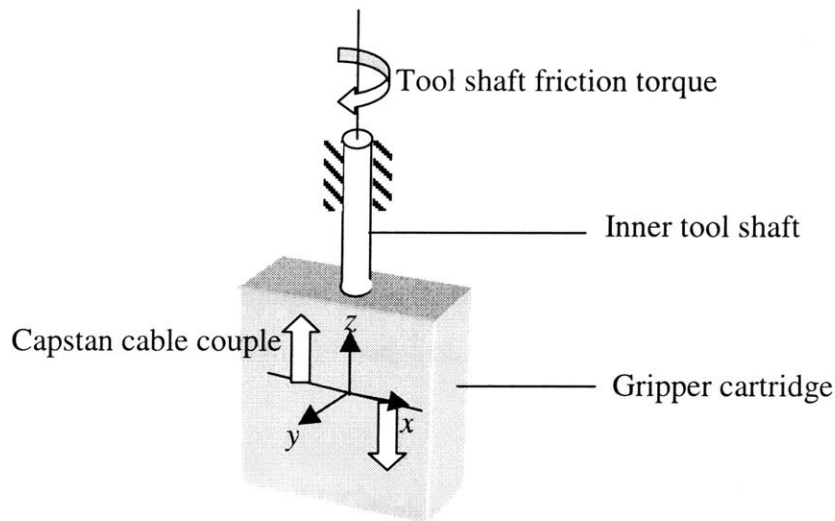


Figure 4-1. Moments and constraints on the gripper cartridge.

A predominant moment would be imposed on the cartridge about the y axis by the force couple resulting from the tension in the cable wrapped around the capstan. A secondary moment that might have been present would have resulted from any friction between the inner and outer shafts of the laparoscopy tool which would tend to induce a twisting moment about the z, or tool

shaft, axis. In the ideal case, the cartridge would already have been fully constrained to resist moments about the x and y axes, since the inner tool shaft, whose end was fixed in the cartridge, was guided by the outer shaft which was in turn fixed in the main housing. However, imposing the cable-induced moment in the real world would likely cause the inside shaft to bind inside the outside shaft and possibly cause the inside shaft to deflect. Furthermore, this constraint would not resist the twisting moment about the z , or tool shaft, axis. It was desired to constrain these three rotations without placing any further geometric constraints on the assembly, so that the insertion of the shaft would fully locate the gripper cartridge without overconstraining it. The option of using a linear rolling element bearing was dismissed for this reason, although a THK miniature linear motion guide was found to be small enough for this application. The two predominant brainstorm ideas for resisting these moment are shown in Figure 4-2.

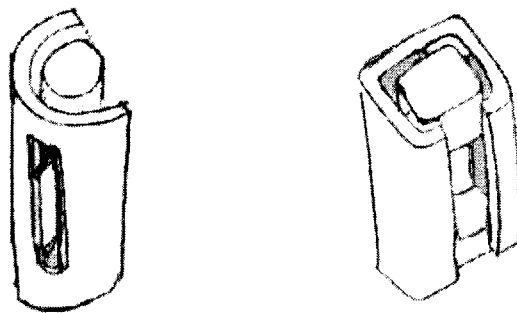


Figure 4-2. Two brainstorming ideas for the gripper motion constraint. At left, a “fin” moving in a slot; at right, the gripper cartridge is nested in the outer housing using delrin corner pads.

These consisted of either using a fin-in-slot configuration, or using fully nested, radially asymmetrical geometry (square or rectangular prism) for the cartridge and housing and providing a bushing of delrin. Following the design heuristic to minimize the information content in the design, the second option was dismissed, since it would require tight tolerances on all angles and dimensions on the exterior of the gripper cartridge and the interior of the housing. The fin concept, on the other hand, dictated only the parallelism of the slot and fin surfaces. The next question regarded whether the cartridge and housing should be round or rectangular; the latter was chosen since the fin/slot, cable mountings, and other features would be better manufactured

on the mill than the lathe, and because the motor and bearings would need to be seated against planar surfaces. The first embodiment of this design is shown in Figure 4-3.

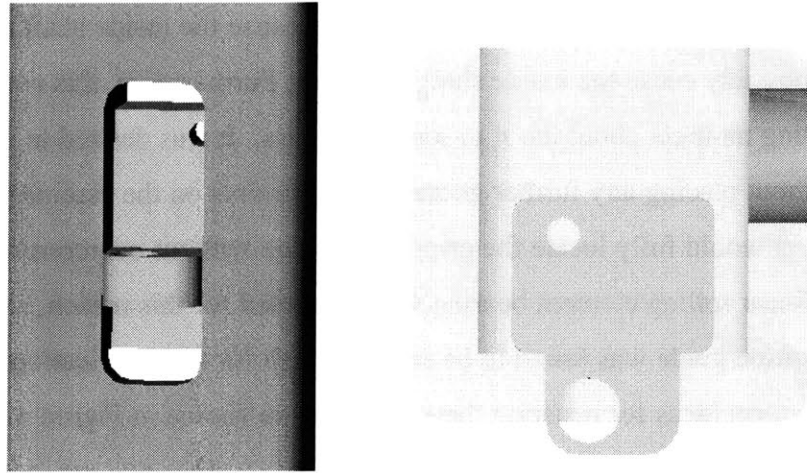


Figure 4-3. First embodiment of gripper motion guide. At left, back view. At right, top cross-section view.

It was observed at this time that the slot in the housing and resulting access to the back of the gripper cartridge would additionally provide an accessible surface on which to mount cable-tensioning components. As such, the fin itself was established as the anchoring surface for the cable tightening screw, and provisions were made for bringing the cable through the cartridge as seen in Figure 4-3. The vertical range of motion available to the cartridge in the slot was designed so as to be larger than the travel of the actual toolshaft. The benefit of this design was that the physical end-of-travel stops for the gripper axis were those in the laparoscopy tool handle, and the device would not be required to bear these “bottoming out” loads. Clearance was established between the outer sides of the cartridge and the housing so that there would not be redundant constraints on motion along the x axis. Furthermore, since two orthogonal surfaces of the gripper cartridge were required to slide on the back of the housing (the back of the cartridge and the sides of the fins), it was determined that the material of the back of the housing in which the slot was cut should be friction-reducing. This suggested making either the back plate, or the entire housing, from a material such as delrin or ABS. The single-piece housing was chosen in order to reduce both part count and the final weight of the device. This design was used in the fabrication of the first gripper cartridge prototype. An attempt was made to machine the gripper

cartridge out of ABS as well, but it was found that the tiny features of this part would not remain sufficiently strong in this material. More importantly, this prototype demonstrated a tendency to jam, and it was observed that the ratio of the fin thickness along the direction of motion to the width of the slot would need to be increased. The following design, shown in Figure 4-4 reflected the new proportions.

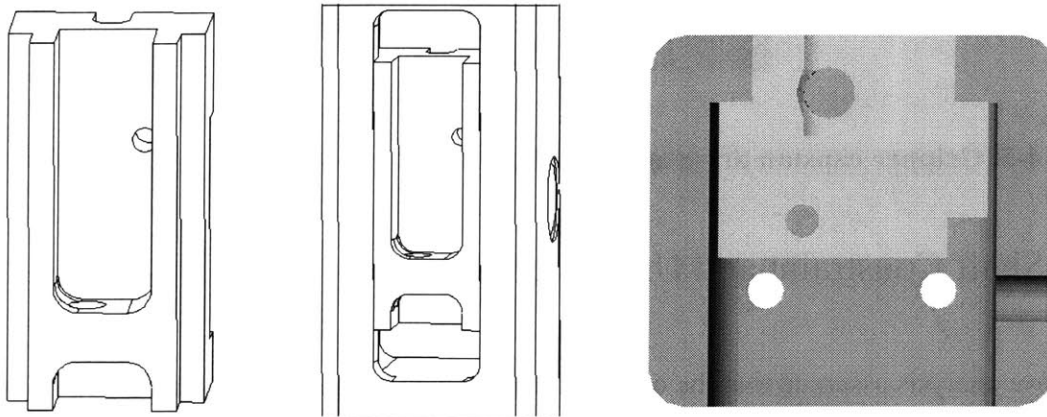


Figure 4-4. Final linear guide design for the gripper cartridge. At left, the final cartridge design having two bearing surfaces; shown mating with the housing in back view at center, and in cross-section at right.

Here the “fins” were extended to the full length of the cartridge, and designed to lie flush with the back of the housing for safety. This design was used in all following prototypes and was characterized by very low friction between the cartridge and housing.

The force couple from the tensioned cable also applied a significant moment to the capstan, and thus the shaft of the motor. The possibility of using two cables in order to make the load symmetrical was considered, but was dismissed based on the considerable added space requirements and complexity involved. It was chosen instead to place a bearing in the wall of the housing opposite the motor, so that the motor shaft was supported on both ends. This essentially overconstrained the shaft, since it attempted to align a third bearing with the pair of bearings inside the motor. Great care was taken in machining all associated dimensions in order to prevent this from becoming a problem. The final capstan axis design is shown in Figure 4-5.

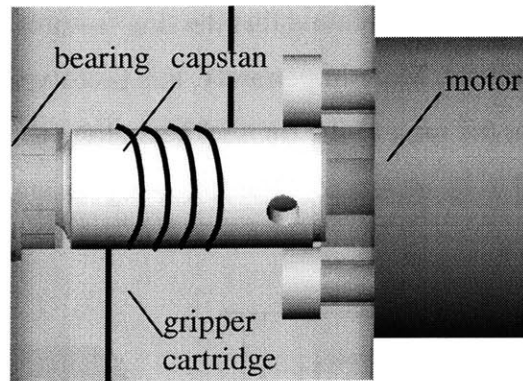


Figure 4-5. Gripper capstan drive axis details.

4.1.2 Shaft Constraint and User Interface

The above analysis assumed that the outer shaft was fixed in the housing, and that the inner shaft was fixed in the gripper cartridge. Designing the mechanisms for securing these shafts involved not only mechanical considerations but also human use ones as well. Mechanical concerns included developing a coupling which could resist axial forces without backlash or compliance, and provide a long enough contact surface along the axis to resist moments. Since each of these connections would need to be released and then re-engaged with each change of trocar position, it was critical to envision the “storyboard” associated with such use. In doing so, a number of parameters associated with connecting/disconnecting the mechanism became important: the number of steps involved, number and kind of tools required, number and size of loose parts, and ease of access to the required parts.

4.1.2.1 Outer shaft – Housing Coupling

With these criteria in mind, a first concept was proposed for the constraint of the outer tool shaft in the main housing, and the subsequent development is shown in Figure 4-6.

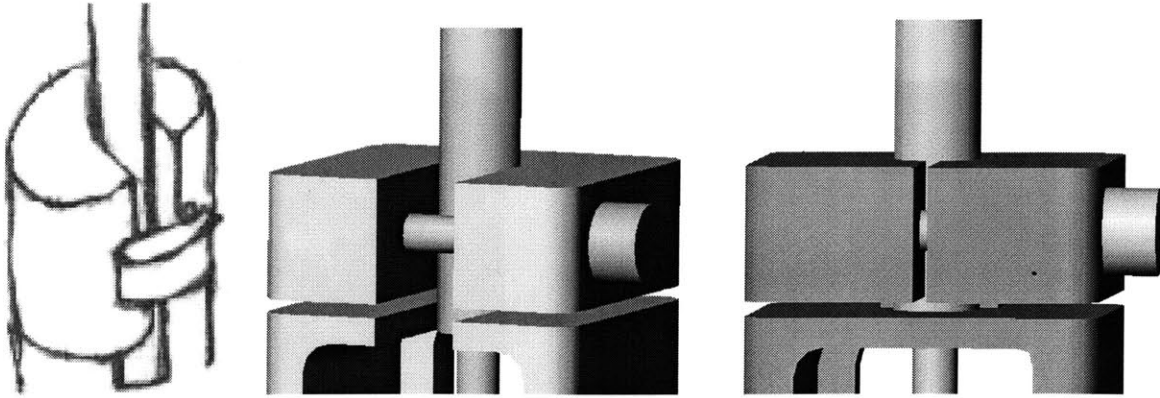


Figure 4-6. Outer shaft clamping concept development.

The initial design suggested a flexure structure with a side- or top- entry slot bearing a commercially available clasp. Driving factors for this idea were to make the clamp integral with the housing with no parts that needed to be removed, and as well as tolerant of manufacturing differences in the diameter of laparoscopic tool shafts. However, clasps of this size were difficult to find, and it quickly became apparent that a clamping screw alone would suffice, and provide a much simpler solution. The first 1 DOF prototype was fabricated using this design; it was discovered that even when high clamping forces were used, the shaft tended to pivot somewhat around the screw in the plane of the slot. Accordingly, in the third and final embodiment the slot width was minimized to support the shaft in nearly 360 degrees. This was also done in the interest of design consistency, anticipating the constraints that would be associated with the 2DOF design, in which the tool would have to be inserted from the top because of the rotary axis bearing. A further addition was that while the hole in the flexure block accommodated the outside shaft diameter, the hole in the housing surface below it was sized to be just larger than the inside shaft. As a result, this surface would serve as a hard stop to fix the position of the outer shaft during insertion. Finally, while socket cap screws were used throughout the construction of the device, the clamping screw was chosen for a flathead screwdriver; first, this tool would be most readily available, and the difference in type would set a demarcation to prevent the accidental loosening of screws such as those which tensioned the cables.

4.1.2.2 Inner Shaft – Cartridge Coupling

Development of the inner shaft clamping design followed a similar pattern. The two predominant ideas are shown in Figure 4-7.

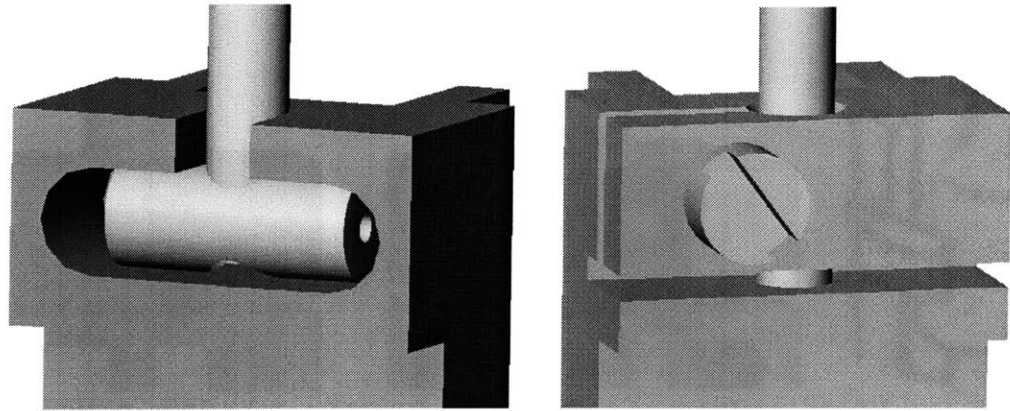


Figure 4-7. Inner shaft clamp concepts.

The first of these was again implemented at the first prototype stage, in which the side-entry paradigm was still in use. Since the outer shaft was in theory fully constrained by the main housing, it was proposed to provide constraint only along the axial direction of motion by outfitting the shaft with an endpiece that could be pressed into a slot in the cartridge. However, it was recognized that it would be difficult to manufacture this coupling so that it would be relatively easy to insert but permit no backlash, or play, in the axial motion even after many uses. Furthermore, while the outer shaft diameter was very consistent between brands of 5mm laparoscopic tools, each had its own interior construction and inner shaft diameter; as a result, it was preferable to minimize the number of custom operations which would need to be performed in order to change the tool handle used. The second and final generation design mirrored that chosen for the outer shaft clamp. A flexure was again used and oriented such that the screw, again flathead, faced out of the main housing cavity for ease of access. A similar surface was provided as a hard stop for the shaft, fully defining the setup distance between the ends of the two shafts and ensuring that the position encoder on this axis could be reset consistently. Finally, a chamfer was added to the insertion hole to guide the inner shaft, which was significantly smaller than the outer shaft, and often not perfectly concentric with it.

4.1.3 Cable Management

The major goals in designing the cabling layout were to make thoughtful use of existing space and to avoid fatiguing the cable by keeping radii over which it traveled as large as possible. The resulting design is shown in Figure 4-8 below.

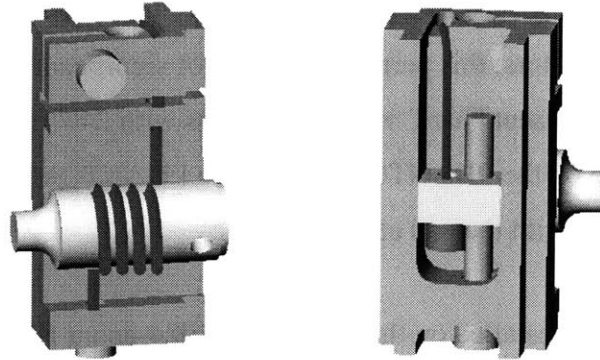


Figure 4-8. Cable fixtures for the gripper axis.

The stationary end of the cable was terminated directly in the base of the cartridge so that the first length of cable would not be required to turn any corners. A 0.25” capstan was used with the 0.024” cable specified in Chapter 3. The standard thread size ¼-20 provided more than ample space to securely seat and orient the cable. Four wraps of cable around the capstan, when fully tensioned, securely fixed the cable and prevented any slipping. Since total displacement was less than one revolution for the capstan, space for only one thread diameter of cable travel was required. As briefly mentioned earlier, the back of the cartridge provided the most space for, and greatest accessibility to, the cable tensioning mechanism. These were of particular importance because the cartridge and capstan needed to be placed inside the main housing before the cable could be fully tensioned. As such, the cable was brought straight up to the top of the cartridge and around to the back. A common scheme was used for the tensioning mechanism. The cable was terminated in a block which was free to slide in a long groove in the back of the cartridge. A threaded hole in the block allowed it to be cinched in by a screw anchored in the “fin” structure of the cartridge.

4.1.4 Actuation and Position Measurement

As described in Chapter 3, a Maxon 16mm Rare Element motor was chosen, and a 19:1 integrated planetary gearbox was specified, based on the maximum continuous current/torque available from the motor. This combination would be sufficient to provide all forces generated by interaction with virtual organ tissue. For interactions with rigid objects (bone and other tools), it was chosen to allow the tool to hit the physical hard stop in the handle rather than to use the force output of the motors; this permitted the use of significantly smaller, lighter motors than would be required to represent “hard” objects. Motors with 24V operating voltage were chosen in order to match those on the PHANTOM so that the PHANTOM amplifier box channels could be used interchangeably with the end effector device.

The first encoder installed on this axis was a 1024-count HP optical encoder with two-channel quadrature output. Taking the gear and capstan transmissions into consideration, this encoder provided one count per 0.001 millimeter of travel for the inner tool shaft. However, unless the gripper handle was moved very slowly, it was discovered that encoder counts were missed during data acquisition, and the position read tended to drift. It became clear that this resolution was actually too fine. These motors were also available for purchase from Maxon with integrated 13mm diameter digital magnetic encoders with quadrature output. At 4 counts per cycle and 16 cycles per revolution, these gave a resolution of 0.016 mm per count. The implementation of the new encoder eliminated count skipping and established consistent position measurement.

The final gripper axis prototype is shown in Figure 4-9 .

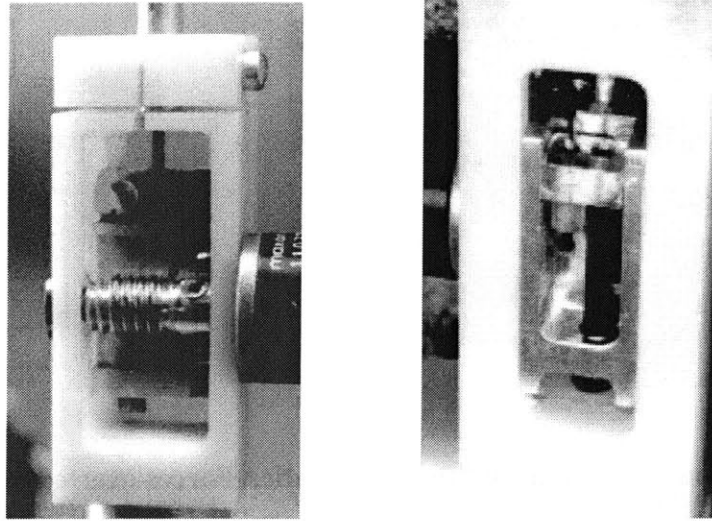


Figure 4-9. Final gripper axis prototype.

4.2 Rotation Axis

A similar sequence of specifications was developed for the rotation axis of the device. These were finalized only after the working prototype of the 1DOF device was tested in order to ensure that any details that might impact the rotary axis were set, and to take advantage of the lessons learned in designing and constructing the first axis.

4.2.1 Configuration and Bearings

Properly constraining the axis of motion was again a primary concern. In this case, the first relevant force was that of the cable pulling the drum toward the capstan when the cable was to be tightened. Secondly, forces in both directions along the tool shaft would be induced when the simulator resisted insertion and withdrawal motions by the user, and in reaction to the gripper actuator forces. The axis design and a schematic depicting these applied forces and their reactions are shown in Figure 4-10.

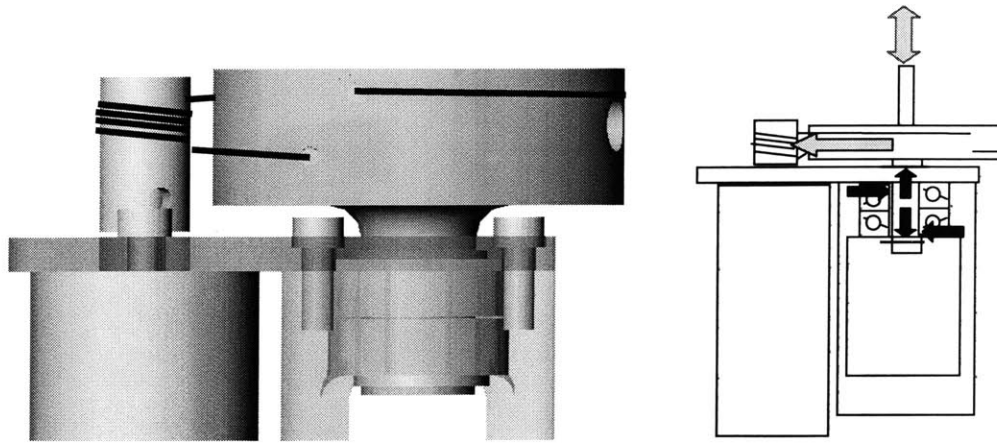


Figure 4-10. Rotation axis detail, and axis schematic. Forces exerted on shaft by cable tension and handle forces are in gray, and reaction forces are in black.

The cable force would tend to tip the cantilevered shaft axis toward the capstan, inducing a force couple at the end of the shaft fixed in the housing. As such it was chosen to support the shaft not with a single rolling element bearing as sketched in the original concept drawing of Figure 3-9, but with a pair of bearings, thus offering a better support spread for resisting this moment. It was clear that a coupling would be required between the tool shaft outer diameter and the bearing inner diameter; in order to insure rotational strength and rigidity, and to reduce total part count, this coupling was designed as an integrated piece with the rotation cable drum, and is described in detail in following sections. Finally, retaining rings were applied to the drum/coupling shaft on either side of the bearing pair to provide constraint and force resistance along the axis of the shaft.

4.2.2 Shaft Constraint and User Interface

The design of the clamp between the outer shaft of the tool and the coupling-drum proved somewhat more difficult than earlier clamps. A primary motivator was to make the design as compact as possible along the tool length, which, as mentioned in Chapter 2, was essential to the maximization of the insertion range of motion. It was recognized early on that an effective way of accomplishing this would be to sink the clamp into the drum itself. The sequence of designs which ensued are shown in Figure 4-11.

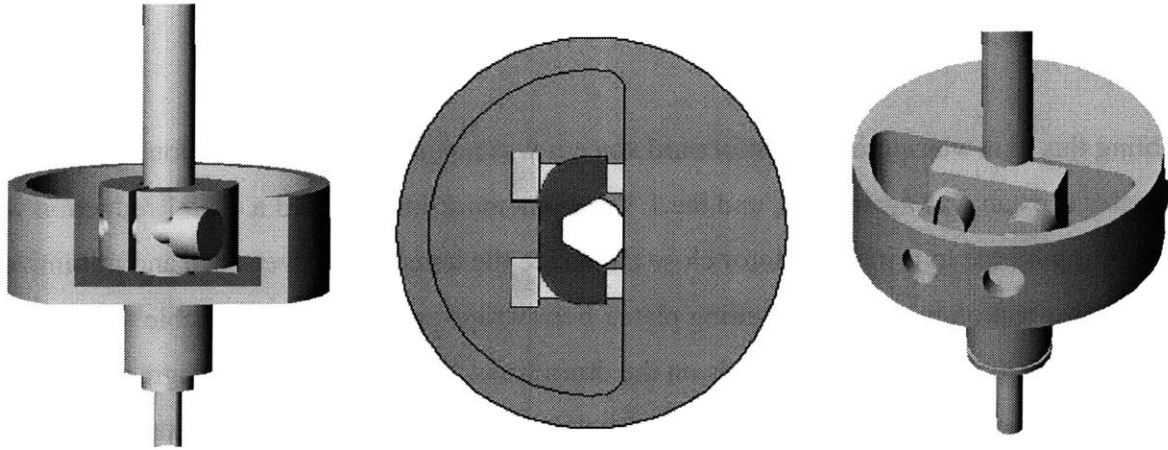


Figure 4-11. Progression of rotary clamp design. Left - flexure; center – kinematic clamp piece; right – circular clamp piece.

Not surprisingly, the first instinct was to use the flexure paradigm chosen for the first two clamps. A cutaway view of the resulting design is shown at the far left of Figure 4-11 in order to show the details of the flexure. Unfortunately, it was quickly ascertained that this design could not be easily machined because there was not sufficient room to lower a slitting saw into the cavity. Therefore, either the drum or the clamp would need to be made as two pieces; the latter was a more logical choice. A new concept was developed in which a separate piece would be clamped to the shaft by two screws threaded into the drum. These would only need to be loosened slightly to accept or release the shaft, so that the clamp-piece could remain attached to the drum at all times during use. The first embodiment of this design was a 3-point kinematic coupling. Here the shaft was pressed against a flat surface on the drum by a piece bearing a 45-degree V-groove. While promising, this design was in turn replaced by a simpler concept in which the drum and clamp-piece together formed a circular cavity (minus clearance for the clamping motion), making the clamp-piece more direct to machine. In addition, holes permitting more direct screwdriver access to the flathead screws were added to the drum. Finally, the last 1/16” of the coupling shaft was designed to accommodate only the inner shaft of the tool, so that a hard stop was again available for inserting the outer shaft to the proper reference position.

4.2.3 Cable Management

Cabling this axis was quite straightforward since it was a pure rotary transmission. A 0.25” diameter capstan was again used, and the 1.13” diameter drum provided a 4.52:1 reduction while making it possible to bring the motor close alongside the housing to save space and minimize the cantilever effect on the motor mounting plate. Four wraps again secured the cable to the capstan. It was chosen to anchor the cable ends on the drum so as to allow nearly 360 degrees of travel, even though the required travel only 180 degrees in order to provide greater versatility. In this case, the capstan would undergo just over 4 rotations, meaning that the cable would walk about 4 thread widths along the capstan. A standard but more compact ¼-28 thread was used in order to save vertical space.

The tensioning mechanism for the cable was designed identically to the one for the gripper axis and placed inside the drum in such a way as to maximize the travel available for drawing in the cable. The cable attached lower on the drum was used for tensioning so that the tensioning mechanism could be more compact and so that the cable would not impose a large moment that would tend to tip the tensioning block. This design is shown in Figure 4-12.

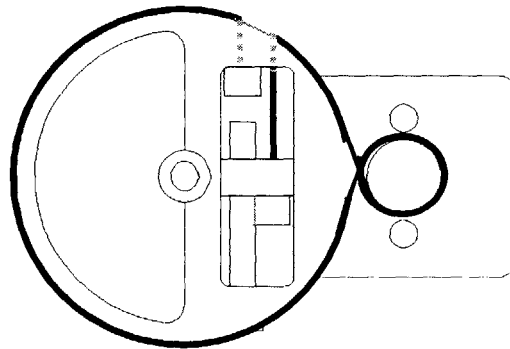


Figure 4-12. Rotation axis cable management configuration.

4.2.4 Actuation and Position Measurement

A 16mm Maxon RE motor was used to actuate this axis as well, and fitted with a 4.4:1 gearbox as suggested in Chapter 3. Again, this arrangement would provide more than enough torque to

simulate tissue interactions, but would not suffice for rigid body representation. This motor was also ordered with an integral 13 mm quadrature digital magnetic encoder, yielding a final resolution of 0.36 degrees per count. The final rotary axis prototype is pictured in Figure 4-13.

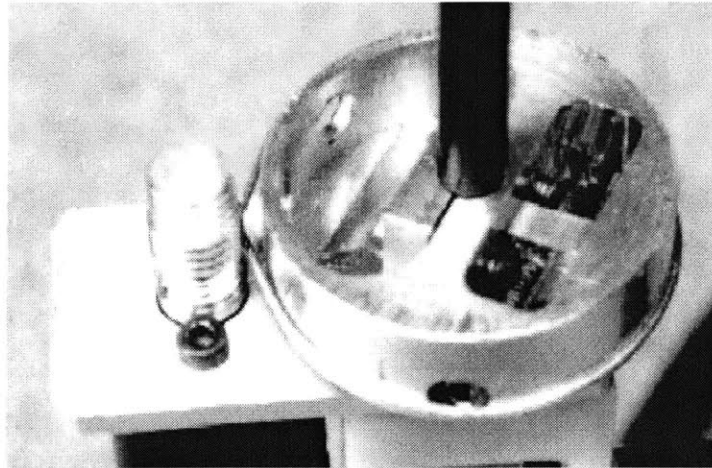


Figure 4-13. Final rotary axis prototype.

4.3 PHANTOM and Simulation configuration

The completed 1- and 2-DOF end effector devices were now ready to be integrated with the PHANTOM hardware, and with the simulation configuration as a whole. It was important to keep the devices interchangeable and to prepare for the use of a PHANTOM encoder gimbal to ascertain the tool orientation for graphics rendering or ray-based haptic modeling. Furthermore, as mentioned earlier, it was possible that an entirely different force-feedback platform might be chosen by this or other research groups to simulate the first three axes in the future.

Accordingly, the coupling between each of the end effector devices and the PHANTOM was designed as a separate module, which attached using identical bolt hole patterns on the underside of each device. For the 1DOF device, the PHANTOM terminal gimbal was used as is, and the coupling consisted of a simple 1/8" diameter post to be inserted in the bearing for the thimble and fitted with a retaining ring. The 2DOF device was intended to both provide and control the final rotational degree of freedom; as such, it was necessary to eliminate this degree of freedom in the gimbal in order for the user to receive the torque output. The fitting in this case replaced

the entire final link of the gimbal. The two devices are shown integrated into the PHANTOM gimbal in Figure 4-14.

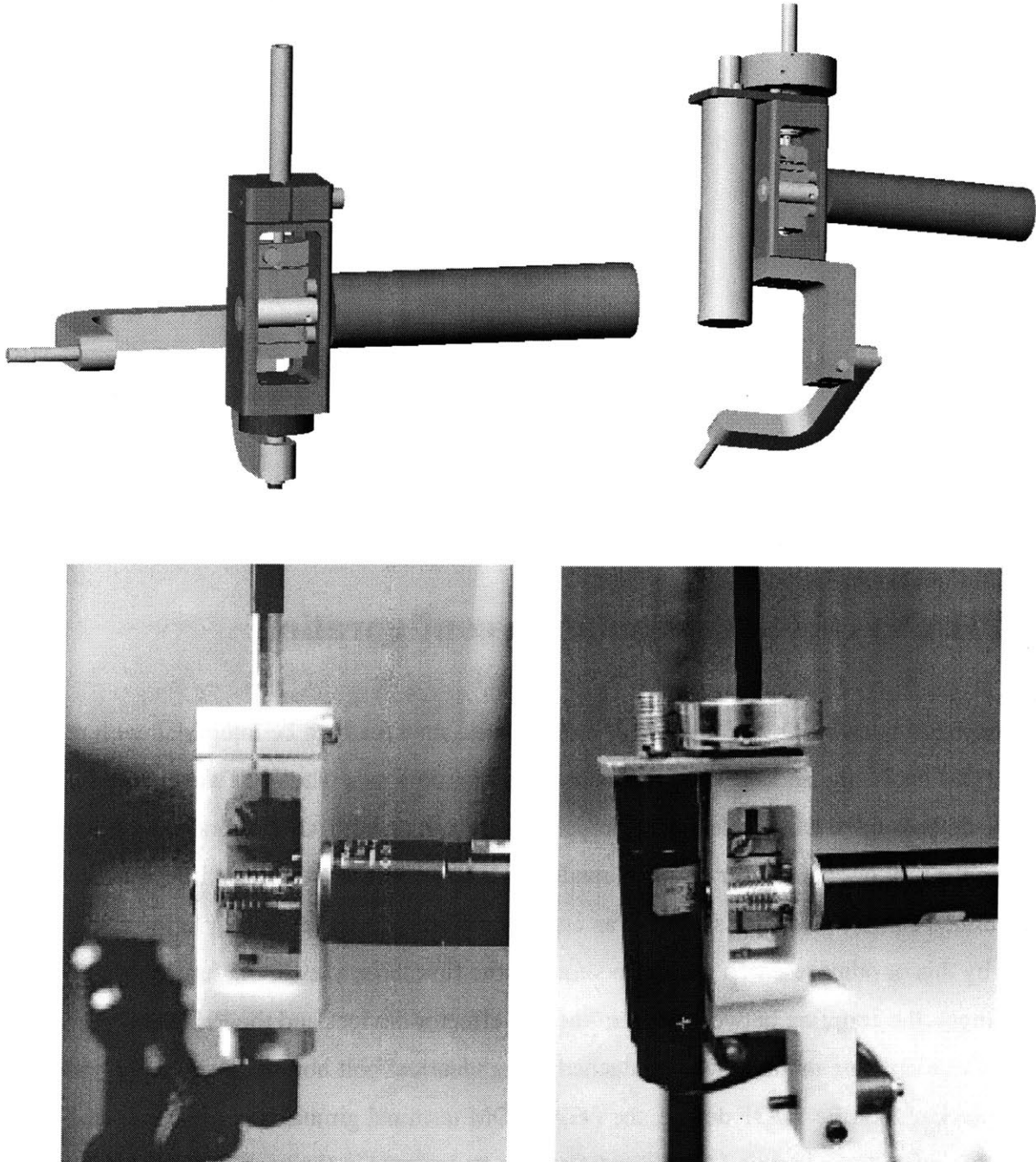


Figure 4-14. The final embodiments of the 1DOF (left) and 2DOF (right) devices, integrated into the PHANTOM gimbal.

The completed simulator hardware, capable of providing 5 DOF force feedback, is pictured in Figure 4-15.

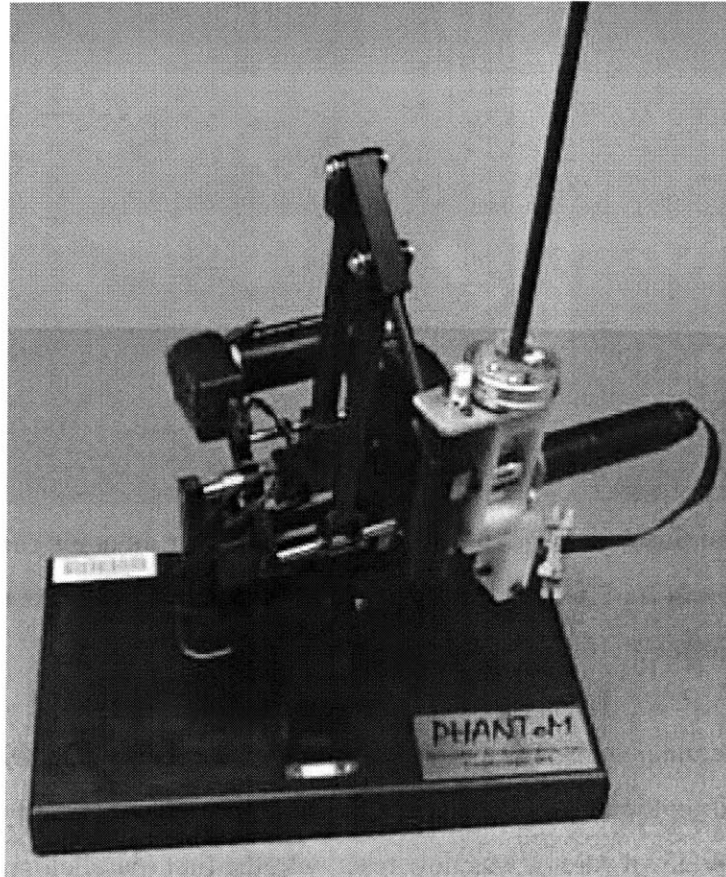


Figure 4-15. Complete 5DOF haptic device.

The initial home for the completed simulator device was inside a cardboard box, outfitted with a wooden lid in which a hole had been cut and covered with a thick layer of latex. The trocar was inserted in the true medical fashion (using the trocar cutting blade) in this material. The box was then covered in a traditional drape configuration. This setup is shown in Figure 4-16.

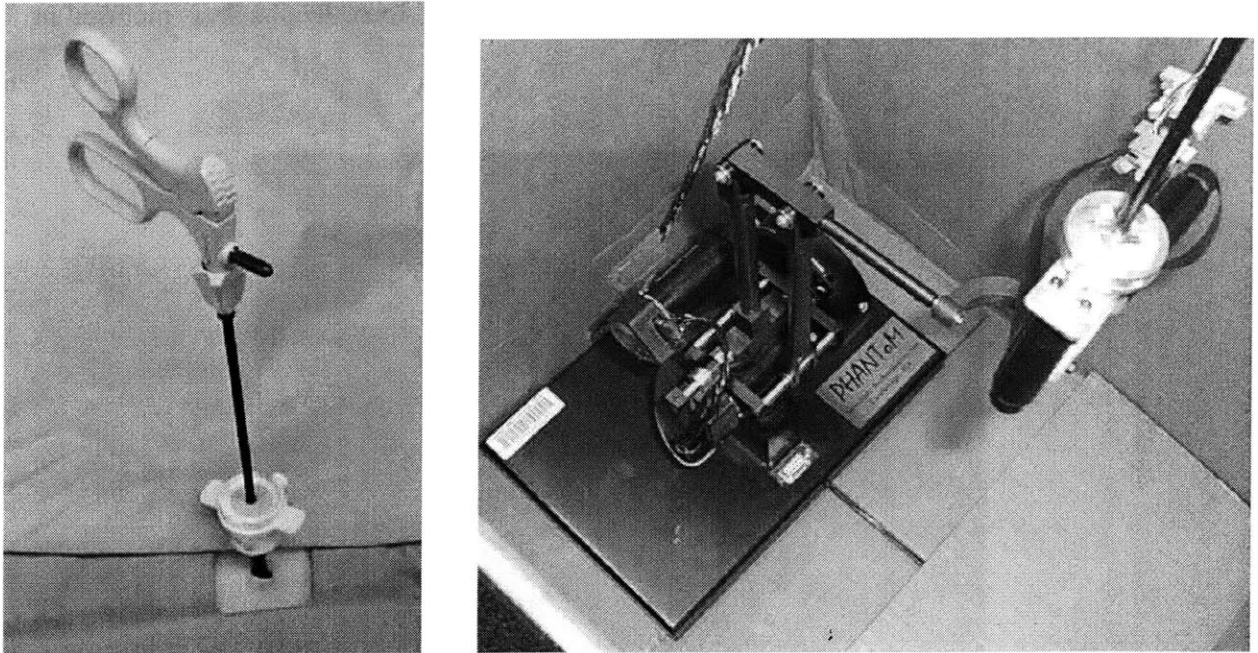


Figure 4-16. Box simulator configuration. At left, simulator exterior consisting of a laparoscopic trocar and tool inserted in the simulated latex “body”. At right, the haptic display hardware within.

This configuration actually suggested a new reset position for the PHANTOM; whereas in the traditional home position the PHANTOM arm was set at a 90 degree angle with the second long link directed vertically downward, it was now reset with the first (parallelogram) link vertically upward and the second link horizontal as shown in the photograph of Figure 4-16. As a result, the usual y and z axes of the PHANTOM were exchanged. A convenient consequence was that while traditional PHANTOM haptics/graphics simulations used the paradigm of a person interacting with a virtual object directly in front of him or her, the simulation was now automatically mapped to reflect the fact that the user was looking down on a surface being palpated from above.

A torso designed for laparoscopic training by the company Simulab was purchased in order to complete the simulation. It consisted of a mannequin-like rigid torso shell with an opening over the abdomen. This opening was covered by a compliant material meant to simulate the abdominal wall. However, this torso was a great disappointment; when it was received it became apparent that the simulated abdominal wall was only a thin piece of foam, with

properties nothing like those of an actual insufflated abdomen. Another company was found, which specialized in developing torso models for incision as well as laparoscopic practice. These appeared to reflect a focused effort to simulate the actual tissues of the abdominal wall, and were composed of the following layers: skin (epidermis, dermis, and subdermis), fat, linea alba, and peritoneum. Although this product was not yet received at the time of writing, it appeared to have the potential to lend significant integrity to the simulator. Both torsos are shown in Figure 4-17.

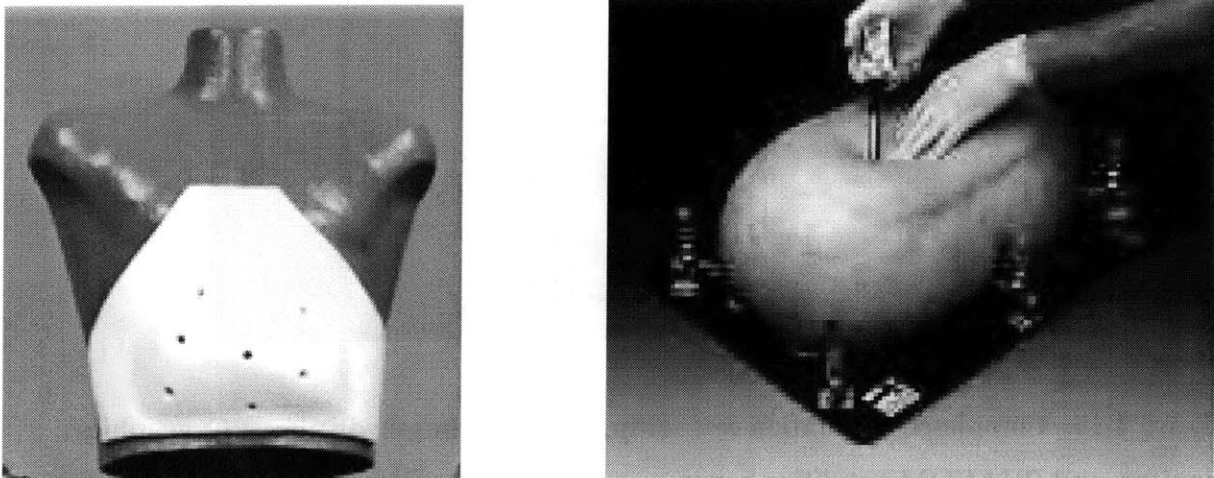


Figure 4-17. Simulab torso (left) and Limbs and Things torso (right). (Simulab, 1999), (Limbs and Things, 1999).

4.4 Controls and Electronics

It was convenient to use a second PHANTOM control card and amplifier box to control the additional device axes. This controller card executed closed-loop PID control on the motor current, which directly commanded the output torque. Conversions based on each transmission ratio and the torque constant of the motors were used to calculate the current corresponding to the force or torque desired for display to the user; these conversions are given in the Device Manual in Appendix E. Each axis of the new device was wired identically to the PHANTOM axis configuration for the sake of consistency. Details of these connections can also be found in

the manual. The completed system including PC, two PHANTOM amplifier boxes, and the device setup, is shown in Figure 4-18.

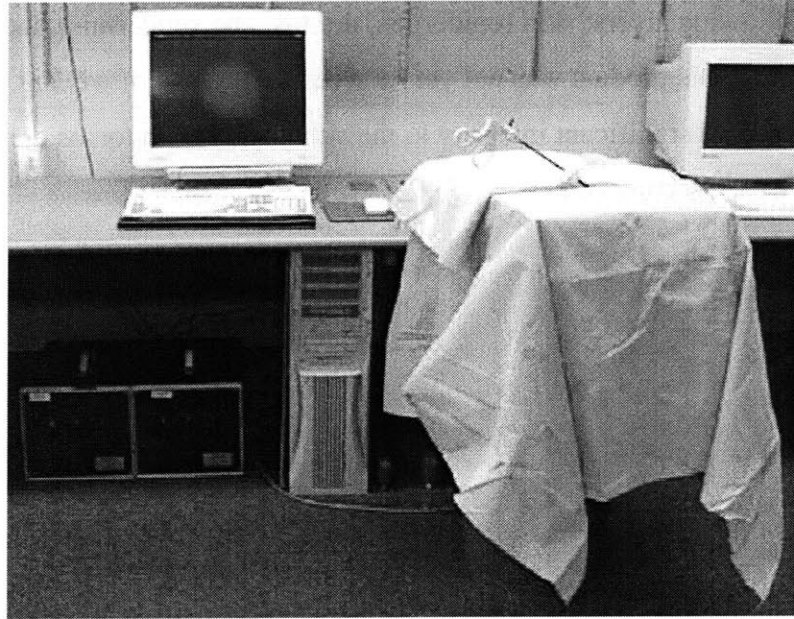


Figure 4-18. Completed simulation test setup, including haptic display, PC, graphics monitor, and PHANOM amplifier boxes.

4.5 Software

Although the bulk of the software simulation development was to be performed by a team at the Draper Laboratory, basic software was developed to control the end-effector device from within a PHANTOM-based haptic/graphical program. It was desired to send currents directly to the card, and to read the encoders directly from it, since the device was characterized by its own transformations between these low-level commands and the position/forces at the user end. Three “levels” of libraries were available for communication with the PHANTOM card: lowest-level I/O commands to the base address through the “lunchbox” functions listed in Appendix F, PHANTOM force commands and position readout through the “PHANTOM IO” library, and high-level object-oriented creation of haptic scene graphs through the “GHOST” library. Using the “lunchbox” or PHANTOM I/O commands alone required the construction of a haptics loop

in the code (generally based on a simple “while” loop), while GHOST and the PHANTOM I/O “OS Extender” libraries each provided an independent scheduler for the haptics loop. Using a scheduler ensured that the haptics refresh rate was maintained near 1KHz (Salisbury and Srinivasan, 1997) as required by human psychophysics in order to produce “smooth” haptic sensations, and permitted the simultaneous execution of other functionalities such as a graphics loop. In anticipation of the desire to integrate the haptics with graphics once all the hardware was controlled satisfactorily, it was necessary to choose one of the scheduler-based libraries as the foundation for the code. Several permutations were attempted using GHOST or PHANTOM I/O to control the PHANTOM and the scheduling operations, and “Lunchbox” commands alone or with PHANTOM I/O to control the specific commands to the end effector device.

Working within these PHANTOM hardware/software realms posed several challenges to integration. The most predominant one was working around the timeout circuit on the PHANTOM amplifier box, which would disable the amps if they did not receive commands at a certain rate. For this reason, it was not possible to use the “lunchbox” functions alone for the end effector device; it had to be initialized as a PHANTOM using one of the scheduler-based sets of commands. The first effort to this effect initialized two GHOST `gst_PHANTOM` objects in GHOST and attempted to send a simple current command to the end-effector device. However, the GHOST program structure appeared to interfere with the command; the axis only underwent vibrations rather than outputting a force, regardless of whether a PHANTOM or the end effector device was connected. Furthermore, each `gst_PHANTOM` was required to be part of the scene graph in order to be updated by the haptics loop, and it was not possible to hide objects in the scene graph from one `gst_PHANTOM` and not the other. This meant that a second actual PHANTOM would receive the same force commands as the first when in the same position within the haptic scene, and that the end effector device would receive extraneous currents if there was to be anything in this scene.

Fortunately, interfacing with PHANTOM I/O libraries was somewhat more smooth. Commands were again sent to initialize two sets of PHANTOM amplifiers; however, it was possible to control the actual PHANTOM separately using PHANTOM I/O force commands. However, it was necessary to send forces regularly to the second box via the

“PHANTOM_send_force” command in PHANTOM I/O to keep the box active. Therefore zero forces were sent this way, and the desired currents sent through the “lunchbox” commands. It was important that the current command follow the zero-force command immediately in the code to avoid a “duty-cycle” effect that occurred in which the current dropped to zero for a significant proportion of each haptic cycle. It is acknowledged that there must be a more elegant way of accomplishing control, but as this one finally produced excellent results further development was not pursued.

A simple demonstration program was developed for the purpose of validating the effectiveness of the hardware designed here. It was based on a large, compliant haptic sphere (stiffness of 0.1 N/mm, typical of some organs) rendered by the PHANTOM, with which the tool tip, modeled visually by a small sphere, could interact. When the user pushed the tool into the sphere, spring-modeled force was applied to the gripper axis and twist axis in both directions; therefore, the user felt resistance upon closing the gripper on the “tissue” as well as when attempting to spread the gripper inside it, analogously to the use of this tool described in Chapter 2. Furthermore, the user was able to grip the tissue and pull out of the sphere, feeling it pull back and feeling resistance upon trying to twist as well. Finally, if the user then released with the gripper, this force was terminated, generating the sensation of the tissue “snapping back”. At all times, “gravity compensation” was implemented; that is, a constant vertical force was applied by the PHANTOM equal in magnitude to the weight of the device so that the user did not feel that the tool bore any additional weight. The graphical display was relatively simple and performed in Open Inventor. The large sphere was represented as a static pink sphere, and did not visually deform; the tool tip cursor was a small gray sphere. The code for this sample program is given in Appendix F.

In addition, the MIT Touch Lab, using the same software tactics described above, integrated the 1DOF device into an existing simulation of a catheter insertion procedure in which graspers were used to guide a catheter into a blood vessel. This simulation offered much more sophisticated haptics (ray-based rendering of finite element models) and graphics (complete rendering of the tool including orientation and gripper motion, as well as texture-mapped organs).

Chapter 5

Evaluation and Recommendations

While no quantitative or systematic user testing was performed, both the 1DOF and 2DOF devices were used in the simulations described in the last section by a number of medical and engineering students and professionals. A great deal of information was obtained from the performance of the devices and the comments received in the course of these system tests, as well as from a closer evaluation of the design of the device itself by the author and several peers.

5.1 Performance Evaluation

Dr. Dawson and the members of the Draper simulation team were very pleased with the finished product. When questioned about the magnitudes of the applied forces and torques as well as the available range of motion on all axes, Dr. Dawson said that these were “good”. He commented however that there appeared to be too much friction in the twist axis, and in particular that he could feel discontinuities in the force. He emphasized that “the body feels wet, slippery, smooth. You don’t feel click, click, click”. It was observed that this friction was not present when the drum was rotated in the bearing before the cable was added, and that it increased as the cable was tensioned. Dr. Salisbury offered the insight that while ungeared motors contain a set of ball bearings and can be used in the cantilevered configuration chosen for the rotary axis, the gear heads bear only a bushing so as not to overconstrain the motor shaft, and cannot support radial loads such as that imposed by the tightening of the cable. The proposed solution involved supporting the end of the motor capstan as sketched in Figure 5-1 below.

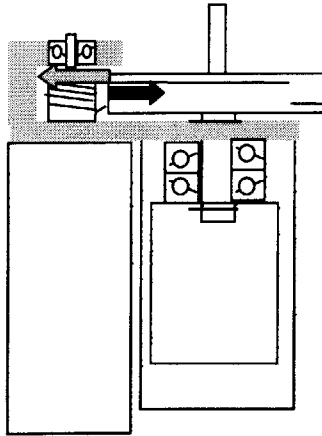


Figure 5-1. Proposed scheme extending the motor bracket to support the shaft of the rotary axis motor.

Furthermore, over the time that this group used the simulation, the upper of the two motors driving the parallelogram linkage on the PHANTOM became very warm. This motor carried most of the continuous load of providing the gravity compensation. Thus, although the 2 DOF device weighed only 0.37 pounds while the PHANTOM maximum force output was specified at 1.9 pounds, applying the smaller load on only one motor drew enough current that in continuous operation this motor could overheat. The proposed solution is to add a counterweight to the PHANTOM so that it the device is once again balanced in the set position and software gravity compensation is unnecessary. There would be a tradeoff involved, however, in the form of a possibly discernable increase in inertia on the three primary axes of motion.

Finally, the usability of the device in terms of the disconnecting/reconnecting operations involved in changing the trocar position was evaluated by the author. One observation was that while these were very fast and straightforward when the device was alone outside the simulation environment, it became more complicated once the device was attached to the PHANTOM and concealed inside the “torso”. In the setup used here, it involved a two-person operation: one to lift the torso up so that the second could have access to the device to disconnect it. It would be preferable if an area of the torso in the immediate vicinity of the trocar could be lifted away and supported independently, as sketched in Figure 5-2.

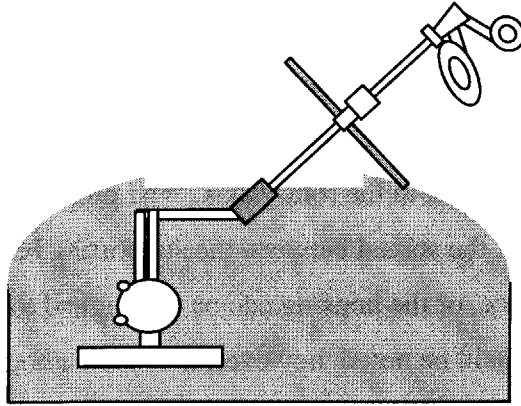


Figure 5-2. Concept for increased device accessibility.

Furthermore, while the flexure clamp for the outside shaft in the ABS housing of the 1DOF device was easy to use in repeated connecting/disconnecting cycles, the similar flexure clamp for the inner shaft in the aluminum gripper cartridges of both devices tended to deform plastically after several cycles, making it difficult to reinsert the tool shaft. It is recommended to fabricate this piece out of a more elastic material, such as ABS or Delrin (to save weight) or steel, or to use a two-piece clamp similar to that designed for the 2 DOF rotary coupling. This latter mechanism worked particularly well, delivering secure clamping forces over many uses.

Finally, although those who used the device did not remark about unusual resistance in the handle, this was measured in the same manner described in Chapter 2. It was found that 0.3N was required to overcome stiction and move the handle at a minimal constant velocity; this met the design specification of being under that for the lowest-friction tool, the grasper, which required 0.4N.

5.2 Design Evaluation

As shown in the preceding account, the design was constantly re-evaluated and updated by the author during the course of design and fabrication. While two generations of the 1DOF device were built in order to reflect several major changes, the current 2DOF device was a first-generation prototype. Two more subtle design issues were raised in the process of building this device. The first of these was that the rigidity of the rotary axis was less than optimal; when

significant tension was applied to the cable, the drum was tilted slightly toward the capstan. This was attributed to the slight oversizing of the hole for the pair of bearings which supported the shaft and possibly to the material properties of the ABS housing. This slight compliance may have also contributed to the discontinuity felt in the rotary axis. The proposed causes will be explored; if further stiffness is required, the spread between the supporting bearings can be increased at the tradeoff of vertical space, or the housing can be redesigned to support one bearing on each side of the drum. It should be noted, however, that such a housing would need to be made in two pieces in order to insert the drum-coupling; this redesign would also incur a loss in stiffness, suggesting that the benefit may be limited. It would further introduce a tradeoff in terms of device weight/volume and design simplicity.

Two cable-management issues in the rotary drum design were addressed as well. The first was the addition of flanges at the rims of the cable pathway in order to prevent accidental slipping of the cable off the drum. The second came as the result of a design review by David Robinson of the MIT Leg Laboratory, and concerned a sharp cable radius in the tensioning device. The original and redesigned drums are shown in Figure 5-3 below.

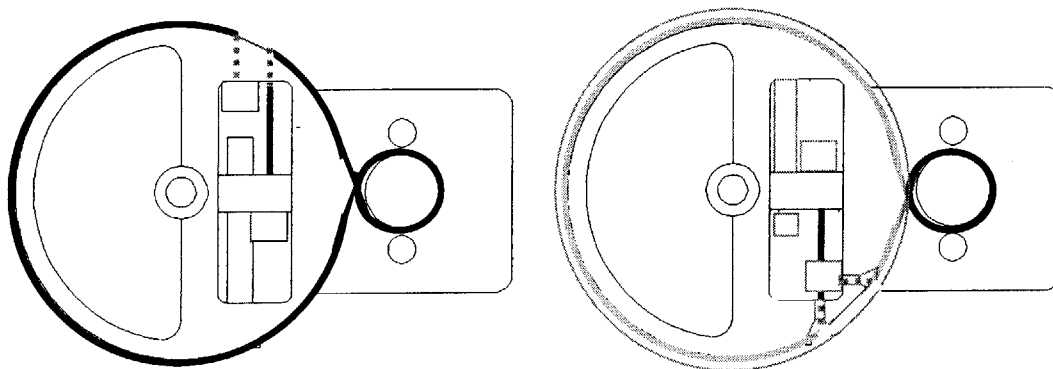


Figure 5-3. Original and redesigned cable management for the rotary drum.

In the new design both angles of entry are greater than 90 degrees, and the entrance holes are chamfered in order to further improve the conditions for the cable.

Chapter 6

Conclusions and Extensions

In conclusion, through a great deal of front-end design work and careful and constant re-evaluation, a force-feedback system which met each category of requirements was developed. The 1DOF device is already in use at the MIT Touch Lab for the simulated catheter insertion procedure mentioned earlier. During winter 1999-2000 the current 2DOF prototype, with the above changes to the rotary drum, will be integrated with the software simulation currently in development at the Draper Laboratory. A second complete haptic display device will be built in order to simulate two-handed tasks such as suturing and complex retraction, and to test the hypothesis that haptic feedback may be even more critical in procedures which require “cooperation” between the surgeons hands.

The need to do more extensive and quantitative user testing is clearly acknowledged. The questions to be answered lie at two levels. First, each device should be used by a number of experienced and training laparoscopic surgeons to gain feedback on the devices, and the simulation setup as a whole, might be further improved. Perhaps more significant, however, would be to answer the initial question – “What is truly important for learning?” – from within the virtual environment. Since it is currently possible to present the surgeon with four of increasing force feedback – (pitch/yaw and insertion using the PHANTOM alone, and added gripper feedback, twist feedback, or both), it would be meaningful to perform experiments to compare the utility of these configurations. It is proposed that the answer may be specific to the surgical task being simulated, since different tasks invoke different motions. A first plausible

test to probe which axes of feedback are important would rate surgeons' performance in designated tasks using each of the tools in random order, so that across surgeons any "learning" effect might be normalized. In this way, it is hoped that a "threshold" device might be defined for each task, as suggested in the sketch of Figure 6-1.

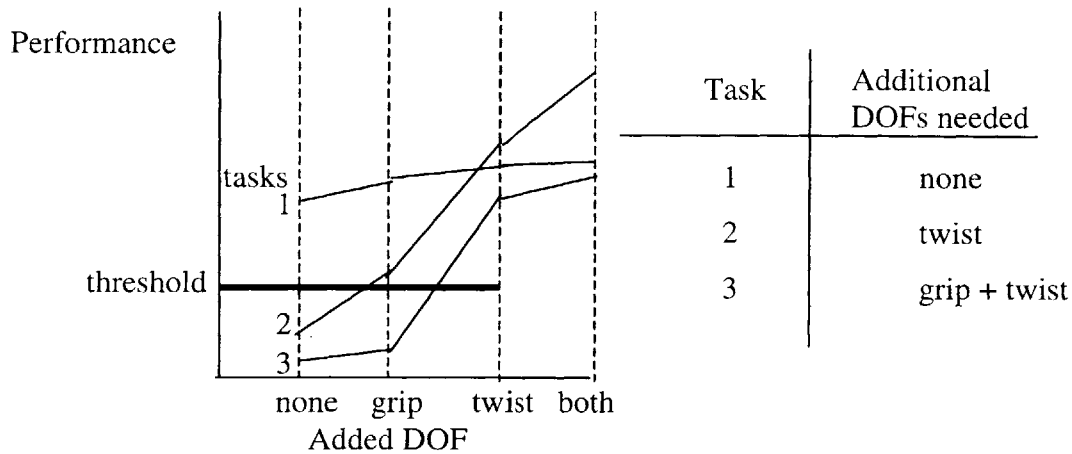


Figure 6-1. Suggested utility test for several tasks.

A second, and likely more important test would be to evaluate the importance of the three different configurations in learning rather than one-time performance. Such a test would require more subjects, since each could be tested on only one of the devices for a given task, and individual learning differences between surgeons would need to be normalized. Fortunately, the researchers at the Touch Lab, who are experienced in psychophysics and user interface investigation methods, have agreed to pursue such investigations. It is further hoped that these devices may see more widespread use, such that meaningful observations from many sources may be contributed.

Bibliography

- Asano, T., Yano, H., and Iwata, H. (1997). Basic Technology of Simulation System for Laparoscopic Surgery in Virtual Environment with Force Display. *Medicine Meets Virtual Reality*, 207-215.
- Burdea, G. (1996). Force and Touch Feedback for Virtual Reality. *John Wiley and Sons*.
- Cao, C., MacKenzie, C., and Payandeh, S. (1996). Task and Motion Analyses in Endoscopic Surgery. *Proceedings of the ASME Dynamics Systems and Control Division*, 58:583-590.
- Carroll, Linda. (1994). Virtual Reality Shapes Surgeons' Skills. *Medical World News*, 35:26-27.
- Dawson, S. (1999). Personal communication.
- Edmond C., Heskamp, D., Sluis, D., Stredney, D. et al. (1997). ENT Endoscopic Surgical Training Simulator, *Studies in Health Technology and Informatics* 39:518-528.
- Gorman, P.J., Lieser, J.D., Murray, W.B., Haluck, R.S., and Krummel, T.M. (1999). Evaluation of Skill Acquisition Using a Force Feedback, Virtual Reality Based Surgical Trainer. *Medicine Meets Virtual Reality*, 121-123.
- Gupta, V., Reddy, N.P. and Pelin, B. (1997). Forces in Laparoscopic Surgical Tools, *Presence* Vol. 6, No. 2 , 218-228.
- Hunter, I.W., Jones, L.A., Sagar, M.A., LaFontaine, S.R., and Hunter, P.J. (1995). Ophthalmic microsurgical robot and Associated Virtual Environment. *Computers in Biology and Medicine*, 25(2):172-182.
- Immersion Corporation (1998), Sales Material for Impulse Engine.
- Immersion Corporation (updated 15 July, 1998, visited 6 August, 1999). "Medical Products". <http://www.immerse.com/>
- Krumm, Hans-Georg (updated 27 June, 1999, visited 6 August, 1999). "Force Feedback for the Karlsruhe Endoscopic Surgery Trainer". Forschungszentrum Karlsruhe. <http://iregt1.iai.fzk.de/DYNAMIK/html/hifee.html>
- Limbs and Things Ltd. (updated 29 June, 1999, visited 6 August, 1999). "Surgical Series – The Body Form". <http://www.limbsandthings.com>
- Madhani, A. (1998) Design of Teleoperated Surgical Instruments for Minimally Invasive Surgery. Doctoral Thesis, Department of Mechanical Engineering, MIT.
- Martin, K.M., Levin, M.D., and Rosenberg, L.B. (1996) Mechanical Interface Having Multiple Grounded Actuators. United States Patent #5,828, 197.

Massie, T.H. and Salisbury, J.K. (1994). The Phantom Haptic Interface: A Device for Probing Virtual Objects. *Dynamic Systems and Control*, pages 295-299.

Rattner, D. (1999) Personal communication.

Rosen, J. , MacFarlene, M., Richards, C., Hannaford, B., and Sinanan, M. (1999). Surgeon-Tool Force/Torque Signatures – Evaluation of Surgical Skills in Minimally Invasive Surgery. *Medicine Meets Virtual Reality*, 290-296.

Rosenberg, L.B. and Stredney, D. (1996). A Haptic Interface for Virtual Simulation of Endoscopic Surgery. *Health Care in the Information Age*, 29: 371-387.

Salisbury, J.K., Srinivasan, M.A. (1997) PHANToM-based haptic interaction with virtual objects, *IEEE Computer Graphics and Applications*, 17(5): 6-10.

Simulab Corporation (visited 6 August, 1999). “Simulab: Surgical Education through Surgical Simulation”. <http://www.simulab.com/GI.html>

Ulrich, K. and Eppinger, S. (1995). *Product Design and Development*. McGraw-Hill, Inc.

Vollenweider, Marc. (6 Aug, 1999). “Project Simulator for Laparoscopic Surgery”. Ecole Polytechnique, Bleuler Laboratory. <http://dmtwww.epfl.ch/isr/mmt/biomed/>

Ward, J.W. (updated 24 January, 1999, visited 6 August, 1999). “Haptic Feedback”. University of Hull, VEGA lab. <http://www2.dcs.hull.ac.uk/VEGA/tech/haptic.html>

Appendices

Appendix A. Requirements analysis data collection forms

A1. Surgeon questionnaire

CURRENT TRAINING:

- procedures, methods, scenario, environment
- most important sensations/cues (visual and haptic) in training

REVIEW OF OTHER SIMULATORS:

- Seen/used other simulators? Which?
- Comments (good, bad, why)?

IMPORTANT FOR GENERAL LAP. TRAINING DEVICE?

- physically removing/inserting tools
- tools free of additional hardware or wires on handle exterior
- appearance of external environment (like OR)
- ability to change trocar insertion points
- rotating tool >360 degrees in trocar (actual angle?)
- feeling tools touching one another
- body wall compliance (motion of trocar insertion point)
- tool end effector forces (e.g. friction from scissors blades w/o tissue between)
- tissue feedback
- proximity of tools -- how close?

PREFERENCE:

A	B
Removable tools	fixed tool (all freedoms) + voice toolchange
Operating room setup	Desktop setup (same haptics) (large w/ bed, tools, etc)

WISH LIST:

- Training Environment/Scenario
- Tools simulated
- Tool proximity (distance between trocars, and between tool tips)
- Motions
- Workspace inside the body
- Range of motion of hands outside the body
 - insertion range
 - angle from perpendicular to body
- Haptic cues
- Tissues palpated
- Other things:

A2. Operating room observation form

	GRASPING		CUTTING			TWISTING		
	tissue	time elapsed	tissue	time elapsed	#cuts	tissue	angle	time elapsed
1								
2								
3								
4								
5								
6								
7								
8								
9								
10								
11								
12								
13								
14								
15								
16								
17								
18								
19								
20								
21								
22								
23								
24								
25								

- tool removals:
- tool proximity:
- workspace:
- tool insertion:
- tool angle:
- body wall motion:
- insertion points:
- teaching comments:

Description of procedure and tools:

Appendix B. Design spreadsheets

B2. Specification Definition

	Metric/Functional Requirement	Specification
Kinematics	DOF	5
	device size "box"	1.5'x2' footprint
	pivot and workspace near surface	
	tool proximity	1 cm
	work volume	6"x6"x6"
	insertion linear travel	6"
	pitch/yaw angular ROM	+/-80 deg
	roll angular ROM	>/= 180 deg
Dynamics/Actuators	max force - insertion	< 8 N
	max tang. force-pitch/yaw torque	<8N/
	max roll (twist) torque	<2.1Nm
	max gripper (shaft) force	17N
	stiffness	as high as possible
	backdrive friction	handle-.4N max force to move
	inertia	as low as possible
	weight comp. Alg.	yes
Configuration	captured + voice control vs. removeable	captured but reconfigurable
	actuate at pivot or at tissue	tissue
	all custom vs. build on other devices	others if appropriate
	actuators on tool exterior	no
	able to enter different ports	yes
	actuated axes	all 5
	tools simulated	graspers, scissors
	tool force signature represented	yes
	real/simulated/none tool interaction	real or simulated
	external environment	real!
	body wall compliance	if possible, not mandatory
Overall	Cost	as low as possible (<\$20K)
	Robustness	important
	Simplicity	yes-use and construction

B3. Benchmarking and Platform Concept Selection

		System						
		Tip actuated			Pivot actuated			
Metric/Functional Requirement		(1)(baseline) PHANToM based	(2) Immersion Patent	(3) Immersion Impulse Engine	(4) Ecole Polytechnique	Force Feedback Device	(6)U. Hull Manipulator	(7) Cable Differential concept
Kinematics	DOF							
	device size "box"	7"x10"						
	pivot and workspace near surface							
	tool proximity							
	work volume	5"x7"x10"						
	insertion linear travel	up to 10"		4"				
	pitch/yaw angular ROM	near +/- 90		+/- 30 deg				
	roll angular ROM	360						
	integration with other axes							
Dynamics/Actuators	max force - insertion	23 oz		28oz			N/A	N/A
	max tang. force-pitch/yaw torque							
	max roll (twist) torque	N/A	N/A	N/A	N/A	N/A	N/A	N/A
	max gripper force	N/A	N/A	N/A	N/A	N/A	N/A	N/A
	high stiffness	20 lb/in						
	low backdrive friction	0.15 oz		<0.5 oz				
	low inertia	<.17lbm						
	weight comp. alg. possible							
Configuration	captured but reconfigurable							
	actuate at tissue							
	building on other devices OK							
	no actuators on tool exterior							
	able to enter different ports							
	all 5 actuated axes							
	tools simulated	N/A	N/A	N/A	N/A	N/A	N/A	N/A
	tool force signature represented	N/A	N/A	N/A	N/A	N/A	N/A	N/A
	real/simulated/none tool interaction							
	realistic external environment body wall compliance							
Overall	low cost	\$10K/\$15K	N/A	8.6K	N/A	N/A	N/A	N/A
	robustness							
	simplicity							
			Better than baseline					
			Same as baseline					
			Worse than baseline					
		NA	Not Applicable					

B4. Gripper Subsystem Concept Selection

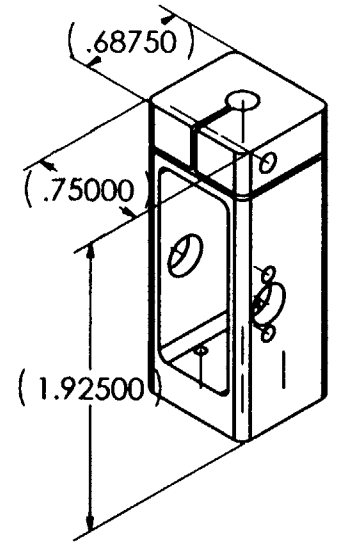
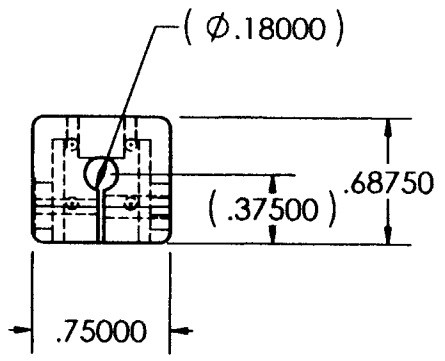
Criterion	Concept		
	linear capstan (baseline)	arc section cable drive	ballscrew
total volume	Same as baseline	Worse than baseline	Worse than baseline
total mass	Same as baseline	Worse than baseline	Worse than baseline
rot inertia	Same as baseline	Worse than baseline	Better than baseline
rot stiffness	Same as baseline	Same as baseline	Same as baseline
rot friction	Same as baseline	Same as baseline	Same as baseline
rot backlash	Same as baseline	Same as baseline	Same as baseline
lin inertia	Same as baseline	Same as baseline	Same as baseline
lin stiffness	Same as baseline	Same as baseline	Same as baseline
lin friction	Same as baseline	Better than baseline	Same as baseline
lin backlash	Same as baseline	Same as baseline	Worse than baseline
lin backdriveability	Same as baseline	Same as baseline	Worse than baseline
useability	Same as baseline	Same as baseline	Same as baseline
simplicity & manufacturing	Same as baseline	Worse than baseline	Worse than baseline
robustness	Same as baseline	Same as baseline	Worse than baseline
cost	Same as baseline	Same as baseline	Worse than baseline

	Better than baseline
	Same as baseline
	Worse than baseline

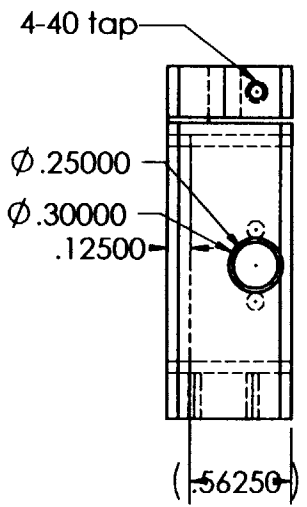
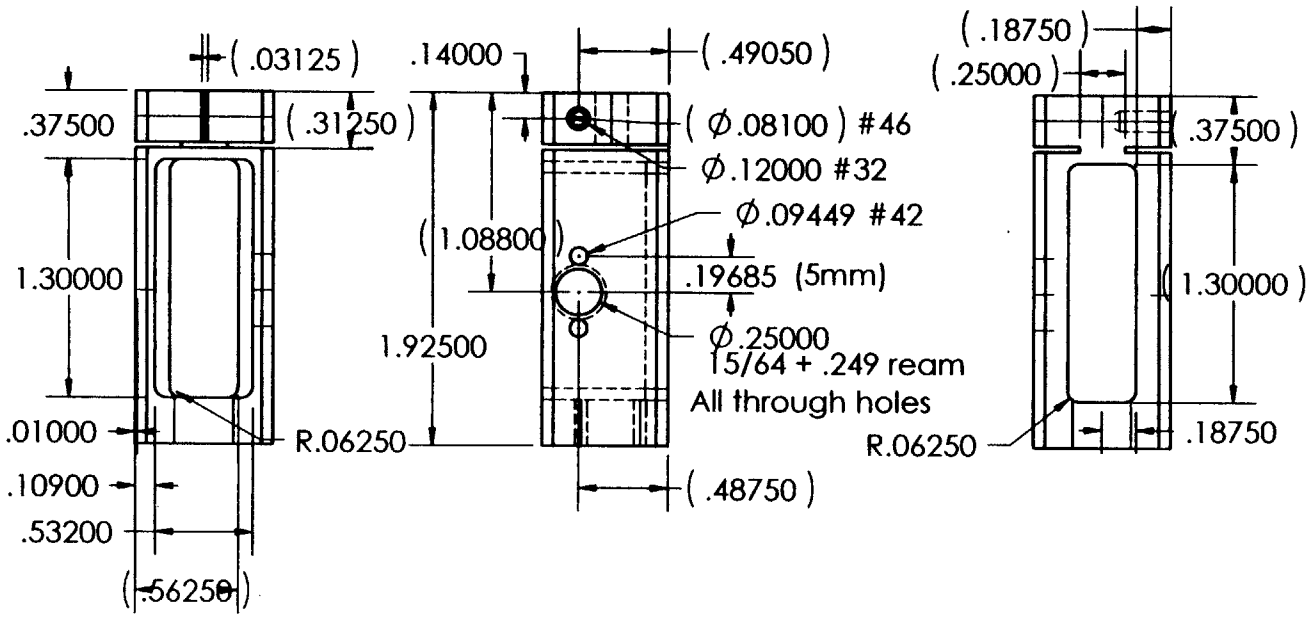
Appendix C. CAD drawings

C1. 1DOF Device

THE INFORMATION CONTAINED IN THIS DRAWING IS THE SOLE PROPERTY OF MIT. ANY REPRODUCTION IN PART OR WHOLE WITHOUT THE WRITTEN PERMISSION OF MIT IS PROHIBITED.

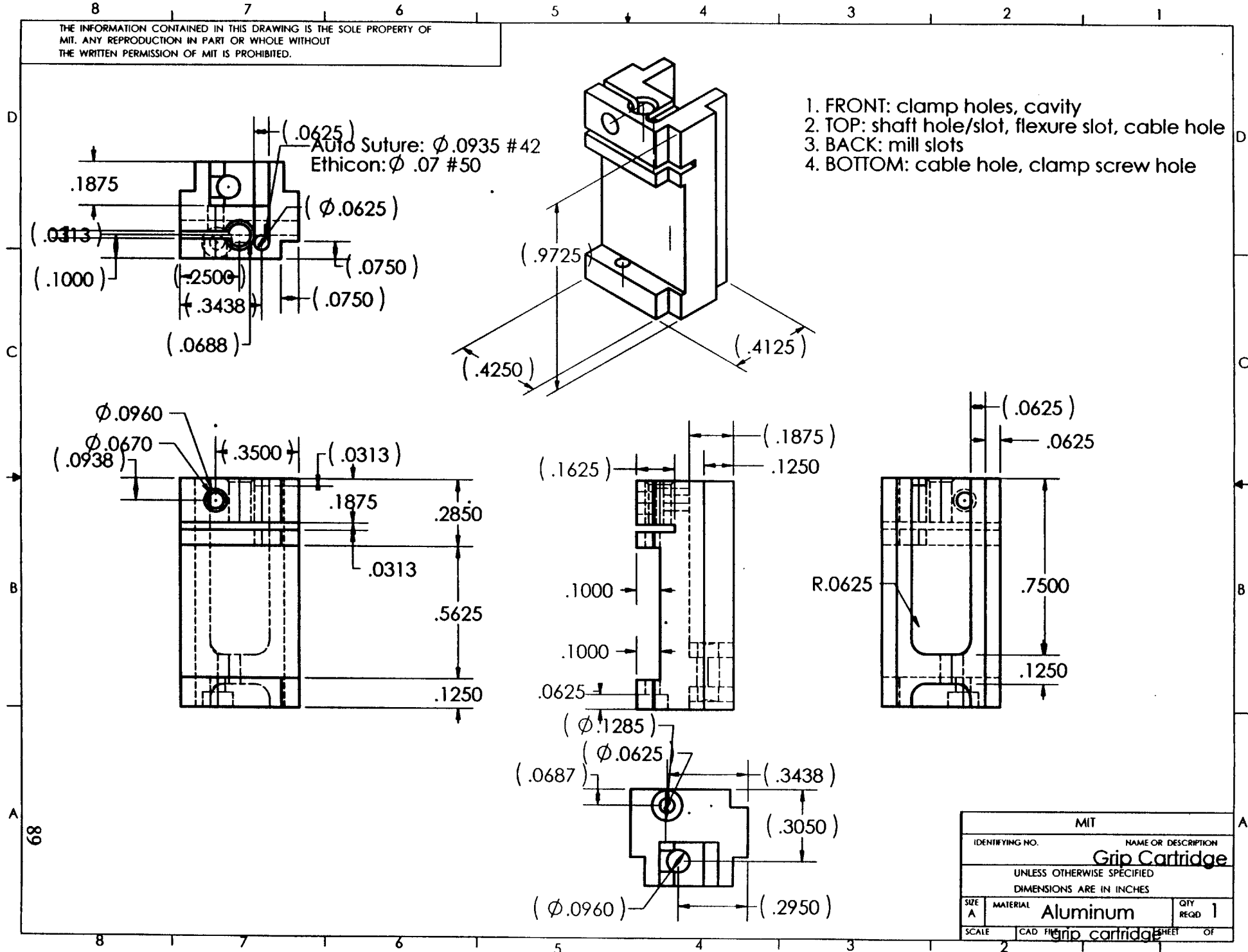


- 1. RIGHT: clamp holes, motor/bearing holes, flexure slot
- 2. FRONT: pocket
- 3. TOP: shaft groove, flexure slots
- 4. BACK: back slot
- 5. LEFT: bearing c-bore, tap clamp hole



MIT			
IDENTIFYING NO.		NAME OR DESCRIPTION	
		1DOF Housing	
UNLESS OTHERWISE SPECIFIED DIMENSIONS ARE IN INCHES			
SIZE	MATERIAL	QTY	REQD
A	Delrin or ABS	1	1
SCALE	CAD FILE	DOF housing	SHEET OF

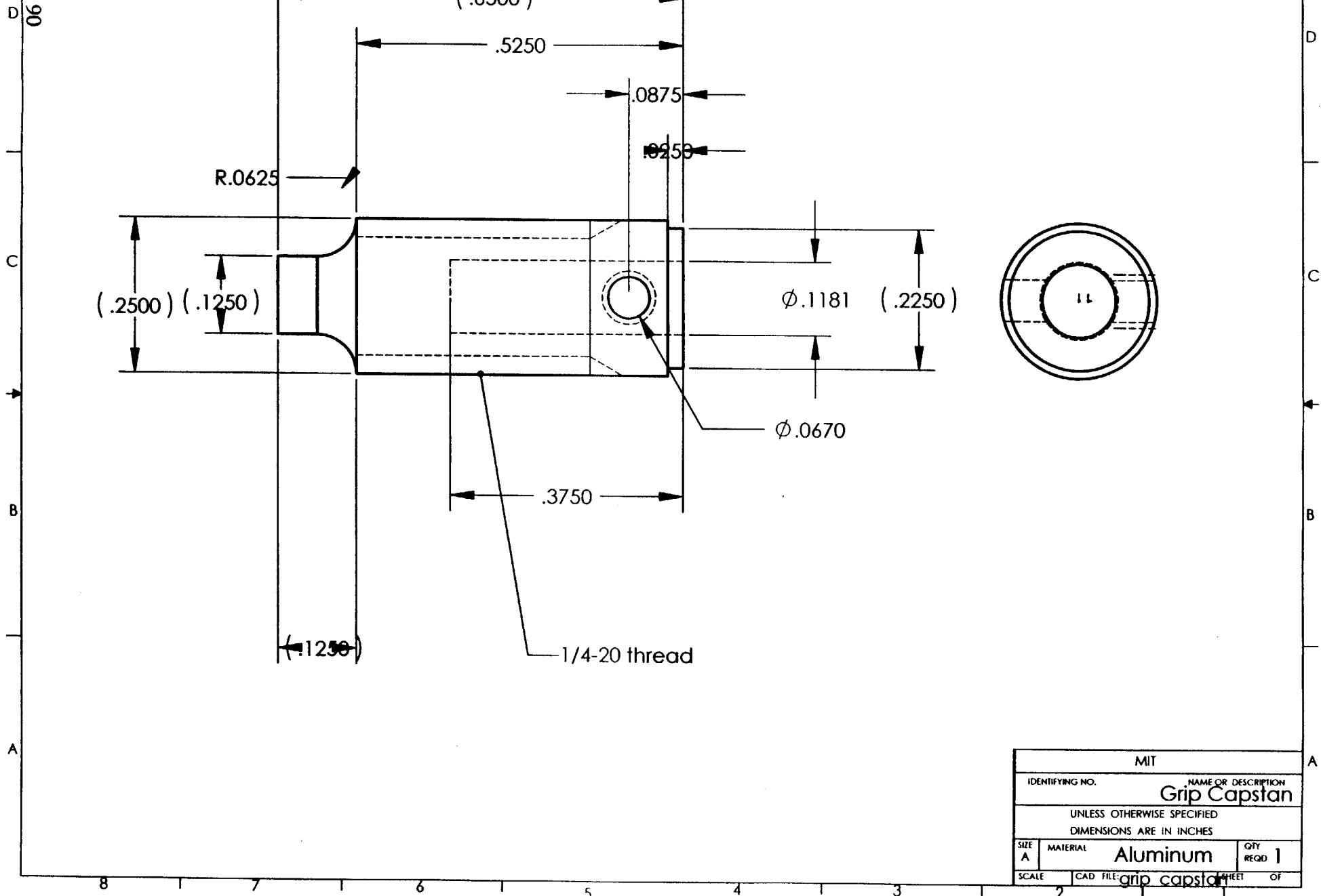
THE INFORMATION CONTAINED IN THIS DRAWING IS THE SOLE PROPERTY OF MIT. ANY REPRODUCTION IN PART OR WHOLE WITHOUT THE WRITTEN PERMISSION OF MIT IS PROHIBITED.



MIT			
IDENTIFYING NO.	NAME OR DESCRIPTION		
	Grip Cartridge		
UNLESS OTHERWISE SPECIFIED			
DIMENSIONS ARE IN INCHES			
SIZE A	MATERIAL	Aluminum	QTY REQD 1
SCALE	CAD FILE	grip cartridge	SHEET OF

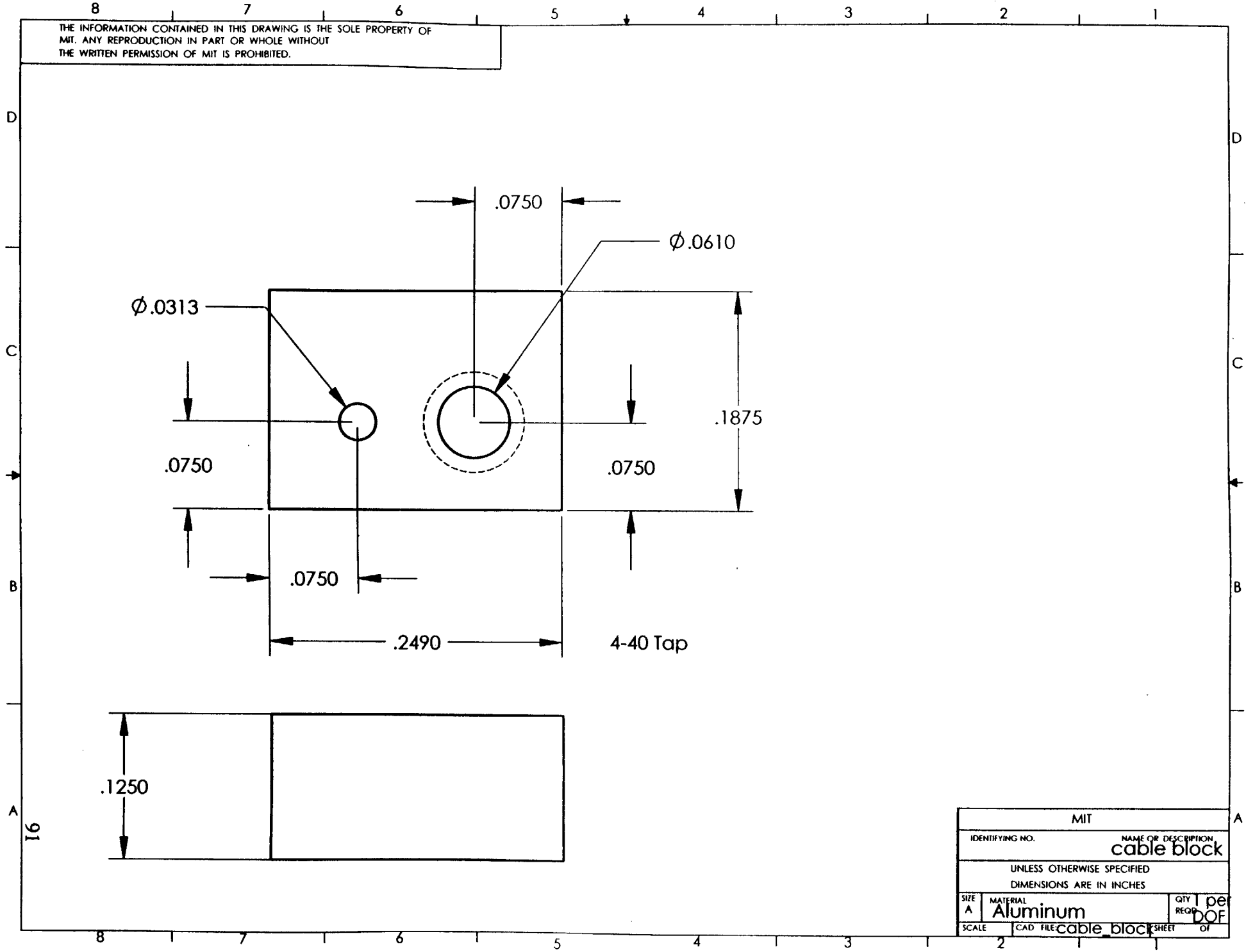
THE INFORMATION CONTAINED IN THIS DRAWING IS THE SOLE PROPERTY OF MIT. ANY REPRODUCTION IN PART OR WHOLE WITHOUT THE WRITTEN PERMISSION OF MIT IS PROHIBITED.

1. Lathe: shaft hole, face & turn motor end
2. Mill: drill & tap setscrew hole
3. Lathe: turn bearing end, threads



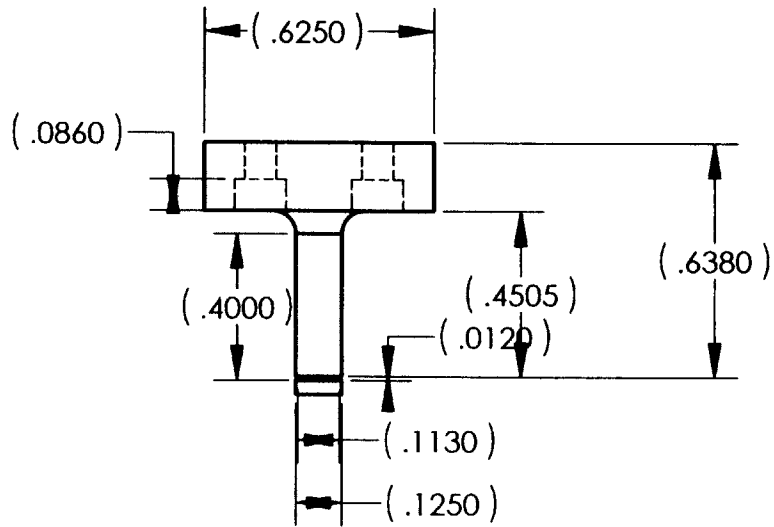
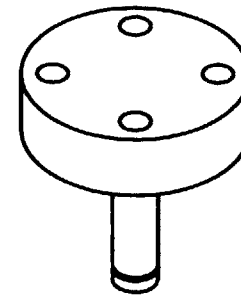
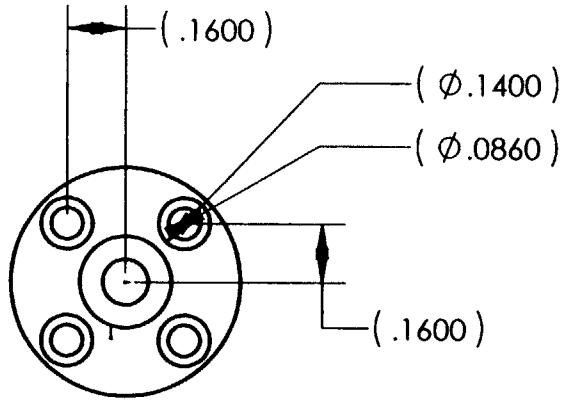
MIT			
IDENTIFYING NO.		NAME OR DESCRIPTION	
		Grip Capstan	
UNLESS OTHERWISE SPECIFIED DIMENSIONS ARE IN INCHES			
SIZE	MATERIAL	QTY	REQD
A	Aluminum	1	1
SCALE	CAD FILE:	SHEET	OF
	grip capstan	1	1

THE INFORMATION CONTAINED IN THIS DRAWING IS THE SOLE PROPERTY OF MIT. ANY REPRODUCTION IN PART OR WHOLE WITHOUT THE WRITTEN PERMISSION OF MIT IS PROHIBITED.



MIT			
IDENTIFYING NO.		NAME OR DESCRIPTION	
		cable block	
UNLESS OTHERWISE SPECIFIED DIMENSIONS ARE IN INCHES			
SIZE A	MATERIAL Aluminum	QTY REQD	1 per DOF
SCALE	CAD FILE: cable_block		SHEET OF

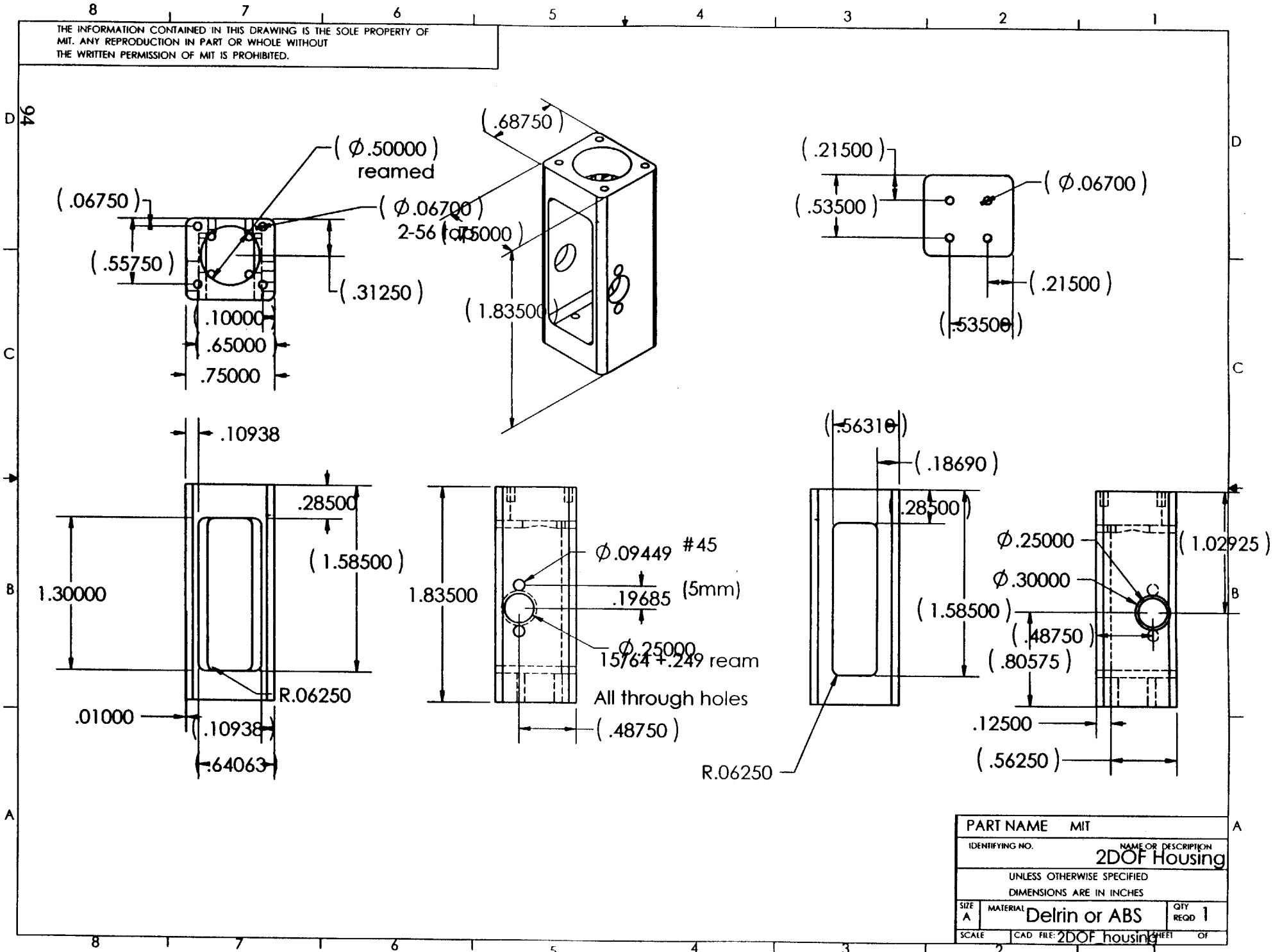
THE INFORMATION CONTAINED IN THIS DRAWING IS THE SOLE PROPERTY OF MIT. ANY REPRODUCTION IN PART OR WHOLE WITHOUT THE WRITTEN PERMISSION OF MIT IS PROHIBITED.



MIT			
IDENTIFYING NO.	NAME OR DESCRIPTION		
	IDOF Mount Post		
UNLESS OTHERWISE SPECIFIED			
DIMENSIONS ARE IN INCHES			
SIZE	MATERIAL	QTY	REQD
A	Aluminum	1	1
SCALE	CAD FILE:	SHEET OF	
	2 IDOF_mount_post_1.dwg	1	

C2. 2DOF Device

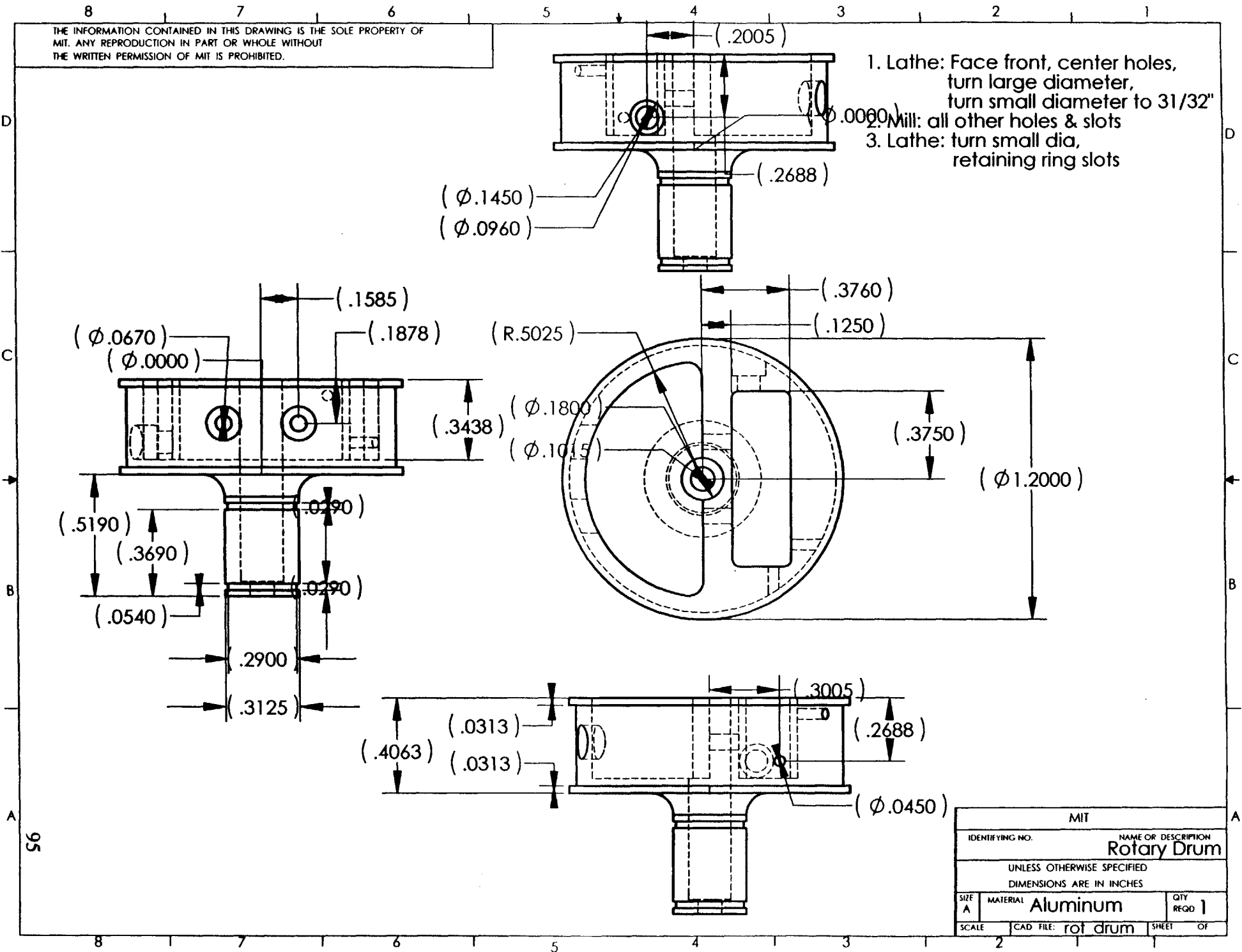
THE INFORMATION CONTAINED IN THIS DRAWING IS THE SOLE PROPERTY OF MIT. ANY REPRODUCTION IN PART OR WHOLE WITHOUT THE WRITTEN PERMISSION OF MIT IS PROHIBITED.



PART NAME		MIT	
IDENTIFYING NO.		NAME OR DESCRIPTION	
		2DOF Housing	
UNLESS OTHERWISE SPECIFIED			
DIMENSIONS ARE IN INCHES			
SIZE	MATERIAL	QTY	REQD
A	Delrin or ABS	1	1
SCALE	CAD FILE:	SHEET	OF
	2DOF housing		

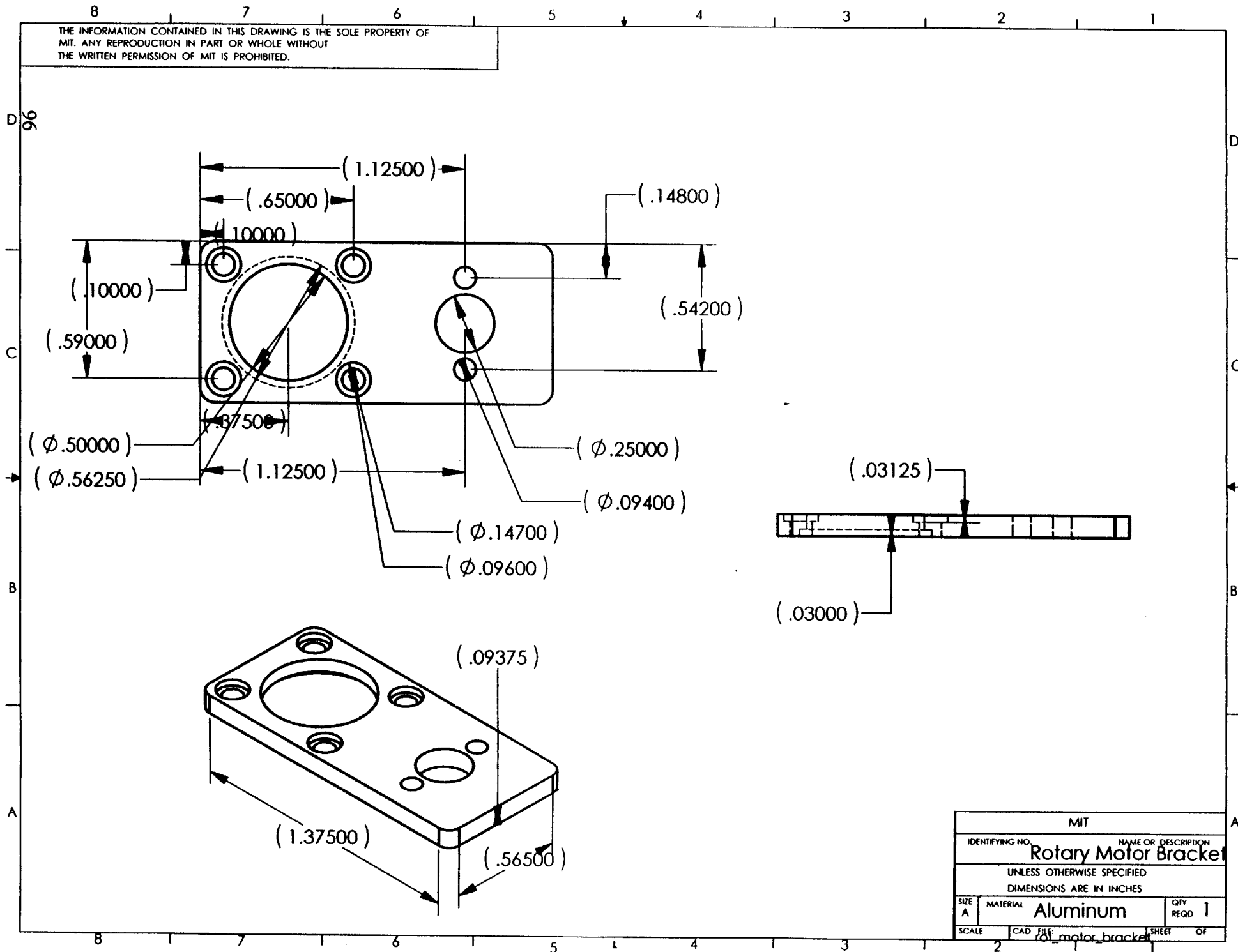
THE INFORMATION CONTAINED IN THIS DRAWING IS THE SOLE PROPERTY OF MIT. ANY REPRODUCTION IN PART OR WHOLE WITHOUT THE WRITTEN PERMISSION OF MIT IS PROHIBITED.

1. Lathe: Face front, center holes, turn large diameter, turn small diameter to 31/32"
2. Mill: all other holes & slots
3. Lathe: turn small dia, retaining ring slots



MIT			
IDENTIFYING NO.		NAME OR DESCRIPTION	
		Rotary Drum	
UNLESS OTHERWISE SPECIFIED			
DIMENSIONS ARE IN INCHES			
SIZE	MATERIAL	QTY	REQD
A	Aluminum	1	1
SCALE	CAD FILE:	SHEET	OF
	rot drum		

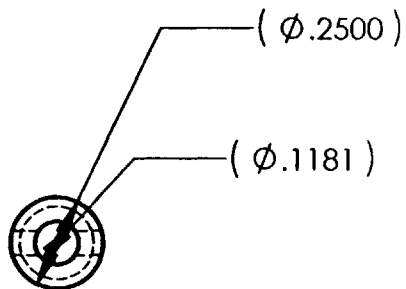
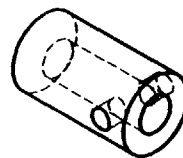
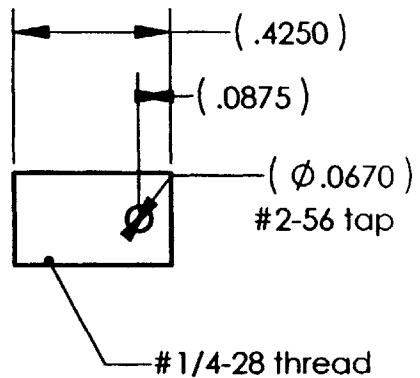
THE INFORMATION CONTAINED IN THIS DRAWING IS THE SOLE PROPERTY OF MIT. ANY REPRODUCTION IN PART OR WHOLE WITHOUT THE WRITTEN PERMISSION OF MIT IS PROHIBITED.



MIT			
IDENTIFYING NO.	NAME OR DESCRIPTION		
	Rotary Motor Bracket		
UNLESS OTHERWISE SPECIFIED			
DIMENSIONS ARE IN INCHES			
SIZE	MATERIAL	QTY	REQD
A	Aluminum	1	
SCALE	CAD FILE	SHEET OF	
	rot_motor_bracket		

THE INFORMATION CONTAINED IN THIS DRAWING IS THE SOLE PROPERTY OF
MIT. ANY REPRODUCTION IN PART OR WHOLE WITHOUT
THE WRITTEN PERMISSION OF MIT IS PROHIBITED.

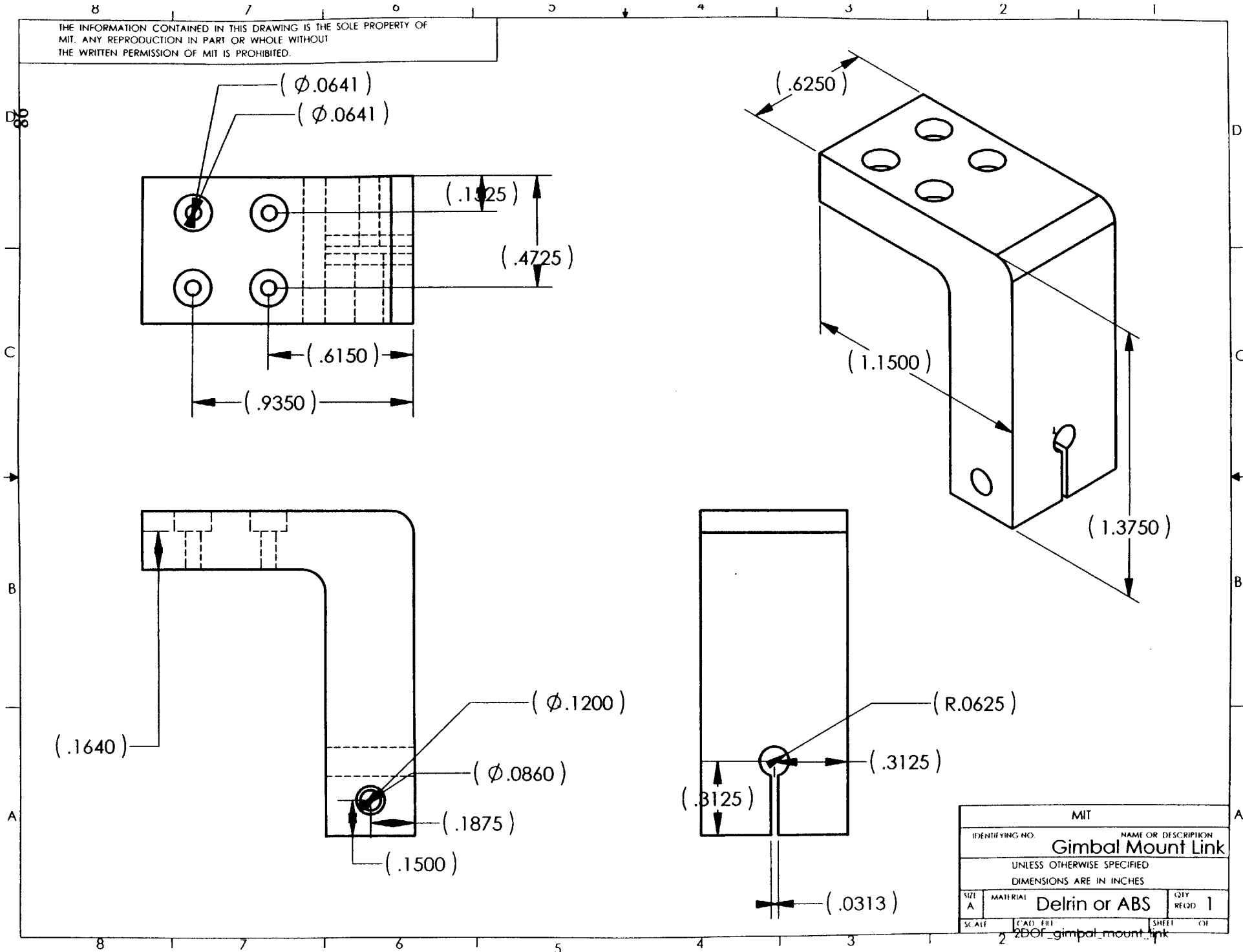
1. lathe: face ends
2. mill: drill (through all) and tap setscrew hole
3. lathe: thread body



97

MIT			
IDENTIFYING NO.		NAME OR DESCRIPTION	
		Rotary Capstan	
UNLESS OTHERWISE SPECIFIED DIMENSIONS ARE IN INCHES			
SIZE A	MATERIAL Aluminum	QTY REQD 1	
SCALE	CAD FILE of capstan	SHEET	OF

THE INFORMATION CONTAINED IN THIS DRAWING IS THE SOLE PROPERTY OF MIT. ANY REPRODUCTION IN PART OR WHOLE WITHOUT THE WRITTEN PERMISSION OF MIT IS PROHIBITED.



MIT			
IDENTIFYING NO.		NAME OR DESCRIPTION	
		Gimbal Mount Link	
UNLESS OTHERWISE SPECIFIED			
DIMENSIONS ARE IN INCHES			
SIZE	MATERIAL	QTY	REQD
A	Delrin or ABS	1	1
SCALE	CAD FILE	SHEET	OF
	2 2DOF_gimbal_mount_link		

Appendix D. Device Manual

PHANToM Requirements

- Sensable Devices PHANToM 1.0 SW (Standard Workspace)
- 6-axis amplifier card and box, or 2 3-axis cards and boxes

Component Specifications

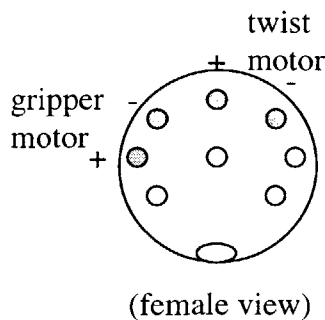
Gripper axis

- 1 Maxon Motor Rare Earth 16mm diameter, 4.5W, 2 shafts, 24V with 16mm diameter metal 19:1 planetary gearbox and 13mm Digital Magnetic Encoder
- 1 Flanged, shielded ball bearing, 0.125in ID, 0.25 in OD

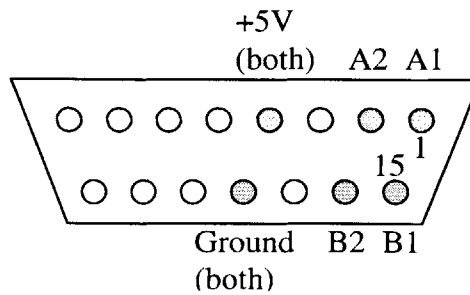
Twist axis

- 1 Maxon Motor Rare Earth 16mm diameter, 4.5W, 2 shafts, 24V with 16mm diameter metal 4.4:1 planetary gearbox and 13mm Digital Magnetic Encoder
- 2 Flanged, shielded ball bearings, 0.3125in ID, 0.5 in OD

Wiring Diagram



+ Brown
- Black



Encoder A - white
Encoder B - green
+5V - red
Ground - black

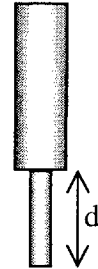
Device Specifications and Simulation Variables

- Device Weight
 - 1DOF: 81.8g
 - 2DOF: 164.3g

- Encoder Count to Position Conversions
 - Gripper: 0.0164mm/count
 - Twist: 0.36 degrees/count
- Output Force/Torque to Input Motor Current Conversions
 - Gripper: 0.1 A/N
 - Twist: 0174 A/Nm

Tool Preparation Specifications

- Cut away end effector.
- Cut back outer shaft (Dremel reinforced cutoff wheel used here).
For handle at mid-travel, $d =$
 - 1DOF: 0.37"
 - 2DOF: 0.30"



Appendix E. Program Code

```
/******
```

```
Ela Ben-Ur  
PHANTOM I/O commands modeled after code by Chris Tarr  
8-6-99
```

This is a simple demonstration program which can be run with either the 1DOF or 2DOF laparoscopic tool actuator devices. It coordinates PHANTOM IO commands for the PHANTOM with "lunchbox" commands for the device, and brings in Open Inventor for graphics. The simulation consists of a large compliant sphere which the user can grab and twist.

```
*****/
```

```
#include <stdlib.h>  
#include <process.h>  
#include <windows.h>  
#include <conio.h>  
#include <fstream.h>  
#include <stdio.h>  
#include <math.h>  
  
#include <typeinfo.h>  
#include <Mmsystem.h>  
// HAPTICS  
#include "lunchbox.h"  
#include "D:\phantom\basicio\lib\iolib\phantom.h"  
#include "D:\phantom\basicio\lib\os_extender\os_extender.h"  
  
// OPENGL  
#include <GL/gl.h>  
#include <GL/glu.h>  
#include <GL/GLaux.h>  
  
// INVENTOR  
#include "stdinventor.h"  
// specific nodes used  
#include <Inventor/nodes/SoCone.h>  
#include <Inventor/nodes/SoRotationXYZ.h>  
#include <Inventor/Xt/viewers/SoXtWalkViewer.h>
```

```

#ifndef TRUE
#define TRUE 1
#define FALSE 0
#endif

/* Device parameters */
#define SIM_BASE_ADDR 0x200
// #define DEVICE_MASS 0.0861 /*1DOF kg*/ / 0.1686 /*2DOF kg*/
#define DEVICE_MASS .14
#define GRIP_COUNTS_TO_MM 0.0164
#define GRIP_NEWTONS_TO_AMPS 0.01
#define TWIST_COUNTS_TO_DEGREES 0.36
#define TWIST_Nm_TO_AMPS 0.174

/* sphere radius in mm */
#define CURSOR_RADIUS 5.0
/* stiffness of sphere in N/mm */
#define GRIP_STIFFNESS 3/7.5
#define TWIST_STIFFNESS .01
/* location of floor in mm */
#define FLOOR_Z -20.0

/* stiffness of floor in N/mm */
#define FLOOR_STIFFNESS 0.1

/* HAPTICS globals */
int phantom_id;
int phantom_id2;
float position[3]={0,0,0}, grip_pos, twist_pos;
long int enc;
static char floor_flag=0;
static char grab_flag=0;
//float grip_force;

/* GRAPHICS globals */
static SoSeparator *g_root;
static SoTransform *g_cursorTransform;
SoXtRenderArea *g_RenderArea;

/* HAPTICS funtion Declarations */
SCHEDULER_CALLBACK servoLoopCallback(void *userData);
SCHEDULER_CALLBACK servoLoopCallback2(void *userData);
void generate_floor_force(float pos[], float force[], float grip_pos, float *grip_force, float
twist_pos, float *twist_torque);

```

```

void grav_comp_force(float force[]);
/* GRAPHICS function declarations */
void __cdecl updateProgramCB(void *data, SoSensor *s);

void main (int, char **argv)
{
// **** GRAPHICS*****
// INITIALIZING ROUTINES*****
    // initialize inventor, get main window
    Widget g_Window=SoXt::init(argv[0]);
    g_RenderArea = new SoXtRenderArea(g_Window);
    //SoDB::init();
    // create scene standards
    g_root=new SoSeparator;

    g_root->ref();
    SoPerspectiveCamera *g_Camera=new SoPerspectiveCamera;
    g_root->addChild(g_Camera);
    SoDirectionalLight *g_light = new SoDirectionalLight;
    g_root->addChild(g_light);

// CUSTOM SCENE CREATION*****
    // SPHERE
        SoSeparator *g_sphereSep = new SoSeparator;
        SoTransform *g_sphereTransform = new SoTransform;
        g_sphereTransform->translation.setValue(SPHERE_X, SPHERE_Y,
SPHERE_Z);
        g_sphereSep->addChild(g_sphereTransform);
        // appearance
        SoMaterial *g_sphereMaterial = new SoMaterial;
        g_sphereMaterial->diffuseColor.setValue(.8, 0.2, 0.0);
        g_sphereMaterial->transparency.setValue(.2);
        g_sphereSep->addChild(g_sphereMaterial);
        //shape
        SoSphere *g_sphere = new SoSphere;
        g_sphere->radius = SPHERE_RADIUS;
        g_sphereSep->addChild(g_sphere);

        g_root->addChild(g_sphereSep);

// CURSOR
        SoSeparator *g_cursorSep = new SoSeparator;

        g_cursorTransform = new SoTransform;

```

```

        g_cursorTransform->translation.setValue(SPHERE_X, SPHERE_Y,
        SPHERE_Z+30);
        g_cursorSep->addChild(g_cursorTransform);

        SoMaterial *g_cursorMaterial = new SoMaterial;
        g_cursorMaterial->diffuseColor.setValue(0.8, 0.8, 0.8);
        g_cursorSep->addChild(g_cursorMaterial);

        SoSphere *g_cursor = new SoSphere;
        g_cursor->radius = CURSOR_RADIUS;
        g_cursorSep->addChild(g_cursor);

        g_root->addChild(g_cursorSep);

// RENDERING ROUTINES *****
        //camera qualities
        g_Camera->viewAll(g_root, g_RenderArea->getViewportRegion());
        //render window qualities
        g_RenderArea->setTitle("Practice");
        //rendering commands
        g_RenderArea->setSceneGraph(g_root);

//*****
//*****HAPTICS*****
//*****
//INITIALIZATION*****
        int dummy;
        /* start OS Extender (must be done first) */
        initOSExtender();

        /* Initialize the phantom */
        phantom_id = init_phantom("phantom.ini");
        if (phantom_id < 0) {
            printf("Error initializing PHANToM 1\n");
            getchar();
            exit(1);
        }

        phantom_id2 = init_phantom("phantom2.ini");
        if (phantom_id2 < 0) {
            printf("Error initializing PHANToM 2\n");
            getchar();
            exit(1);
        }

```



```

/* Tell user to hold phantom in reset position */
printf("Hold PHANToM in neutral position and press enter\n");
printf("Do not use reset arm on PHANToM model 3.0\n");
getchar();

/* reset the phantom - this calibrates the sensors on the PHANToM.
   It must be done before reading position or writing forces. This function
   must be called while the PHANToM is in the reset position otherwise the
   positions read from the PHANToM will be incorrect. */
if (phantom_reset(phantom_id)) {
    disable_phantom(phantom_id);
    printf("Error resetting PHANToM 1\n");
    getchar();
    exit(1);
}
if (phantom_reset(phantom_id2)) {
    disable_phantom(phantom_id2);
    printf("Error resetting PHANToM 2\n");
    getchar();
    exit(1);
}

/* start the servo loop - it does all the work:
   updates phantom, calculates reaction forces
   and sends forces to the phantom. We use os_extender
   function startServoLoop so that this will run in real time.
   Pass startServoLoop phantom id as user data
   it will need for other iolib functions. */
startServoLoop(servoLoopCallback, (void *) &dummy);

//SET UP CALLBACKS/SENSORS
SoIdleSensor *updateProgramSensor = new SoIdleSensor(updateProgramCB,
NULL);
updateProgramSensor->schedule();

//RENDERING ROUTINES *****
// g_RenderArea->show();
// SoXt::show(g_Window);
// SoXt::mainLoop();
}

void __cdecl updateProgramCB(void *data, SoSensor *s)
{

```

```

    g_cursorTransform->translation.setValue(position[0],position[1],position[2]);
    g_RenderArea->render();
    s->schedule();
}

SCHEDULER_CALLBACK servoLoopCallback(void *userData)
{
//    int phantom_id = *((int *) userData);
    int error;

    /* gripper variables */

    /*PHANToM variables*/

    float grip_current= 0.0, twist_current = 0.0;
    float force[3], object_force[3], zero_forces[3]={0,0,0}, grip_force, twist_torque;
    static int first_time = TRUE;

    /* the time first through the loop we need to enable the PHANToM forces.
       We don't do this before starting the servo loop because the
       hardware timeout circuit will disable the forces before the servo loop
       begins. */
    if (first_time)
    {
        if (error = enable_phantom_forces(phantom_id)) {
            disable_phantom(phantom_id);
            printf("Error enabling PHANToM 1 forces\n");
            getchar();
            exit(1);
        }
        /*if (error = enable_phantom_forces(phantom_id2)) {
            disable_phantom(phantom_id2);
            printf("Error enabling PHANToM 2 forces\n");
            getchar();
            exit(1);
        }

        first_time = FALSE;
    }

    /* Update the PHANToM
       This updates the current state (position, velocity etc...)
       of the PHANToM. Must be called once and only once every servo loop
       otherwise values returned by get_phantom_pos, get_phantom_vel, etc..

```

```

        will not be correct */
if (update_phantom(phantom_id)) {
    disable_phantom(phantom_id);
    printf("Error updating PHANToM\n");
    getchar();
    exit(1);
}

/* Get the position from memory */
get_phantom_pos(phantom_id, position);
/*grip position */
    static long int old_enc=0;
    enc=EncoderRead(0,old_enc, SIM_BASE_ADDR); /*encoder counts*/
    grip_pos=enc*GRIP_COUNTS_TO_MM;

/*twist position*/
    enc=EncoderRead(1,old_enc, SIM_BASE_ADDR);
    twist_pos=enc*TWIST_COUNTS_TO_DEGREES;

/* Rezero the forces - must be done every servo loop */
zero_vector(force);
zero_vector(object_force);
grip_force=twist_torque=0;

/* Create force for the sphere */
//generate_sphere_force(position, object_force, grip_pos, &grip_force, twist_pos,
&twist_torque);
//add_vectors(force, object_force);

/* Create force for the floor */
generate_floor_force(position, object_force, grip_pos, &grip_force, twist_pos,
&twist_torque);
add_vectors(force, object_force);

//grav_comp_force(object_force);
add_vectors(force, object_force);
grip_current = (float)(grip_force*GRIP_NEWTONS_TO_AMPS)-0.07;
twist_current=(float)(twist_torque*TWIST_Nm_TO_AMPS)+0.11;

/* In this example we simply superimpose (add) all the force vectors.
    For some configurations of virtual environments, this may not be valid */

/* Send the force information to the PHANToM and error check */
if (send_phantom_force(phantom_id, force)) {
    disable_phantom(phantom_id);
    printf("Error sending PHANToM 1 forces\n");
}

```

```

        getchar();
        exit(1);
    }/**/
    if (send_phantom_force(phantom_id2, zero_forces)) {
        disable_phantom(phantom_id2);
        printf("Error sending PHANToM 2 forces\n");
        getchar();
        exit(1);
    }/**/

AmpOutput(0, grip_current, SIM_BASE_ADDR);
AmpOutput(1, twist_current, SIM_BASE_ADDR);
}

/*    generate_floor_force
 *    Given the phantom position this function
 *    calculates the reaction force for the floor.
 */
void generate_floor_force(float pos[], float force[], float grip_pos, float *grip_force, float
twist_pos, float *twist_torque)
{
    /* if phantom point is below floor we need to calculate reaction
        force otherwise reaction force is zero */
    if (pos[PHTM_Z] < FLOOR_Z)
    {
        /* reaction force is stiffness times penetration of floor */
        force[PHTM_Z] = FLOOR_STIFFNESS * (FLOOR_Z - pos[PHTM_Z]);
        if (floor_flag==0)
        {
            EncoderReset(0, SIM_BASE_ADDR);
            EncoderReset(1, SIM_BASE_ADDR);
        }
        floor_flag=1;
        grab_flag=1;
        *grip_force=(float)(GRIP_STIFFNESS*grip_pos);
        *twist_torque=(float)(TWIST_STIFFNESS*twist_pos);

    }
    else
    {
        if (grab_flag==1)
        {
            if (grip_pos<-1)
            {
                force[PHTM_Z] = FLOOR_STIFFNESS * (FLOOR_Z -
pos[PHTM_Z]);
                *grip_force=(float)(GRIP_STIFFNESS*grip_pos);
                *twist_torque=(float)(TWIST_STIFFNESS*twist_pos);
            }
        }
    }
}

```

```

        }
        else
        {
            grab_flag=0;
            force[PHTM_Z] = 0.0;
        }
    }

    else
    {
        force[PHTM_Z] = 0.0;
        floor_flag=0;
    }
}

/* since floor is x-z plane there is never any reaction force
   along x and z axes */
force[PHTM_X] = 0.0;
force[PHTM_Y] = 0.0;
}

void grav_comp_force(float force[])
{
    force[0]=force[1]=0.0;
    force[2]=DEVICE_MASS*9.8;
}

```

```

/*****
*
* Vinay Shah
* 01-14-97
*
* This subprogram contains functions used by the SensAble Technologies
* Power Amplifier Box. One function is used to read optical encoders.
* The box provides 16 bits of information. This subprogram returns 32
* bits of information by checking for wrap-around. The next two functions
* are used to enable and disable the amplifiers. Since the default
* amp setting on the box is on-full-power, amp output is first commanded
* to zero before enabling or disabling.
*
* Functions Provided:
* LunchboxInit - resets encoders, zeros amp output, and enables amps
* AmpDisable - disables amps and zeros amp output
* AmpEnable - zeros amp output and enables amps
* AmpOutput - output desired current
* EncoderReset - resets individual encoder and zeros amp output
* EncoderRead - reads individual encoder
* DevFault - checks for device fault
*
* Additional functions written by Mark Ottensmeyer
* PhantResetAll - resets encoders without cycling amplifiers
* PhantReadAngles - returns current joint angles in radians
* PhantGetPos - returns endpoint position in meters (assumes
* EncoderReset() was called at
origin)
* PhantForceOut - calculates current output for desired force input
*
*****/

```

```

/** include files */

```

```

#include "d:\users\canuck\utils\lunchbox.h"

```

```

void LunchboxInit(int baseaddr)
/* baseaddr - base address of the PC Interface Card for the amp */
{
    int axis;

    AmpDisable(baseaddr);
    for(axis = 0; axis < 3; axis++) EncoderReset(axis, baseaddr);
    AmpEnable(baseaddr);
}

```

```

void AmpDisable(int baseaddr)
/* baseaddr - base address of the PC Interface Card for the amp */
{
    int axis;

    LB_BYTE_OUT(baseaddr, LB_DIGITAL, 0xBF);
    for(axis = 0; axis < 3; axis++) AmpOutput(axis, 0.0, baseaddr);
}

void AmpEnable(int baseaddr)
/* baseaddr - base address of the PC Interface Card for the amp */
{
    int axis;

    for(axis = 0; axis < 3; axis++) AmpOutput(axis, 0.0, baseaddr);
    LB_BYTE_OUT(baseaddr, LB_DIGITAL, 0x3F);
}

void EncoderReset(int channel, int baseaddr)
/* channel - integer between 0 and 5 indicating which encoder channel */
/* baseaddr - base address of the PC Interface Card for the amp */
{
    AmpDisable(baseaddr);
    LB_BYTE_OUT(baseaddr, LB_DIGITAL, 0xff - (0x1 << channel));
    LB_BYTE_OUT(baseaddr, LB_DIGITAL, 0xff);
}

long EncoderRead(int channel, long old_enc, int baseaddr)
/* channel - integer between 0 and 5 indicating which encoder channel */
/* baseaddr - base address of the PC Interface Card for the amp */
/* old_enc - previous encoder reading (used to detect overflow) */
{
    char high, low;
    long dif;

    high = (char) LB_BYTE_IN(baseaddr, 2*channel);
    low = (char) LB_BYTE_IN(baseaddr, 2*channel+1);

    dif = ((0xff & (long) high) << 8) + (0xFF & (long) low) - old_enc;
    if(dif & (long) 0x8000) dif |= -(long) 0x8000;
    else dif &= (long) 0x7fff;

    old_enc += dif;
    return(old_enc);
}

```

```

void AmpOutput(int channel, float amps, int baseaddr)
/* channel - integer between 0 and 5 indicating which encoder channel */
/* amps    - desired current (A) from amplifier */
/* baseaddr - base address of the PC Interface Card for the amp */
{
    long value, zero;

    switch(channel){
        case 0: zero = LB_DAC_ZERO_0; break;
        case 1: zero = LB_DAC_ZERO_1; break;
        case 2: zero = LB_DAC_ZERO_2; break;
        case 3: zero = LB_DAC_ZERO_3; break;
        case 4: zero = LB_DAC_ZERO_4; break;
        case 5: zero = LB_DAC_ZERO_5; break;
    }

    value = LB_AMP_TO_DAC(amps, zero);

    if (value > LB_DAC_MAX) value = LB_DAC_MAX;
    else if(value < LB_DAC_MIN) value = LB_DAC_MIN;

    LB_BYTE_OUT(baseaddr, 2*channel+1, (value >> 8) & 0xFF);
    LB_BYTE_OUT(baseaddr, 2*channel,  value & 0xFF);
}

int DevFault(int baseaddr)
/* baseaddr - base address of the PC Interface Card for the amp */
{
    return(LB_BYTE_IN(baseaddr, LB_DIGITAL) & 0x01);
}

int StylusSwitch(int baseaddr)
{
    return(LB_BYTE_IN(baseaddr, LB_DIGITAL) & 0x02);
}

/* here-on written by Mark Ottensmeyer */
void PhantResetAll(int baseaddr) {
    int channel;
    for(channel=0;channel<3;channel++) {
        LB_BYTE_OUT(baseaddr, LB_DIGITAL, 0x3f - (0x1 << channel));
        LB_BYTE_OUT(baseaddr, LB_DIGITAL, 0x3f);
    }
}

```



```

void PhantReadAngles(int baseaddr, float radians[3])
{
    static long int old_enc[3]={0,0,0};
    char i;

    for(i=0;i<3;i++) {
        radians[i]=(float)EncoderRead(i,old_enc[i],baseaddr)/21164.;
    }
}

void PhantGetPos(int baseaddr, float millimeters[3])
{
    /* angle 1 is corrected to include the offset due to the Phantom
       arm "dogleg" */
    float angles[3], S0, C0, S1p, C1p, S2, C2;
    PhantReadAngles(baseaddr, angles);
    S0=sin(angles[0]); C0=cos(angles[0]);
    S1p=sin(angles[1]+Ang23); C1p=cos(angles[1]+Ang23);
    S2=sin(angles[2]); C2=cos(angles[2]);
    millimeters[POSX]=-S0*(L_1*C2-L_23*S1p);
    millimeters[POSY]=(L_1*S2+L_23*C1p) - L_2;
    millimeters[POSZ]=C0*(L_1*C2-L_23*S1p) - (L_1+L_3);
    return;
}

void PhantForceOut(int baseaddr, float newtons[3]) {
    float torque[3];
    PhantForceOut2(baseaddr,newtons,torque,GCOMP_ON);
    return;
}

void PhantForceOut2(int baseaddr, float newtons[3], float torque[3], int gcomp)
{
    int i;
    float angles[3], amps[3], forcemag=0, S0, C0, S1p, C1p, S2, C2;
    float S1, C1;

    for(i=0;i<3;i++) forcemag+=newtons[i]*newtons[i];
    // nosound();
    if((forcemag=sqrt(forcemag))>MAXFORCE) {
    //     sound(200);
        for(i=0;i<3;i++) newtons[i]=newtons[i]*MAXFORCE/forcemag;
    }
    PhantReadAngles(baseaddr,angles);
    S0=sin(angles[0]); C0=cos(angles[0]);
    S1p=sin(angles[1]+Ang23); C1p=cos(angles[1]+Ang23);
}

```

```

S1=sin(angles[1]); C1=cos(angles[1]);
S2=sin(angles[2]); C2=cos(angles[2]);
torque[0]= -C0*(L_1*C2 - L_23*S1p)*newtons[FX]
           -S0*(L_1*C2 - L_23*S1p)*newtons[FZ];
torque[1]= -1*(L_23*S0*C1p*newtons[FX] - L_23*S1p*newtons[FY]
           - L_23*C0*C1p*newtons[FZ]);
torque[2]= -1*(L_1*S0*S2*newtons[FX] + L_1*C2*newtons[FY]
           - L_1*C0*S2*newtons[FZ]); /**/
/* torque[0]= -C0*(L_1*C2 - L_23*S1)*newtons[FX]
           -S0*(L_1*C2 - L_23*S1)*newtons[FZ];
torque[1]= -1*(L_23*S0*C1*newtons[FX] - L_23*S1*newtons[FY]
           - L_23*C0*C1*newtons[FZ]);
torque[2]= -1*(L_1*S0*S2*newtons[FX] + L_1*C2*newtons[FY]
           - L_1*C0*S2*newtons[FZ]); /**/
if(gcomp==GCOMP_ON) {
    torque[2]+= (-61.2)*cos(angles[2])
               + 7.6*(sin(angles[1])*sin(angles[1]-angles[2])
               + cos(angles[1])*cos(angles[1]-angles[2]));
/**/
/* torque[2]+= (-68.0)*cos(angles[2])
               + 8.5*(sin(angles[1])*sin(angles[1]-angles[2])
               + cos(angles[1])*cos(angles[1]-angles[2]));
/**/
}
for(i=0;i<3;i++) {
    amps[i]=torque[i]/TORQUECONST;
    AmpOutput(i,amps[i],baseaddr);
}
return;
}

```

2976-64